Journal of the Anatomical Society of India

Print ISSN: 0003-2778

GENERAL INFORMATION

About the Journal

Journal of the Anatomical Society of India (ISSN: Print 0003-2778) is peer-reviewed journal. The journal is owned and run by Anatomical Society of India. The journal publishes research articles related to all aspects of Anatomy and allied medical/surgical sciences. Pre-Publication Peer Review and Post-Publication Peer Review Online Manuscript Submission System Selection of articles on the basis of MRS system Eminent academicians across the globe as the Editorial board members Electronic Table of Contents alerts Available in both online and print form. The journal is published quarterly in the months of January, April, July and October.

Scope of the Journal

The aim of the *Journal of the Anatomical Society of India* is to enhance and upgrade the research work in the field of anatomy and allied clinical subjects. It provides an integrative forum for anatomists across the globe to exchange their knowledge and views. It also helps to promote communication among fellow academicians and researchers worldwide. The Journal is devoted to publish recent original research work and recent advances in the field of Anatomical Sciences and allied clinical subjects. It provides an opportunity to academicians to disseminate their knowledge that is directly relevant to all domains of health sciences.

The Editorial Board comprises of academicians across the globe.

JASI is indexed in Scopus, available in Science Direct.

Abstracting and Indexing Information

The journal is registered with the following abstracting partners:

Baidu Scholar, CNKI (China National Knowledge Infrastructure), EBSCO Publishing's Electronic Databases, Ex Libris – Primo Central, Google Scholar, Hinari, Infotrieve, Netherlands ISSN center, ProQuest, TdNet, Wanfang Data

The journal is indexed with, or included in, the following:

SCOPUS, Science Citation Index Expanded, IndMed, MedInd, Scimago Journal Ranking, Emerging Sources Citation Index.

Impact Factor® as reported in the 2019 Journal Citation Reports® (Clarivate Analytics, 2020): 0.227

Information for Authors

Article processing and publication charges will be communicated by the editorial office. All manuscripts must be submitted online at www.journalonweb.com/jasi.

Subscription Information

A subscription to JASI comprises 4 issues. Prices include postage. Annual Subscription Rate for non-members-		
Rates of Membership (with effect from 1.1.2019)		
	India	**International**
Ordinary membership	INR 1500	US $ 100
Couple membership	INR 2250	
Life membership	INR 8000	US $ 900
Subscription Rates (till 31st August)		
Individual	INR 4500	US $ 600
Library/Institutional Trade discount of 10% for agencies only	INR 10000	US $ 900
Subscription Rates (after 31st August)		
Individual	INR 5000	
Library/Institutional	INR 10500	
The Journal of Anatomical Society of India (ISSN: 0003-2778) is published quarterly **Subscriptions** are accepted on a prepaid basis only and are entered on a calendar year basis. Issues are sent by standard mail Priority rates are available upon request.		

Information to Members/Subscribers

All members and existing subscribers of the Anatomical Society of India are requested to send their membership/existing subscription fee for the current year to the Treasurer of the Society on the following address: Prof (Dr.) Punit Manik, Treasurer, ASI, Department of Anatomy, KGMU, Lucknow - 226003. Email: punitamanik@yahoo.co.in. All payments should be made through an account payee bank draft drawn in favor of the **Treasurer, Anatomical Society of India,** payable at **Lucknow** only, preferably for **Allahabad Bank, Medical College Branch, Lucknow.** Outstation cheques/drafts must include INR 70 extra as bank collection charges.

All complaints regarding non-receipt of journal issues should be addressed to the Editor-in-Chief, JASI at editorjasi@gmail.com. The new subscribers may, please contact wkhlrpmedknow_subscriptions@wolterskluwer.com.

Requests of any general information like travel concession forms, venue of next annual conference, etc. should be addressed to the General Secretary of the Anatomical Society of India.

For mode of payment and other details, please visit www.medknow.com/subscribe.asp

Claims for missing issues will be serviced at no charge if received within 60 days of the cover date for domestic subscribers, and 3 months for subscribers outside India. Duplicate copies cannot be sent to replace issues not delivered because of failure to notify publisher of change of address. The journal is published and distributed by Wolters Kluwer India Pvt. Ltd. Copies are sent to subscribers directly from the publisher's address. It is illegal to acquire copies from any other source. If a copy is received for personal use as a member of the association/ society, one cannot resale or give-away the copy for commercial or library use.

The copies of the journal to the subscribers are sent by ordinary post. The editorial board, association or publisher will not be responsible for non receipt of copies. If any subscriber wishes to receive the copies by registered post or courier, kindly contact the publisher's office. If a copy returns due to incomplete, incorrect or changed address of a subscriber on two consecutive occasions, the names of such subscribers will be deleted from the mailing list of the journal. Providing complete, correct and up-to-date address is the responsibility of the subscriber.

Nonmembers: Please send change of address information to subscriptions@medknow.com.

Advertising Policies

The journal accepts display and classified advertising. Frequency discounts and special positions are available. Inquiries about advertising should be sent to Wolters Kluwer India Pvt. Ltd, advertise@medknow. com.

The journal reserves the right to reject any advertisement considered unsuitable according to the set policies of the journal.

The appearance of advertising or product information in the various sections in the journal does not constitute an endorsement or approval by the journal and/or its publisher of the quality or value of the said product or of claims made for it by its manufacturer.

Addresses

Editorial Office

Dr. Vishram Singh, Editor-in-Chief, JASI
OC-5/103, 1st floor, Orange County Society,
Ahinsa Khand-I, Indirapuram, Ghaziabad,
Delhi, NCR- 201014.
Email: editorjasi@gmail.com

Published by

Wolters Kluwer India Pvt. Ltd
A-202, 2nd Floor, The Qube,
C.T.S. No.1498A/2 Village Marol, Andheri (East),
Mumbai - 400 059, India.
Phone: 91-22-66491818
Website: www.medknow.com

Printed at

Dhote Offset Tech. P. Ltd
Goregaon (E), Mumbai, India

Journal of the Anatomical Society of India

Print ISSN: 0003-2778

EDITORIAL BOARD

Journal of the Anatomical Society of India

Print ISSN: 0003-2778

EXECUTIVE COMMITTEE

Journal of the Anatomical Society of India

Volume 70 | Issue 1 | January-March 2021

CONTENTS

Journal of the Anatomical Society of India on Web

http://www.journalonweb.com/jasi

The Journal of the Anatomical Society of India now accepts articles electronically. It is easy, convenient and fast. Check following steps:

1 Registration

- Register from http://www.journalonweb.com/jasi as a new author (Signup as author)
- Two-step self-explanatory process

2 New article submission

- Read instructions on the journal website or download the same from manuscript management site
- Prepare your files (Article file, First page file and Images, Copyright form & Other forms, if any)
- Login as an author
- Click on 'Submit new article' under 'Submissions'
- Follow the steps (guidelines provided while submitting the article)
- On successful submission you will receive an acknowledgement quoting the manuscript ID

3 Tracking the progress

- Login as an author
- The report on the main page gives status of the articles and its due date to move to next phase
- More details can be obtained by clicking on the ManuscriptID
- Comments sent by the editor and reviewer will be available from these pages

4 Submitting a revised article

- Login as an author
- On the main page click on 'Articles for Revision'
- Click on the link "Click here to revise your article" against the required manuscript ID
- Follow the steps (guidelines provided while revising the article)
- Include the reviewers' comments along with the point to point clarifications at the beginning of the revised article file.
- Do not include authors' name in the article file.
- Upload the revised article file against New Article File - Browse, choose your file and then click "Upload" OR Click "Finish"
- On completion of revision process you will be able to check the latest file uploaded from Article Cycle (In Review Articles-> Click on manuscript id -> Latest file will have a number with 'R', for example XXXX_100_15R3.docx)

Facilities

- Submission of new articles with images
- Submission of revised articles
- Checking of proofs
- Track the progress of article until published

Advantages

- Any-time, any-where access
- Faster review
- Cost saving on postage
- No need for hard-copy submission
- Ability to track the progress
- Ease of contacting the journal

Requirements for usage

- Computer and internet connection
- Web-browser (Latest versions - IE, Chrome, Safari, FireFox, Opera)
- Cookies and javascript to be enabled in web-browser

Online submission checklist

- First Page File (rtf/doc/docx file) with title page, covering letter, acknowledgement, etc.
- Article File (rtf/doc/docx file) - text of the article, beginning from Title, Abstract till References (including tables). File size limit 4 MB. Do not include images in this file.
- Images (jpg/jpeg/png/gif/tif/tiff): Submit good quality colour images. Each image should be less than 10 MB) in size
- Upload copyright form in .doc / .docx / .pdf / .jpg / .png / .gif format, duly signed by all authors, during the time mentioned in the instructions.

Help

- Check Frequently Asked Questions (FAQs) on the site
- In case of any difficulty contact the editor

Discovery of New Organs in Human Throat: The Tubarial Salivary Glands

"*Scientists discover new human salivary glands*" was the title of the article which hogged the limelight of most medical journal bulletins and newsletters on October 16, 2020.

According to the classical description in the textbooks of anatomy, there are three pairs of large salivary glands, namely parotid around the ears, submandibular below the mandible, and sublingual under the tongue.[1,2] In addition to these glands, there are a number of minor salivary glands located in the mucosa of the oral cavity and named as lingual, labial, buccal, and palatine glands concurrent to their location. These glands are made up of serous, mucous, or seromucous acini and produce saliva. The saliva is poured into the oral cavity to help in mastication, digestion, tasting, swallowing, and dental hygiene.

It is worth mentioning that in addition to the salivary glands mentioned above, there are a number of discrete seromucous glands located in the mucosa of various parts of the aerogastric tract for the purpose of lubrication, protection, etc., The mucosa around the openings of the auditory tubes also contains discrete microscope seromucous glands for the lubrication of mucosa around the tubal openings. However, a large pair of new salivary glands was reported to be present in the human throat by the scientists from the Netherlands Cancer Institute (NCI) which was never noticed earlier.[3]

The scientists from NCI while doing a routine screening of 100 prostate cancer patients using prostatic-specific membrane antigen (PSMA) positron-emission tomography/computed tomography scan accidentally found the presence of large masses of glandular tissue in human nasopharynx in all patients. It was located above the torus tubarius, an elevation produced by a cartilage guarding the opening of auditory tube.

The scans of all the 100 patients clearly showed the PSMA-positive area (shinning yellow-like gold) above torus tubarius on either side in the region of the nasopharynx [Figure 1a]. This area extended from the skull base above to downward along the posterolateral wall of the pharynx [Figure 1b].

The glands were characterized by performing histological and histochemical examinations. The tissue was obtained from freshly donated dead bodies.

The three-dimensional reconstruction of histology slides showed salivary tissue in newly discovered glands (in yellow) and ducts in blue. These glands consisted of serous and mucous acini. The number of mucous acini was much more than serous acini similar to that of the sublingual salivary gland. The cells showed the cytoplasmic expression of PSMA. The ducts of these glands were opening in the posterolateral pharyngeal wall.

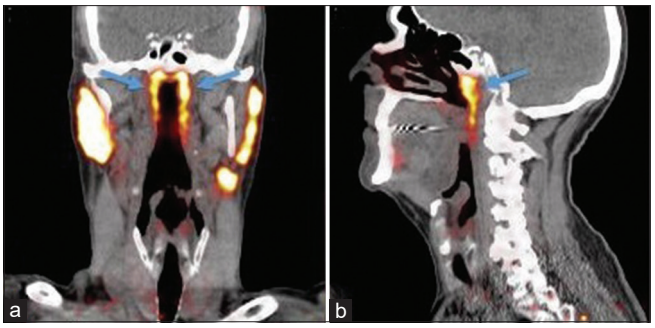

Figure 1: [3]Prostatic-specific membrane antigen positron-emission tomography/computed tomography scan of head-and-neck region. The slices at the level of torus tubarius in the nasopharynx showing an orange signal at the site of salivary tissues expressing prostatic-specific membrane antigen. (a) Coronal slice showing bilateral presence of tubarial salivary glands. (b) Sagittal slice showing unilateral presence of tubarious salivary glands

On an average, they are about 4 cm (1.5 inches) long. These glands were categorized as seromucous glands with ducts by histological histochemical studies. According to Woulter Vogel, co-author and radiation oncologist at NIC, the radioactive tracer used in this technique not only binds with the cells of prostate glands but also binds well with PSMA of cells of salivary glands.[4]

The above finding showed that the glands are part of the salivary system, thus forming the fourth pair of major salivary glands.[5-7] The scientists therefore named them as tubarial salivary glands. The secretions of these glands are poured onto the dorsolateral wall of the nasopharynx and lubricate and moisten the upper part throat located behind the nose (nasopharynx) and behind the mouth (oropharynx).

It is a bit surprising that these macroscopic glands were left unnoticed by anatomists, histologists, ear, nose, and throat surgeons, and histopathologists so far long.

Since, the salivary glands both major and minor pour their secretions into the oral cavity where it mixes up with food during mastication to help in digestion and swallowing of food bolus. Therefore, according to our opinion instead of calling these glands tubarial salivary glands, they should be simply named as tubarial glands.

The sparing of these glands during radiotherapy of head-and-neck cancer patients will relieve them from common posttherapy symptoms such as dryness of the mouth (xerostomia) and difficulty in swallowing (dysphagia).

Vishram Singh, Krishna Chaitanya Reddy[1]

Department of Anatomy, Kasturba Medical College, Mangalore, MAHE, Karnataka, [1]Department of Anatomy, Kamineni Academy of Medical Sciences and Research Center, L. B Nagar, Hyderabad, Telangana, India

Address for correspondence: *Prof. Vishram Singh, OC-5/103, 1st Floor, Orange County Society, Ahinsa Khand-I, Indirapuram, Ghaziabad, Delhi-NCR - 201 014, Uttar Pradesh, India. E-mail: drvishramsingh@gmail.com*

References

1. Standring S. Gray's Anatomy: The Anatomical Basis of Clinical Practice. 41st ed. London, UK:Elsevier; 2015.
2. Moore KL, Agur AM, Dalley AF. Clinically Oriented Anatomy. 7th ed. Philadelphia, Pennsylvania, United States: Lippincot Williams and Wilkins; 2018.
3. Valstar MH, de Bakker BS, Steenbakkers RJ, de Jong KH, Smit LA, Klein Nulent TJ, *et al*. The tubarial salivary glands: A potential new organ at risk for radiotherapy. Radiother Oncol 2021;154:292-8.
4. Klein Nulent TJ, Valstar MH, de Keizer B, Willems SM, Smit LA, Al-Mamgani A, *et al*. Physiologic distribution of PSMA-ligand in salivary glands and seromucous glands of the head and neck on PET/CT. Oral Surg Oral Med Oral Pathol Oral Radiol 2018;125:478-86.
5. Tos M. Mucous glands in the developing human rhinopharynx. Laryngoscope 1977;87:987-95.
6. Richardson MS. Non-neoplastic lesions of salivary glands. In: Thomson I, editor. Head and Neck Pathology. 2nd ed. Woodland Hills, CA:Elsevier Saunders; 2013. p. 228.
7. Berger G. Eustachian tube submucosal glands in normal and pathological temporal bones. J Laryngol Otol 1993;107:1099-105.

Article Info

Received: 01 November 2020
Accepted: 09 March 2021
Available Online: ***

Access this article online

Quick Response Code:

Website: www.jasi.org.in

DOI: 10.4103/jasi.jasi_240_20

How to cite this article: Singh R, Reddy KC. Discovery of New Organs in Human Throat: The Tubarial Salivary Glands. J Anat Soc India 2021;XX:XX-XX.

Original Article

Morphometric Study of the Knee Joint in Saudi Arabian Population based on Magnetic Resonance Imaging Scan

Abstract

Introduction: Total knee arthroplasty (TKA) is considered a highly recommended procedure, to improve the life of patients suffering from knee arthritis by relieving pain and deformity. Knee morphology and anthropomorphic features have evolved as the most reliable source of information to design TKA prostheses. But unfortunately, the amorphic features of Western patients are the preferred choice of data for the development of suitable implants. This study is conducted for commencing to evaluate the geometric parameters of the knee joints of Saudi Arabian male and female subjects which is indispensable to the design of knee prosthesis used for compatriotic patients. **Material and Methods:** A total of 13 parameters of tibia and femur were studied in a group of 150 normal subjects including 110 females and 40 males. A subsequent magnetic resonance imaging scan was done for all the studied cases and a reproducible result was obtained. **Results:** The Saudi females were found to have smaller dimensions of parameters of tibia and femur than those in Saudi males. The results when compared with other reports from different countries, we find marked difference in their dimensions. **Discussion and Conclusion:** Our study suggests that there exists a morphological mismatch between the knee anatomy of people of Saudi Arabia and people of other countries. Implantation of such implants prepared on the basis of outsider data could not justified to use in the Saudi population.

Keywords: *Anatomical conformity, knee arthritis, Saudi knee morphology, total knee arthroplasty*

Daifallah Alharbi, Zaheer Ahmed

Department of Orthopaedics, College of Medicine, Majmaah University, Al Majmaah, Saudi Arabia

Introduction

The knee is an important hinge joint that is responsible for weight-bearing and movement. The femur (thigh bone), tibia (shin bone), and patella (knee cap) make up the bones of the knee joint. The knee joint keeps these bones in place with additional support of different ligaments.

Osteoarthritis of Knee is known to be the most common degenerative disease around the world,[1] it is a result of progressive wear and tear of articular cartilage of the joint. The occurrence of OA varies from 3.8% to 70% around the world depending on the methodologies used for its diagnosis and the studied populations.[2-4] It is most common in elderly women and men. Knee OA can be divided into two types, primary and secondary. Primary OA is articular degeneration without any apparent underlying reason. Secondary OA is the consequence of either an abnormal concentration of force across the joint as with posttraumatic causes or abnormal articular cartilage, such as rheumatoid arthritis. OA is typically a progressive disease that may eventually lead to disability. Knee joint instability is also one of the common sources of problem from which both athletes and nonathletes suffer which leads to OA of the knee joint in long run. It affects a varied population, including professional athletes, older adults, and recreational exercisers.[5] Knee instability has a high incidence rate and has been extensively studied over the last decade. Many countries have health-care systems focused on value-based care, which are systems focused on understanding the cost drivers, implementing high-value therapies, and improving methods and/or techniques to assess knee instability and rehabilitation therapies that could potentially reduce the health-care costs associated with knee injury.[6-10]

Total knee replacement (TKR) is a surgical procedure in which an artificial joint or prosthesis replaces a damaged knee joint. In recent years, knee prosthesis has improved greatly and it has become one of the most

How to cite this article: Alharbi D, Ahmed Z. Morphometric study of the knee joint in Saudi Arabian population based on magnetic resonance imaging scan. J Anat Soc India 2021;XX:XX-XX.

Article Info

Received: 15 July 2020
Accepted: 26 December 2020
Available online: ***

Address for correspondence:
Dr. Zaheer Ahmed, Department of Orthopaedics, College of Medicine, Majmaah University, Al Majmaah 11952, Saudi Arabia.
E-mail: z.mohammed@mu.edu.sa

Access this article online

Website: www.jasi.org.in
DOI: 10.4103/JASI.JASI_135_20
Quick Response Code:

reliable joint replacements. The aim of TKR is pain relief and restoration of knee function and mobility. In fact, TKR is widely considered as an effective treatment for end-stage knee degenerative pathologies.[11-14] It has a great clinical success rate of nearly 95% after 10 years follow-up. The main prosthesis design has to satisfy specific anatomical, biological, mechanical, and industrial requirement.[15-18]

In recent years, many studies have identified shape differences in the knee within the Caucasian population. The analyses based on shape have identified sex differences in the femoral midshaft, distal femur, and patella. Using automated three-dimensional (3D) morphologic analysis, difference in knee morphology between the sexes has been identified. Reports of anthropometric studies have confirmed that there is a striking difference in knee morphology between males and females, where females having a smaller mediolateral to anteroposterior ratio and more narrow distal femurs.[19-22] Furthermore, research on implant mismatching carried out in various Asian countries has suggested that the selection of total knee arthroplasty (TKA) implants blindly is not rationalized since their designs are based on morphological data of a limited studied population of a certain region.[23]

It is thus a great concern that if ethnical differences in the shape and size of the distal femur and proximal tibia exist, there is a need to identify the clinical impact of the current TKA design. Thus, it has become essential to compare the resected knees of the subject population with the existing western implants and quantify the morphological differences so that the performance of TKA can be improved. The aim of the present study is to investigate the morphology of the Saudi Arabian population using three-dimensional knee models and compare the results with the similar studies conducted in different parts of the world for judicial selection of commercially available TKA implants.

Material and Methods

This cross-sectional observational study was conducted in the Department of Orthopaedic Surgery, College of Medicine, Majmaah University, Al Majmaah Saudi Arabia, from May 2019 to January 2020. The study was conducted after prior approval from the Central Research Committee, of our university and the Ministry of Health with Central IRB log number: 2019-0057E.

During the study period, a total of 180 magnetic resonance imaging (MRI) scans of knee joints were done and all of them were considered for the study. Out of which, 23 MRI scans of knee joint had posttraumatic changes in the knee and 7 MRI scans were skeletally immature. Hence, out of 180, 30 MRI scans were excluded and the final sample size of 150 was analyzed in this study. The knee joint data included all patients during the study period which included 40 males and 110 females' knees. As skeletal maturity occurs completely at the age of 18 years and there would not much difference in the morphometric measurements of knee joints, all individuals aged from 18 years to 73 years were included in the study.

These data were collected using MRI scans. MRI scans were used as an assessment tool to study the bony structures and soft tissues, Patients in whom ligament and meniscus injury was identified on MRI were excluded from the study. Only complete and fully ossified bones were included and knee joints with any fracture, unossified or pathological abnormalities such as tumors, deformities, congenital deformities, and metabolic diseases of bones were excluded from this study.

MRI scans of 150 normal subject's dataset of knee joints were obtained from the hospital which covers all geographical regions of Al Majmaah province. The total number of scanning slices was 120 and the range of scanning covered the complete knee joints of both legs with the knee in full extension. The slice thickness was 3 mm. The Digital Imaging and Communications in Medicine (DICOM) images were loaded to 3D SLICER, which is an advanced software platform for the analysis (including registration and interactive segmentation) and visualization (including volume rendering) of medical images and for research in image-guided therapy was used for accurate extraction of all parameters.[24]

Magnetic resonance imaging study

In this study, about 13 morphological features measured were tibia anteroposterior (tAP), tibia medial condyle anteroposterior (tMAP), tibia lateral condyle anteroposterior (tLAP), and tibia medial-lateral (tML), femur epicondylar width (fEW), femur medial condyle anteroposterior (fMAP), femur lateral condyle anteroposterior (fLAP), femoral mediolateral length (fML), femur medial condyle width (fMW), femur lateral condyle width (fLW), intercondylar fossa width (ICW), intercondylar fossa height (ICH), and femoral aspect ratio (ration of femoral ML/AP). To avoid interobserver errors, the measurements were extracted using a highly specific software, namely 3D SLICER using DICOM images in three different view planes such as transverse plane, sagittal plane, and coronal plane of the scan and the same is presented in Figure 1a-c.

Femoral cuts

The distal femur plane is selected 9 mm above the most inferior point of femoral condyles in the sagittal plane, which is represented in Figure 2a. The posterior condylar axis (PCA) is represented in Figure 2b. PCA is the line tangent to the most posterior part of the medial and lateral condyles and this axis is made as the horizontal reference.

Transepicondylar axis (TEA) is measured and it is the distance between the lateral and medial epicondyles. fMAP,

fLAP, and fML are illustrated in Figure 2c. The femur lateral condyle is measured at the level of the narrowest width of the intercondylar notch in the lateral condyle. Femur medial and lateral condyle is measured at the level of the narrowest width of the intercondylar notch in medial condyle as shown in Figure 2c and d. ICH is the distance between the most anterior point in the intercondylar notch to the point on the PCA and this measurement is taken perpendicular to the PCA as shown in Figure 2e. The femoral characteristics are expressed in Figure 2a-e.

A line is drawn at the most inferior part of the femoral condyles. A line parallel to this line at the level of the popliteal groove is shown in Figure 2e, where the notch width, medial condyle width (MCW), and lateral condyle width (LCW) were measured as shown in Figure 2d. Femoral condyle anteroposterior diameter is measured at a section of axial slice where the maximum anteroposterior diameter of lateral condyle is present. A horizontal line is drawn touching both the posterior surfaces of medial and lateral femoral condyles. The femoral mediolateral length (fML) was referenced by the femoral epicondyle axis, defined as the most salient point between the medial and lateral attachment on the femoral condyle. The femoral medial condyle anteroposterior length (fMAP) was defined as the distance from the most anterior point on the femur medial condyle to the posterior condylar line. The femoral lateral condyle anteroposterior length (fLAP) was taken as the distance from the most anterior point on the femur lateral condyle, Figure 2c.

The intercondylar fossa height (FH) is the perpendicular distance from the apex of the notch to the horizontal line at the level of the articular margins of the medial and lateral femoral condyles. It is illustrated in Figure 2e.

Tibial cuts

The tML was the maximum length between medial and lateral tibia plateau, parallel to the axis of the femoral condyle. The tibial lateral anteroposterior length (tLAP) was the length from the anterior lateral tibia plateau to the posterior plateau. The tibial medial anteroposterior length (tMAP) was the length from the anterior medial tibia plateau to the posterior plateau, which are illustrated in Figure 3a and b. The femoral aspect ratio (fML/fAP) and tibial aspect ratio (tML/tAP) were considered in our study to interpreting the results of knee shape. All measurements were recorded in millimeters.

Measurements

The resected femur was oriented perpendicular to the transverse plane and all measurements were performed on this distal resection plane. The mediolateral axis was taken as the TEA, a line connecting the lateral epicondylar prominence and the medial epicondylar prominence. Tangents parallel to the TEA and passing through the anterior and posterior extremities were constructed.

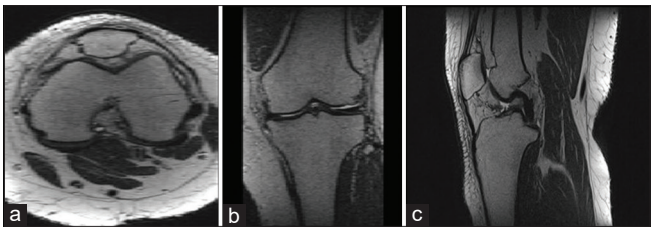

Figure 1: (a) Transverse plane view femur. (b) Coronal plane view femur. (c) Sagittal plane view femur

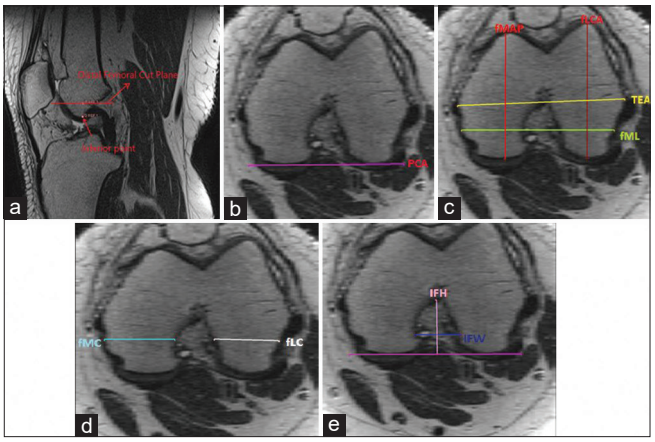

Figure 2: (a) Distal femur plane. (b) Posterior condylar axis. (c) Transepicondylar axis of the femur. (d) Femur lateral and medial condyles. (e) Intercondylar fossa width and height

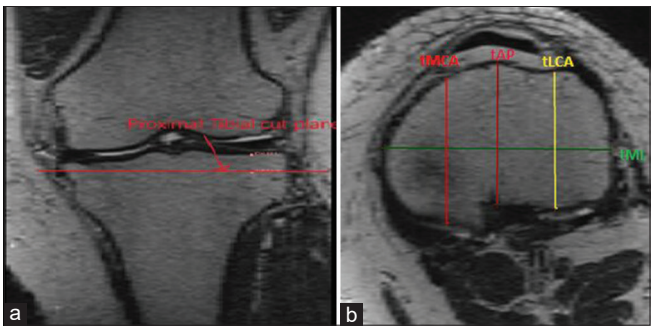

Figure 3: (a) Proximal tibial plane. (b) Axial plane of the tibia

Distance between two medial and lateral extremities in the resected plane measured collinear to the TEA was defined as the femoral mediolateral width (fML). Distance between two tangents parallel to TEA and passing through anterior and posterior extremities of the distal femur was defined as the femoral Anteroposterior width (fAP).

The resected tibia was oriented perpendicular to the transverse plane and all measurements were performed on this proximal resection plane. The mediolateral axis was constructed parallel to the femoral TEA. Tangents parallel to the TEA and passing through the anterior and posterior extremities were constructed. Distance between medial and lateral extremities in the resected plane measured parallel to the mediolateral axis was defined as tibial mediolateral width (tML). Distance between two tangents parallel to TEA and passing through anterior and posterior extremities

of the proximal tibia was defined as tibial anteroposterior width (tAP).

Comparison

To compare the result of our study (i.e., Saudi Arabian knees morphological measurements) with other reports, an extensive literature survey was carried out by retrieving the literature. The aspect ratios were defined as mentioned above in order to make our data coherent with the anthropometric data of other ethnic groups. The data of various parameters of our measurements were compared with that of Chinese, Caucasian, Japanese, Korean, Germany, France, Brazil, Turkey, Malaysia, and Indian population as shown in Tables 1-4.

Statistical analysis

The data were entered and analyzed using SPSS [25.0]. Statistics. Armonk, New York, USA: IBM Corp. Frequencies and percentages are reported for qualitative variables, whereas the quantitative variables were expressed as mean ± standard deviation. One-way analysis of variance was applied to compare the Saudi population parameters with the other countries. *Post hoc* Scheffe test was further applied to observe with group mean differs. $P < 0.05$ was considered as statistically significant.

Results

The results of the morphological study conducted on Saudi males and females are summarized in Tables 1-3. The measurements of tibial parameters include tAP (ranges from 45.95 ± 4.14 for male to 43.13 ± 3.76 for female), tMAP (ranges from 48.23 ± 3.75 for males to 43.87 ± 3.62 for female), tLAP (ranges from 45.17 ± 3.82 for males to 39.90 ± 3.56 for female), and tML (ranges from 75.93 ± 4.32 for male to 68.06 ± 4.88 for female) this data is summarized in Table 1.

The measurements of femoral characteristics include fEW (ranges from 79.56 ± 4.43 for males to 71.31 ± 4.98 for female),

Table 1: Comparison of different parameters studied between Saudi Arabia and other countries

Parameter	Reference range in mm (different countries)				Turkey	*P*
	Saudi (present study)	China	Caucasians	Korea		
Tibia						
Tibia anteroposterior	45.95±4.14 male	52.8±4.3 male*	53.9±4.6 male*	48.2±3.3 male*	-	<0.001
	43.13±3.76 female	50.0±1.4 female*	51.3±2.6 female*	43.2±2.3 female		<0.001
Tibia medial condyle anteroposterior	48.23±3.75 male	54.1±3.1 male*	54.7±2.3 male*	48.5±3.7 male	-	<0.001
	43.87±3.62 female	49.9±1.5 female*	50.6±2.2 female*	43.5±2.9 female		<0.001
Tibia lateral condyle anteroposterior	45.17±3.82 male	49.9±3.9 male*	49.3±3.38 male*	43.5±2.9 male*	-	<0.001
	39.90±3.56 female	44.6±1.2 female*	44.3±2.1 female*	39.8±2.5 female		<0.001
Tibia medial-lateral	75.93±4.32 male	73.6±3.4 male*	74.9±2.9 male	76.1±4.0 male	-	0.001
	68.06±4.88 female	67.4±2.6 female	66.5±7.4 female	67.6±3.1 female		0.286
Femur						
Femur lateral condyle anteroposterior	61.26±3.82 male	68.2±3.2 male*	68.7±2.5 male*	64.63±3.1 male*	-	<0.001
	56.00±3.27 female	62.2±1.9 female*	63.0±2.9 female*	58.39±3.1 female*		<0.001
Femur medial condyle anteroposterior	58.83±4.21 male	66.1±3.5 male*	67.1±2.8 male*	61.22±2.9 male*	-	<0.001
	53.16±3.72 female	59.7±1.6 female*	62.6±2.1 female*	55.25±2.5 female*		<0.001
Epicondylar width (transepicondylar axis)	79.56±4.43 male				83.1±7.7 male*	<0.001
	71.31±4.98 female				74.4±4.3 female*	<0.001
Femoral mediolateral length	72.61±5.23 male	87.2±4.4 male*	87.7±4.6 male*	-		<0.001
	65.09±4.71 female	74.1±3.5 female*	79.0±3.9 female*			<0.001
Femur lateral condyle width	24.70±2.83 male	32.1±1.9 male*	32.8±1.7 male*	27.96±2.5 male*	26.6±2.8 male*	<0.001
	26.35±3.83 female			24.05 female	23.2±2.3 female	<0.001
Femur medial condyle width	27.09±2.89 male	28.1±1.9 female	31.4±2.0 female*	25.78±2.6 male*	27.0±2.1 male	<0.001
	24.57±2.50 female			23.46±1.74 female*	23.7±2.2 female*	0.006
Intercondylar fossa width	22.16±2.78 male	16.3±2.2 male*	17.2±2.4 male*	21.66±2.3 male	21.3±2.4 male	<0.001
	20.24±2.37 female	14.0±1.0 female*	15.0±1.5 female*	18.97±4.2 female*	19.1±2.0 female	<0.001
Intercondylar fossa height	30.13±3.89 male	33.2±2.8 male*	33.2±2.8 male*	30.50±2.3 male	33.2±2.8 male*	<0.001
	25.95±3.55 female	29.0±2.6 female*	29.0±2.6 female*	27.16±3.1 female*	29.0±2.6 female*	<0.001
Femoral aspect ratio (ML/AP)	1.18±0.08 male	1.27±0.03 male*	1.27±0.03 male*	-	-	<0.001
	1.15±0.06 female	1.24±0.04 female*	1.24±0.04 female*			<0.001

*When ANOVA is applied then we have to apply POST-HOC tests to see which group means significantly differ. In this case the ANOVA p-value is mentioned at the last column and asterisk shows that these groups mean significantly differ

Table 2: Comparison of different parameters studied between Saudi Arabia and other countries

Parameter	Reference range in mm (different countries)					*P*
	Saudi (present study)	Japan	Germany	France	Brazil	
Tibia						
Tibia anteroposterior	45.95±4.14 male	53.8±6.6 male*	-	-	53.9±6.1 male*	<0.001
	43.13±3.76 female	46.6±3.6 female*			46.0±4.0 female*	<0.001
Tibia medial condyle anteroposterior	48.23±3.75 male	-	55.3±3.32 male*	-	-	<0.001
	43.87±3.62 female		49.1±2.86 female*			<0.001
Tibia lateral condyle anteroposterior	45.17±3.82 male	-	49.1±1.62 male*	-	-	<0.001
	39.90±3.56 female		42.7±2.52 female*			<0.001
Tibia medial-lateral	75.93±4.32 male	83.0±6.2 male*	81.0±3.35 male*	-	79.8±5.8 male*	<0.001
	68.06±4.88 female	71.7±4.0 female*	72.2±3.80 female*		69.6±4.3 female	<0.001
Femur						
Femur lateral condyle anteroposterior	61.26±3.82 male	-	69.3±2.50 male*	65.3±4 male*	70.3±4.7 male*	<0.001
	56.00±3.27 female		63.1±3.82 female*	60.4±3.8 female*	61.5±4.9 female*	<0.001
Femur medial condyle anteroposterior	58.83±4.21 male	63.6±3.3 male*	69.3±2.42 male*	66.7±4.2 male*	-	<0.001
	53.16±3.72 female	58.1±3.1 female*	62.3±4.28 female*	60.4±3.9 female*		<0.001
Epicondylar width(transepicondylar axis)	79.56±4.43 male					-
	71.31±4.98 female					
Femoral mediolateral length	72.61±5.23 male	72.7±4.2 male	70.5±3.79 male	85.1±4.9 male*	77.7±4.9 male*	<0.001
	65.09±4.71 female	63.4±3.4 female*	61.5±3.39 female*	75.5±3.7 female*	67.8±4.0 female*	<0.001
Femur lateral condyle width	24.70±2.83 male	-	30.6±1.25 male*	-	-	<0.001
	26.35±3.83 female		26.0±0.85 female			0.562
Femur medial condyle width	27.09±2.89 male	-	32.3±4.22 male*	-	-	<0.001
	24.57±2.50 female		28.4±2.40 female*			<0.001
Intercondylar fossa width	22.16±2.78 male	-	19.3±1.99 male*	-	-	<0.001
	20.24±2.37 female		19.0±2.74 female			0.004
Intercondylar fossa height	30.13±3.89 male	-	32.5±2.63 male*	-	-	0.003
	25.95±3.55 female		30.3±2.46 female*			<0.001
Femoral aspect ratio (ML/AP)	1.18±0.08 male	-	-	-	-	-
	1.15±0.06 female					

*When ANOVA is applied then we have to apply POST-HOC tests to see which group means significantly differ. In this case the ANOVA p-value is mentioned at the last column and asterisk shows that these groups mean significantly differ.

fMAP (ranges from 58.83 ± 4.21 for males to 53.16 ± 3.72 for female), fLAP (ranges from 61.26 ± 3.82 for males to 56.00 ± 3.27 for female), fML (ranges from 72.61 ± 5.23 for males to 65.09 ± 4.71 for female), fMW (ranges from 24.70 ± 2.83 for male to 26.35 ± 3.83 for female), ICW (ranges from 22.16 ± 2.78 for males to 20.24 ± 2.37 for female), ICH (ranges from 30.13 ± 3.89 for males to 25.95 ± 3.55 for female), femoral aspect ratio, ML/AP (ranges from 1.18 ± 0.08 for males to 1.15 ± 0.06 for female) (P < 0.001) corresponding data is summarized in Table 1. The result of the present study was compared with the other similar studies which are shown in Tables 1-3.

Discussion

The present study entitled, "Morphometric Study of Knee Joint in Saudi Arabian Population by MRI scan Images" hereby conducted in 150 study subjects of both sex and varied age group in the Saudi population. From the result, it is clear that all the studied parameters of tibia, i.e., tAP, tMAP, tLAP, and tML have larger size in males than in females. Similar results are seen in all measurements of the femur, i.e., fEW, fMAP, fLAP, fML, fMW, ICW, ICH, and femoral aspect ratio (ML/AP) ($P < 0.001$). However, fLW was high in females than studied males ($P < 0.001$). Our results are in good compliance with the results reported

Table 3: Comparison of different parameters studied between Saudi Arabia and other countries

Parameter	Reference range in mm (different countries)				*P*
	Saudi (present study)	Turkey	Malaysia	India	
Tibia					
Tibia anteroposterior	45.95±4.14 male	47.6±3.8 male*	-	-	0.001
	43.13±3.76 female	40.9±3.1 female*			<0.001
Tibia medial condyle anteroposterior	48.23±3.75 male	53.9±4.2 male*	-	-	<0.001
	43.87±3.62 female	47.5±3.9 female*			<0.001
Tibia lateral condyle anteroposterior	45.17±3.82 male	45.9±3.7 male	-	-	0.065
	39.90±3.56 female	39.9±3.0 female			0.925
Tibia medial-lateral	75.93±4.32 male	77.1±5.1 male*	-	-	0.021
	68.06±−4.88 female	68.7±3.6 female			0.144
Femur					
Femur lateral condyle anteroposterior	61.26±3.82 male	-	-	-	0.246
	56.00±3.27 female				0.887
Femur medial condyle anteroposterior	58.83±4.21 male	-	63.93±3.36 male*	61.09±3.74 male*	<0.001
	53.16±3.72 female		57.39±3.29 female*	54.47±1.91 female	<0.001
Epicondylar width(transepicondylar axis)		79.56±4.43 male			-
		71.31±4.98 female			
Femoral mediolateral length	72.61±5.23 male	-	74.88±3.55 male*	-	<0.001
	65.09±4.71 female		64.53±3.12 female		<0.001
Femur lateral condyle width	24.70±2.83 male	-	-	69.64±3.11 male*	<0.001
	26.35±3.83 female			61.06±3.11 female*	<0.001
Femur medial condyle width	27.09±2.89 male	-	-	-	-
	24.57±2.50 female				
Intercondylar fossa width	22.16±278 male	-	-	-	-
	20.24±2.37 female				
Intercondylar fossa height	30.13±3.89 male	-	-	-	-
	25.95±3.55 female				
Femoral aspect ratio (ML/AP)	1.18±0.08 male	-	-	-	-
	1.15±0.06 female				

*When ANOVA is applied then we have to apply POST-HOC tests to see which group means significantly differ. In this case the ANOVA p-value is mentioned at the last column and asterisk shows that these groups mean significantly differ.

Table 4: Comparison of sample size, gender ratio, and radiological tool employed among different countries for the measuring the geometry of knee joint

Different countries	Sample size	Male	Female	Assessment tool
Saudi Arabia (present study)	150	40	110	MRI
China	50	29	21	CT
Caucasians	37	27	10	CT
Korea	202	88	114	CT
Turkey	200	100	100	MRI
Japan	179	25	154	CT
Germany	41	16	25	Digital caliper
France	256	122	134	CT
Brazil	118	33	84	Metal pachymeter
Malaysia	100	50	50	CT
India	47	21	26	CT

MRI: Magnetic resonance imaging, CT: Computed tomography

in earlier studies conducted in Chinese,[25] Caucasian,[25] Japanese,[26] Korean,[27] Germany,[15] France,[28] Brazil,[29] Turkey,[30] Malaysia,[31] and Indian[32] population.

Saudi males had lower tAP, tMAP, tLAP, fLAP, fMAP, fEW, fML, fMW, ICH, and femoral aspect ratio (ML/AP) than those of Chinese, Caucasian, Japan, Germany, France,

Brazil, Turkey, Malaysian, and Indian population. The tLAP value of males in Saudi Arabia was found to be larger than that of Korean. Similar results were seen with the fMW value of Saudi male and Korean male studied. The fLW value of Saudi males was less than that of Indian males. The tML value of Saudi males was found to be greater than that of Chinese and Caucasian reports, however this was lower in comparison to that exhibited by Korean, Japanese, Germany, Brazilian, and Turkey. Report on tML value was not available in France, Malaysia, and Indian studies. Similar results were seen in ICW values where this parameter was found to have higher value than Chinese, Caucasian, Korean, and German males; however, the result of similar parameters was not studied in the reports from Germany, France, Malaysia, Japan, and India.

Saudi females had lower value of a tMAP, tLAP, fMAP, and fLAP than the other compared reports. The fLW and fMW values for Saudi females were found to be higher in comparison to Korean and German females. The value of Saudi females was however very less than that of Indian females. Reports from the rest of the countries do not include data of fLW and fMW values for females.

The ICW of Saudi females was found to be greater than that of Chinese, Caucasian, Korean, Turkey, and German females, however reports from Japan, France, Brazil, Malaysia, and India do not include this parameter. The ICH of Saudi females was found to be smaller than that of Chinese, Caucasian, Korean, Turkey, and German females; however, reports from Japan, France, Brazil, Malaysia, and India do not include these parameters. The tAP value for Saudi females was found to be smaller than the reported values from all other countries except Germany and France which are otherwise not reported. Data of tML value for Saudi females were found to be greater than tML value from all other countries. The tML was significantly and positively correlated with the tMAP, while the aspect ratio (tML/tMAP) was significantly and negatively correlated with the tMAP. The epicondylar and fML value for Saudi females were lower in comparison to those from Turkey. However, this parameter was not studied in other countries. Based on the reported data, the femoral aspect ratio for females was calculated which comes to be lower for Saudi females than that of other countries, however due to lack of data, it could not be calculated for Korean females. The fML was significantly and positively correlated with the fMAP while the fML/fMAP was significantly and negatively correlated with the fMAP. It is also observed that gender showed significant differences in aspect ratio (tML/tMAP) and nationality showed significant differences in aspect ratio (tML/tMAP) in both males and females. These significant differences in aspect ratio can facilitate the tibial component of TKR prosthesis to be designed more specifically based on gender and ethnicity.

Conclusion

The study is a milestone in the rational designing of knee prostheses for the patients undergoing TKR. The study suggested that not only the TKA prosthesis design should consider the sex factor but also the nationality differences. The morphological differences of femora between Saudi and other countries males and females ($P < 0.001$) cannot be accounted by the differences in size alone, but also the shape variation between these nationalities. An overhanging prosthesis is more likely to cause soft-tissue imbalance and unfavorable patella-femoral stress distribution. It is often needed to downsize the femoral components during TKA operation to avoid this clinical overcome. However, this may also result in an undesirable complication. For example, notching of the anterior cortex can predispose to periprosthetic fractures and over resection of the posterior femoral condyles resulting in an imbalance between the flexion and extension gaps. Therefore, it is important to consider the morphological factor of the tibia and femur as a whole for the prosthesis design.

The limitations of the present study were a limited study population, a larger study population could have been far better in giving good comparison of study results, and could have been more effective as identical parameters were assessed using similar techniques such as MRI or computed tomography scan.

From the study, we can draw a conclusion that the MRI technique has emerged as a promising semi-quantitative and quantitative approaches for imaging the morphology of the knee. Still the comparison of similar parameters under nonenhanced MRI and contrast-enhanced MRI could enable more accurate assessment for the study of knee morphology.

Acknowledgment

All the authors of the research article are thankful to the Deanship of Scientific Research, Majmaah University, KSA, for giving us the support and opportunity to conduct this research. We also thank all the medical practitioners of King Khalid general hospital and Biostatician Dr. Waqas Sami from the College of Medicine, Majmaah University, KSA, and all the people who took part in this study.

Financial support and sponsorship

The authors are highly thankful to the Deanship of Scientific Research, Majmaah University, KSA for the financial assistance provided for the conduction of the present study under the project number: 1439-78.

Conflicts of interest

There are no conflicts of interest.

References

1. Neogi T. The epidemiology and impact of pain in osteoarthritis. Osteoarthritis Cartilage 2013;21:1145-53.

2. Palazzo C, Nguyen C, Lefevre-Colau MM, Rannou F, Poiraudeau S. Risk factors and burden of osteoarthritis. Ann Phys Rehabil Med 2016;59:134-8.
3. Singer SP, Dammerer D, Krismer M, Liebensteiner MC. Maximum lifetime body mass index is the appropriate predictor of knee and hip osteoarthritis. Arch Orthop Trauma Surg 2018;138:99-103.
4. Alrowaili MG. Magnetic resonance evaluation of knee osteoarthritis among the Saudi Population. Pak J Med Sci 2019;35:1575-81.
5. Urabe K, Miura H, Kuwano T, Matsuda S, Nagamine R, Sakai S, *et al*. Comparison between the shape of resected femoral sections and femoral prostheses used in total knee arthroplasty in Japanese patients: Simulation using three-dimensional computed tomography. J Knee Surg 2003;16:27-33.
6. Westrich GH, Haas SB, Insall JN, Frachie A. Resection specimen analysis of proximal tibial anatomy based on 100 total knee arthroplasty specimens. J Arthroplasty 1995;10:47-51.
7. Uehara K, Kadoya Y, Kobayashi A, Ohashi H, Yamano Y. Anthropometry of the proximal tibia to design a total knee prosthesis for the Japanese population. J Arthroplasty 2002;17:1028-32.
8. Shah DS, Ghyar R, Ravi B, Shetty V. 3D morphological study of the Indian arthritic knee: Comparison with other ethnic groups and conformity of current TKA implant. Open J Rheumatol Autoimmune Dis 2103;3:263-9.
9. Kim HA, Kim S, Seo YI, Choi HJ, Seong SC, Song YW, *et al*. The epidemiology of total knee replacement in South Korea: National registry data. Rheumatology (Oxford) 2008;47:88-91.
10. Jones GG, Logishetty K, Clarke S, Collins R, Jaere M, Harris S, *et al*. Do patient-specific instruments (PSI) for UKA allow non-expert surgeons to achieve the same saw cut accuracy as expert surgeons? Arch Orthop Trauma Surg 2018;138:1601-8.
11. Song Y, Zhu F, Lin F, Zhang F, Zhang S. Bone quality, and the combination and penetration of cement-bone interface: A comparative micro-CT study of osteoarthritis and rheumatoid arthritis. Medicine (Baltimore) 2018;97:e11987.
12. Metcalfe AJ, Ahearn N, Hassaballa MA, Parsons N, Ackroyd CE, Murray JR, *et al*. The Avon patellofemoral joint arthroplasty: Two- to 18-year results of a large single-centre cohort. Bone Joint J 2018;100-B: 1162-7.
13. Conley S, Rosenberg A, Crowninshield R. The female knee: Anatomic variations. J Am Acad Orthop Surg 2007;15 Suppl 1:S31-6.
14. Dai Y, Bischoff JE. Comprehensive assessment of tibial plateau morphology in total knee arthroplasty: Influence of shape and size on anthropometric variability. J Orthop Res 2013;31:1643-52.
15. Dargel J, Michael JW, Feiser J, Ivo R, Koebke J. Human knee joint anatomy revisited: Morphometry in the light of sex-specific total knee arthroplasty. J Arthroplasty 2011;26:346-53.
16. Ethgen O, Bruyère O, Richy F, Dardennes C, Reginster JY. Health-related quality of life in total hip and total knee arthroplasty. A qualitative and systematic review of the literature. J Bone Joint Surg Am 2004;86:963-74.
17. Gillespie RJ, Levine A, Fitzgerald SJ, Kolaczko J, DeMaio M, Marcus RE, *et al*. Gender differences in the anatomy of the distal femur. J Bone Joint Surg Br 2011;93:357-63.
18. Greene KA. Gender-specific design in total knee arthroplasty. J Arthroplasty 2007;22:27-31.
19. Guy SP, Farndon MA, Sidhom S, Al-Lami M, Bennett C, London NJ. Gender differences in distal femoral morphology and the role of gender specific implants in total knee replacement: A prospective clinical study. Knee 2012;19:28-31.
20. Hitt K, Shurman JR 2nd, Greene K, McCarthy J, Moskal J, Hoeman T, *et al*. Anthropometric measurements of the human knee: Correlation to the sizing of current knee arthroplasty systems. J Bone Joint Surg Am 2003;85-A Suppl 4:115-22.
21. Ho WP, Cheng CK, Liau JJ. Morphometrical measurements of resected surface of femurs in Chinese knees: Correlation to the sizing of current femoral implants. Knee 2006;13:12-4.
22. Hosaka K, Saito S, Ishii T, Mori S, Sumino T, Tokuhashi Y. Asian-specific total knee system: 5-14 year follow-up study. BMC Musculoskelet Disord 2011;12:251.
23. Hsu RW, Himeno S, Coventry MB, Chao EY. Normal axial alignment of the lower extremity and load-bearing distribution at the knee. Clin Orthop Relat Res 1990;255:215-27.
24. Fedorov A, Beichel R, Kalpathy-Cramer J, Finet J, Fillion-Robin JC, Pujol S, *et al*. 3D slicer as an image computing platform for the quantitative imaging network. Magn Reson Imaging 2012;30:1323-41.
25. Ma QL, Lipman JD, Cheng CK, Wang XN, Zhang YY, You B. A comparison between Chinese and Caucasian 3-Dimensional bony morphometry in presimulated and postsimulated osteotomy for total knee arthroplasty. J Arthroplasty 2017;32:2878-86.
26. Nishikawa M, Owaki H, Kaneshiro S, Fuji T. Preoperative morphometric differences in the distal femur are based on skeletal size in Japanese patients undergoing total knee arthroplasty. Knee Surg Sports Traumatol Arthrosc 2014;22:2962-8.
27. Cho HJ, Kwak DS, Kim IB. Morphometric evaluation of Korean femurs by geometric computation: Comparisons of the sex and the population. Biomed Res Int 2015;2015:1-9.
28. Cavaignac E, Savall F, Chantalat E, Faruch M, Reina N, Chiron P, *et al*. Geometric morphometric analysis reveals age-related differences in the distal femur of Europeans. J Exp Orthop 2017;4:21.
29. Loures FB, de Araújo Góes RF, da Palma IM, Labronici PJ, Granjeiro JM, Olej B. Anthropometric study of the knee and its correlation with the size of three implants available for arthroplasty. Rev Bras Ortop 2016;51:282-9.
30. Erkocak OF, Kucukdurmaz F, Sayar S, Erdil ME, Ceylan HH, Tuncay I. Anthropometric measurements of tibial plateau and correlation with the current tibial implants. Knee Surg Sports Traumatol Arthrosc 2016;24:2990-7.
31. Murshed KA, Ciçekcibaşi AE, Karabacakoğlu A, Seker M, Ziylan T. Distal femur morphometry: A gender and bilateral comparative study using magnetic resonance imaging. Surg Radiol Anat 2005;27:108-12.
32. Hussain F, Abdul Kadir MR, Zulkifly AH, Sa'at A, Aziz AA, Hossain G, *et al*. Anthropometric measurements of the human distal femur: A study of the adult Malay population. Biomed Res Int 2013;2013:1-5.

Original Article

Aberrant Right Subclavian Artery: A Multi-Detector Computed Tomography Study

C. S. Ramesh Babu, Om Prakash Gupta[1], Arjun Kumar[1]

Department of Anatomy, Muzaffarnagar Medical College, Muzaffarnagar, [1]Dr. O.P. Gupta Imaging Centre, Meerut, Uttar Pradesh, India

Abstract

Introduction: Aberrant right subclavian artery (ARSA) arises as the last branch of normally positioned aortic arch and its prevalence estimated as 0.16%–2.0% varies between different ethnic groups. Our aim was to assess the prevalence and associated branching anomalies of ARSA in the Indian participants. **Material and Methods:** Chest computed tomographic scans of 710 patients were analyzed to study the ARSA and its associated vascular anomalies. **Results:** We have observed 11 cases (5 in males and 6 in females) of ARSA with an estimated prevalence of 1.54%. In seven cases, there were four branches arising from the arch of aorta in the order of right common carotid, left common carotid, left subclavian, and aberrant right subclavian. In three cases, there were three branches – bicarotid trunk (common trunk of right and left carotids), left subclavian, and the aberrant right subclavian. In one case, there were five branches in the order of right common carotid, left common carotid, left vertebral, left subclavian, and aberrant right subclavian. Only two participants reported mild symptoms of dysphagia. In all the cases, the ARSA had retroesophageal course. Kommerell diverticulum was not observed. ARSA remain asymptomatic in most cases, but its presence should alert the clinician to look for associated vascular and any cardiac anomalies. **Discussion and Conclusion:** Awareness of the presence of ARSA is crucial for successful outcome of mediastinal, esophageal, and thoracic spine surgeries. Preprocedural computed tomography for the evaluation of aortic arch branching pattern will be beneficial for the successful performance of various surgical and radiological interventions.

Keywords: *Arteria lusoria, bicarotid trunk, dysphagia, retroesophageal right subclavian artery, variant aortic arch branching*

Introduction

Arch of aorta (AA) passes from right to left arching over the root of the left lung and gives three branches brachiocephalic trunk (BT) which further divides into right common carotid (RCCA) and right subclavian arteries (RSA), left common carotid artery (LCCA), and left subclavian artery (LSA) in that order from right to left. This normal branching pattern is reported to occur in 64.9%–94.3% of population.[1] A recent systematic review and meta-analysis of 23,882 arches from 51 articles by Popieluszko *et al*.(2018) found normal branching pattern in 80.9% cases (95% confidence interval [CI] 76.3–82.4).[2] Another review of 20,030 cases estimated the prevalence of normal branching pattern as 84.52%.[3] Increased attention is being paid to study variations in the branching pattern of aortic arch since the advent of surgical and radiological interventional procedures on supra-aortic branches. One of the common congenital anomaly of AA is the presence of aberrant right subclavian artery (ARSA), which arises as the last branch of the arch to the left of the spine and generally ascends between the esophagus and spine. In such cases, the BT is absent, and the RCCA arises as the first branch and ARSA as the last branch. Clinicians name it as "Arteria Lusoria." Although asymptomatic, its presence may cause dysphagia – Dysphagia lusoria. Reported prevalence is 0.16%–2.0% but varies widely between different ethnic groups.[4,5] This anomaly has a preponderance in females.[6,7] About 7%–10% of adults with this anomaly develop symptoms such as dysphagia, dyspnoea, retrosternal pain, chronic cough, and weight loss implying that this anomaly remains latent and innocuous in 90%–93% participants. It may be associated with some congenital anomalies such as patent ductus arteriosus, ventricular septal defect,

How to cite this article: Babu CS, Gupta OP, Kumar A. Aberrant right subclavian artery: A multi-detector computed tomography study. J Anat Soc India 2021;70:XX-XX.

Article Info

Received: 08 July 2020
Accepted: 08 February 2021
Available online: ***

Address for correspondence:
Prof. C. S. Ramesh Babu, Muzaffarnagar Medical College, N.H. 58, Opp. Begrajpur Industrial Area, Muzaffarnagar - 251 203, Uttar Pradesh, India.
E-mail: csrameshb@gmail.com

Access this article online

Website: www.jasi.org.in
DOI: 10.4103/JASI.JASI_129_20
Quick Response Code:

and conotruncal anomalies.[8] The most common vascular anomalies associated with ARSA include bicarotid trunk (BCT) (common origin of both RCCA and LCCA), aortic arch origin of left vertebral artery (LVA), and Kommerell's diverticulum.[6]

Different types of aortic arch branching pattern associated with ARSA have been reported in the literature which is classified into three types by Adachi-Williams. In Type I or Type G, four branches arise from the arch in the order of RCCA, LCCA, LSA, and ARSA [Figure 1a]. In Type II or Type CG, five branches arise from the arch in the order of RCCA, LCCA, LVA, LSA, and ARSA [Figure 1b]. In Type III or Type H, three branched pattern is seen with BCT, LSA followed by ARSA [Figure 1c].[5]

Our aim was to assess the prevalence and associated branching anomalies of ARSA in Indian participants by contrast-enhanced multi-detector computed tomography (CT). Most of the Indian studies are cadaveric studies and case reports. Only few radiological reports are available. Hence, the present, retrospective, observational study was undertaken.

Material and Methods

This retrospective observational study was done in 710 participants (males – 435 and females – 275) who underwent contrast-enhanced CT chest examination for various suspected lung and mediastinal pathologies during the period September 2015 to March 2018. The scans of the patients with malignancies likely to distort the anatomy of aorta and supra-aortic branches, poorly enhanced scans, and those with thoracic aortic disease were excluded leaving 710 participants suitable for the study. The imaging center routinely obtains informed consent before contrast injection. Volume rendered images and maximum intensity projection were obtained from the axial scans. The presence of ARSA, its course and relationship with esophagus, and associated vascular anomalies was noted.

Results

In 11 participants (males – 5 and females – 6) ARSA was noted arising as the last branch of the AA (1.54%; 11/710). Type I (Type G) which can be described as an isolated ARSA was observed in seven participants (males – 2 and females – 5) (0.98%; 7/710) [Figure 2]. Although overall incidence did not show much gender difference, the isolated ARSA has a predominance in females. In three participants (males-2; female-1) Type III (Type H) with BCT, LSA and ARSA was noted (0.42%; 3/710) [Figures 3 and 4]. In a male subject Type II (Type CG) was seen with the sequence of RCCA, LCCA, LVA, LSA, and ARSA (0.14%; 1/710) [Figure 5]. In all cases, ARSA had a retroesophageal course crossing the spine obliquely from left to right [Figure 6]. Kommerell's diverticulum was not observed in our study. In one case, the ARSA made an indentation in the esophagus and trachea [Figure 7]. Only two patients reported mild symptoms of dysphagia.

Discussion

ARSA, also named as retroesophageal right subclavian artery, arteria lusoria, arteria subclavia dextra lusoria, is a more frequently encountered congenital anomaly of aortic arch predominantly observed in females. Its presence is generally detected incidentally in cadaveric and autopsy studies, barium esophagogram, upper GI endoscopy, and many radiological modalities (such as conventional angiography, CT and magnetic resonance (MR) angiography, endoscopic ultrasound, endobronchial ultrasound, and transesophageal echocardiography). Developmentally, the aortic arch and its branches develop from pharyngeal arch arteries which appear symmetrically in the pharyngeal arches. Normally, the AA develops from left aortic sac, left fourth arch artery, and part of left dorsal aorta. Right subclavian artery develops from right fourth arch artery, proximal part of right dorsal aorta, and right seventh intersegmental artery. The part of right dorsal aorta

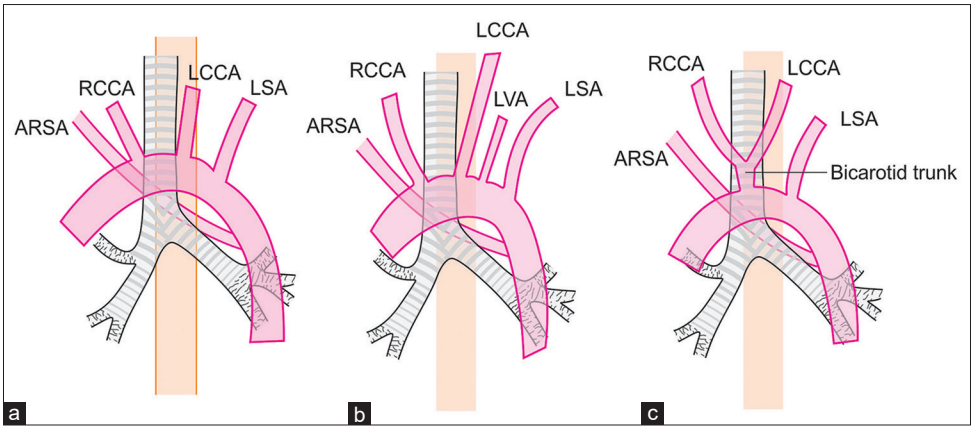

Figure 1: Schematic figure showing Adachi-William's classification of aberrant right subclavian artery. (a) Type I (Type-G) Four branched pattern in the sequence of RCCA, left common carotid artery, left subclavian artery and Aberrant right subclavian artery. (b) Type II (Type CG) Similar to Type I but with additional branch left vertebral artery arising in between the origin of left common carotid artery and left subclavian artery. (c) Type III (Type H) with three branches– the bicarotid trunk (common trunk of both common carotids), left subclavian artery and aberrant right subclavian artery

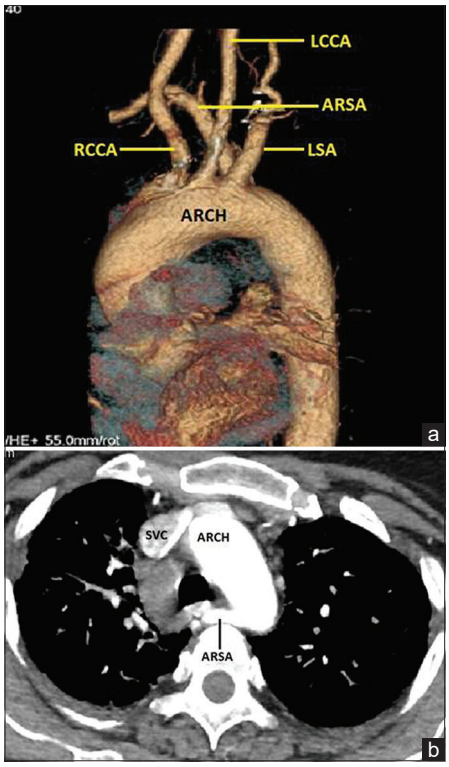

Figure 2: (a) Volume rendered image showing Type I Aberrant right subclavian artery with four branches from aortic arch. Note the absence of brachiocephalic trunk and the direct arch origin of right common carotid (RCCA) as the first branch. (b) Axial image showing the aberrant right subclavian artery passing to the right behind the esophagus. SVC: Superior vena cava

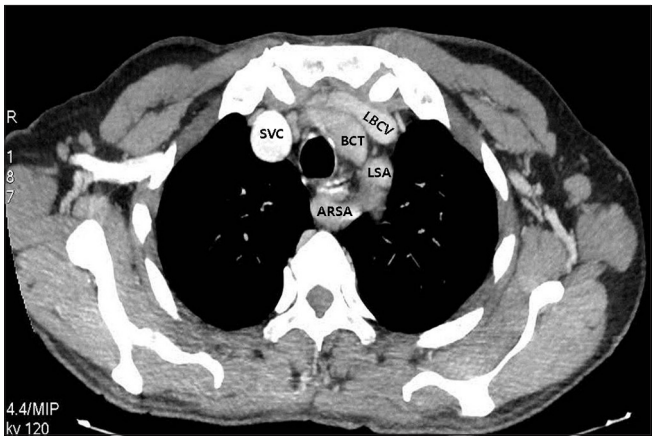

Figure 4: Axial image showing Type III Aberrant right subclavian artery with bicarotid trunk, left subclavian artery and aberrant right subclavian artery sequence. Note the position of aberrant right subclavian artery between the esophagus and the vertebral body. SVC: Superior vena cava, LBCV: Left brachiocephalic vein

distal to seventh intersegmental artery normally involutes. Abnormal involution of the right fourth arch artery and proximal right dorsal aorta and persistence of distal part of right dorsal aorta gives rise to ARSA as the last branch of AA [Figure 8].

A recent systematic review and meta-analysis of 51 articles comprising 23,882 arches indicated that overall incidence

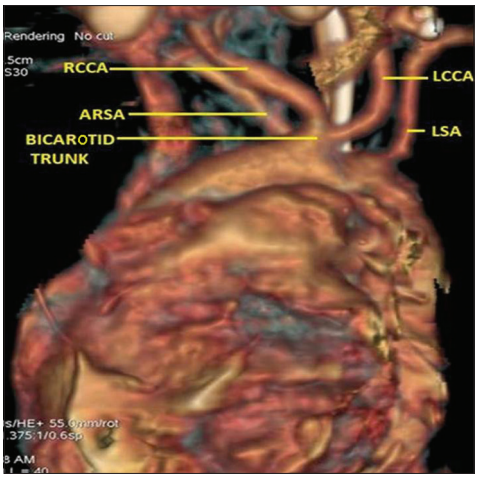

Figure 3: Volume rendered image showing Type III Aberrant right subclavian artery with the Bicarotid trunk as the first branch followed by left subclavian artery and aberrant right subclavian artery

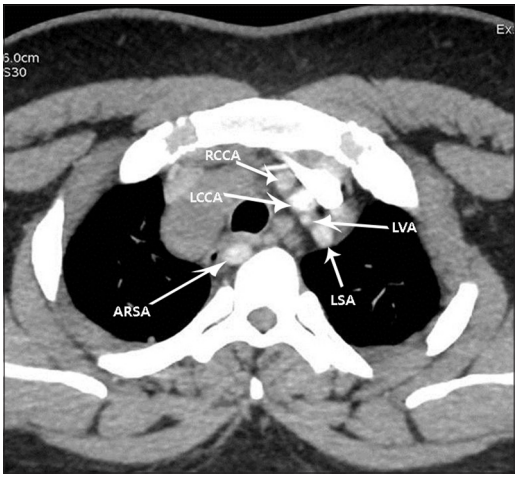

Figure 5: Axial image showing Type II aberrant right subclavian artery with five branched pattern and presence of left vertebral artery between left common carotid artery and left subclavian artery. Aberrant right subclavian artery is passing to the right behind esophagus

of ARSA is 0.7% (95% CI is 0.2%–1.5%). If only imaging studies are included (32 articles, 20141 cases), the incidence is 0.9% (95% CI is 0.2–1.8), and in cadaveric studies (20 articles, 3740 cases), the incidence is 1.0% (95% CI 0.0–3.3).[2] Another systematic review analyzing 20,030 cases reported an incidence of 0.91% (183/20,030) out of which 176 cases had isolated ARSA and seven cases were accompanied by secondary arteries from the arch.[3] The present study reports a prevalence of 1.54% (11/710), which is within the range estimated by meta-analysis. The prevalence of ARSA exhibits racial differences and country-wise prevalence by radiological studies is given in Table 1.

Natsis *et al*. in their study on 267 Greek cadavers reported a prevalence of 2.2% (6/267), and in one cadaver, the ARSA had a course between the trachea and esophagus.[36] Reviewing 15 cadaveric studies initially, they estimated the incidence of ARSA as ranging from 0.2% to 13.3% but later

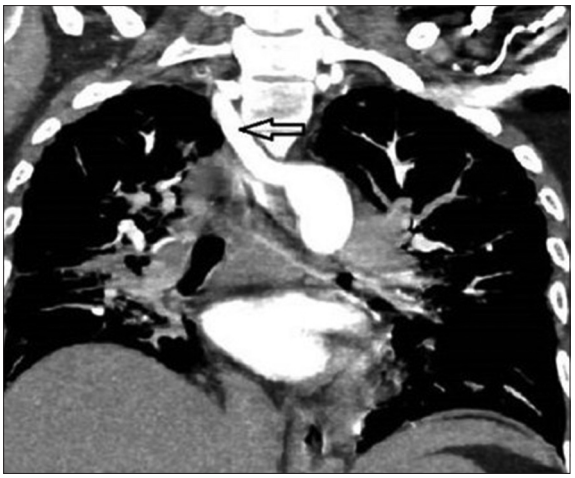

Figure 6: Coronal section showing the oblique course of aberrant right subclavian artery (arrow) in front of the spine to reach the right side

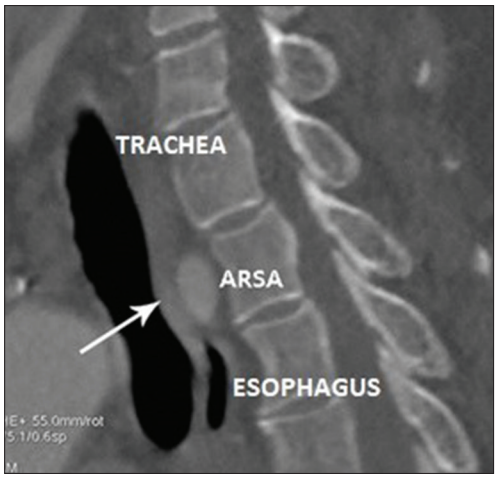

Figure 7: Sagittal section in bone window showing aberrant right subclavian artery causing an indentation (arrow) in the esophagus and trachea

modified it to 1.2% (range 0.19%–2.5%) after exclusion of four studies.[36,37] Polednak using meta-analysis estimated the unweighted prevalence as 1.23% and pooled prevalence as 1.30% (95% CI 0.86%–1.82%).[38] Extracting data from the published reports Molz and Burri found a prevalence of 0.7% (593 ARSAs out of 68,049 autopsy cases) and 2.3% (517/22,201 patients).[7] Country-wise prevalence of ARSA in cadaveric studies is given in Table 2.

ARSA also shows gender differences in its prevalence as suggested by published literature. Polguj *et al*. analyzing 141 published reports suggested that gender distribution was 55.3% in females and 44.7% in males.[6] It is also suggested that isolated ARSA shows 58%–75% female predominance.[7] In our study also isolated ARSA has a female predominance (5 female versus 2 male).

One of the vascular anomaly most commonly associated with ARSA is the presence of BCT, present in 19.2% (27/141) cases with ARSA[6] This is classified as Type III (Type H) and its estimated prevalence is <0.05%.[47] We have observed this type in three participants (Male 2; Female-1; 0.42%). Natsis *et al*. reported two cases of this variant, both in males, in a study involving 72 Greek cadavers (2.78%; 2/72) and reviewed the earlier literature.[48] The combination of BCT with ARSA is mainly reported as case reports.[49-51] Gluncic and Marusic reported the presence of BCT, common trunk of left subclavian and left vertebral followed by ARSA in a female cadaver.[52] In another case report, the sequence of LSA as first branch, then BCT followed by ARSA was observed in a female patient.[53] It must be noted that the sequence of RSA, BCT, and LSA is also observed as a variant branching pattern of aortic arch.

Another rare vascular anomaly associated with ARSA is the five-branched pattern with RCCA, LCCA, LVA, LSA, and ARSA classified as Type II (Type CG) observed in 1 male patient (0.14%). This type was found in two cases (2/2370) by Wang *et al*.[29] and two cases (2/3460) by Choi *et al*.[34] In a cadaveric case report, an accessory LVA was found to arise directly from the aortic arch proximal to ARSA and the normal LVA from LSA was hypoplastic.[54] MR angiography of a female patient revealed a very rare branching pattern with BCT, LVA, LSA, and ARSA, and in this case, the right vertebral artery arose from RCCA.[55] Tsai *et al*. investigated the anomalies of vertebral and common carotid arteries in 102 patients with ARSA. They reported vertebral artery anomalies in 15.7% cases (16/102 patients) and common carotid trunk (BCT) in 20.6% cases (21/102 patients). They also noted that in 84.3% (86/102 patients) cases both vertebral arteries had normal origin from corresponding subclavian arteries.[56] In a most recent review, Plotkin *et al*. analyzed the data of 312 patients having aberrant subclavian arteries (both right and left) and studied the associated vascular anomalies and aortic pathology. The study included 281 ARSA patients and 31 aberrant LSA (ALSA) patients. In ARSA group the LVA had direct arch origin in 9 patients only and subclavian artery origin in 271 cases. On the contrary, in ALSA group, the LVA arose from LSA in all cases.[57]

Kommerell diverticulum (KD) appears as a dilatation at the origin of the ARSA and coexist in 14.9% cases.[6] In our study, none of the 11 patients exhibited KD. It was observed that KD was more common in men with aberrant subclavian arteries and was more frequently associated with ALSA in comparison to ARSA.[57]

Clinical implications

Awareness of the presence of ARSA is crucial for successful outcome of mediastinal, esophageal, and thoracic spine surgeries. Association with Kommerell's diverticulum and aneurysm of the diverticulum is a high-risk feature. The presence of this variant makes right radial artery approach for cardiac catheterization extremely difficult and unsuccessful. Manipulation of endoscopes and other instruments through the esophagus may damage this aberrant vessel leading to catastrophic

Table 1: Incidence of aberrant right subclavian artery in radiological studies

Author, year	Modality of study	Country	Total number of cases	Number of ARSA (%)	Gender distribution	Any associated anomaly
Haesemeyer and Gavant, 1999[9]	MDCT	USA	7174	29 (0.4)		
De Luca *et al*. 2000[10]	EUS	Netherlands	3334	12 (0.36)	Male=6; female=6	
Abhaichand *et al*. 2001[11]	Coronary angiography	France	3730	11 (0.3)		
Kelly 2007[12]	Gastroscopy	Great Britain	920	1 (0.11)		
Yusuf *et al*. 2007[4]	EUS	USA	7513	27 (0.36)	Male=10; female=17	KD in 1 case
Nie *et al*. 2009[13]	Angiography	China	3000	3 (0.1)		
Natsis *et al*. 2009[1]	Angiography	Greece	622	1 (0.16)	Male=1	
Berko *et al*. 2009[14]	MDCT	USA	1000	12 (1.2)		
Piyavisetpat *et al*. 2011[15]	MDCT	Thailand	687	9 (1.31)	Male=2; female=7	One case with BCT
Muller *et al*. 2011[16]	CT	Germany	2033	20 (1.0)		
Sunitha and Narasinga Rao 2012[17]	CT angiography	India	300	1 (0.33)		
Mata-Escolanto *et al*. 2012[18]	MDCT	Spain	900	4 (0.44)		
Celikyay *et al*. 2013[19]	MDCT	Turkey	1136	8 (0.70)		
Uchino *et al*. 2013[20]	MDCT	Japan	2352	11 (0.47)		BCT=4
Shakeri *et al*. 2013[21]	CT	Iran	503	2 (0.4)		
Basti and Kumar, 2014[22]	MDCT	India	306	1 (0.3)		
Rea *et al*. 2014[23]	MDCT	Italy	1359	4 (0.5)		
Karacan *et al*.[24]	MDCT	Turkey	1000	13 (1.3)	Male=3; female=10	BCT=7
Lale *et al*. 2014[25]	MDCT	Turkey	881	17 (1.9)	Male=6; female=11	
Boyaci et al. 2015[26]	MDCT	Turkey	1170	26 (2.2)	Male=18; female=8	
Ergun *et al*. 2015[27]	Angiography	Turkey	270	3 (1.1)		
Tapia *et al*. 2015[28]	CT	China	1050	4 (0.38)	Male=3; female=1	
Wang *et al*. 2016[29]	CECT	China	2370	18 (0.75)	Male=7; female=11	BCT=5 LVA=2
Jalali Kondori *et al*. 2016[30]	MRA	Iran	226	4 (1.8)		
Sankhe *et al*. 2016[31]	MDCT	India	830	5 (0.6)	Male=1; female=4	
Skouroumouni *et al*. 2017[32]	MDCT	Greece	6488	38 (0.59)	Male=13; female=25	KD=10 BCT=12
Krupiński *et al*. 2019[33]	MDCT	Poland	6833	32 (0.47)	Male=13; female=19	KD=9 cases BCT=9 cases
Choi *et al*. 2019[34]	MDCT	Korea	3460	17 (0.49)	Male=4; female=13	KD=9 cases BCT=10 cases LVA=2 cases
Krishnan *et al*. 2019[35]	CECT	India	1116	8 (0.7)		BCT=4
Present study, 2020	MDCT	India	710	11 (1.54)	Male=5; female=6	BCT=3; LVA=1

ARSA: Aberrant right subclavian artery, MDCT: Multidetector-row computed tomography, EUS: Endoscopic ultrasound, CT: Computed tomography, KD: Kommerell diverticulum, BCT: Bicarotid trunk, LVA: Left vertebral artery

bleeding. Pathological formation of arterio-esophageal fistula leads to life-threatening upper GI bleeding. This anomaly is associated with nonrecurrent inferior laryngeal nerve whose presence can complicate thyroid, parathyroid, and lower neck surgeries. May be associated with Di George syndrome, Trisomy-21 and some congenital cardiac anomalies such as tetralogy of Fallot and conotruncal anomalies. It has also been suggested that the presence of aberrant subclavian artery is an anatomical marker for 22.q11 deletion syndrome.

Conclusion

Recent application of various endovascular, surgical, neurological, and radiological interventional procedures

Table 2: Incidence of aberrant right subclavian artery in cadaveric studies globally

Author, year	Country	Total number of cases	Number of ARSA (%)	Gender distribution	Associated anomalies
Zapata *et al*. 1993[39]	USA	6898 (without CHD)	11 (0.15)		
		4102 (with CHD)	117 (2.9)		
		Total/11,000	128 (1.2)		
Saito *et al*. 2005[40]	Japan	516	1 (0.2)		
Nayak *et al*. 2006[41]	India	62	1 (1.6)		
Poonam *et al*. 2013[42]	India	45	1 (2.2)		
Chavda *et al*. 2014[43]	India	70	1 (1.4)		
Panchal *et al*. 2017[44]	India	67	1 (1.5)		
Natsis *et al*. 2017[36]	Greece	267	6 (2.2)	Male=2; female=4	BCT=2 KD=2
Qiu *et al*. 2019[45]	China	120	5 (4.1)	Male=4; female=1	
Keet *et al*. 2019[46]	South Africa	733	11 (1.5)		

ARSA: Aberrant right subclavian artery, KD: Kommerell diverticulum, BCT: Bicarotid trunk, CHD: Congenital heart disease

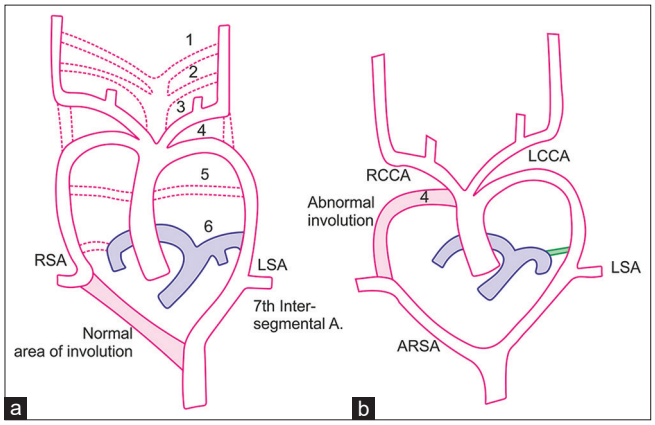

Figure 8: Schematic diagram showing the developmental basis of aberrant right subclavian artery. (a) Normal development of right subclavian artery from right fourth arch artery, proximal right dorsal aorta and right seventh intersegmental artery. The distal part of right dorsal aorta normally involutes. Left fourth arch artery along with left dorsal aorta forms arch of aorta and left seventh intersegmental artery develops into left subclavian artery. Parts which disappear are shown in dotted lines. (b) Aberrant right subclavian artery develops due to abnormal involution of right fourth arch artery and proximal right dorsal aorta and persistence of distal right dorsal aorta. The common carotid arteries develop from proximal part of respective third arch arteries

has kindled interest to evaluate branching pattern variations of aortic arch. ARSA is generally detected incidentally and its presence should alert the clinician to look for any associated vascular and cardiac anomalies. Multi-detector CT is the modality of choice as it accurately depicts vascular anomalies and can be used before planning any interventions.

Acknowledgment

The authors acknowledge the technical assistance rendered by Mr. Sushil Kumar of Muzaffarnagar Medical College, Muzaffarnagar and Mr. Pran Prakash of Jaswant Rai Superspeciality Hospital, Meerut in preparation of images.

Financial support and sponsorship

Nil.

Conflicts of interest

There are no conflicts of interest.

References

1. Natsis KI, Tsitouridis IA, Didagelos MV, Fillipidis AA, Vlasis KG, Tsikaras PD. Anatomical variations in the branches of the human aortic arch in 633 angiographies: Clinical significance and literature review. Surg Radiol Anat 2009;31:319-23.
2. Popieluszko P, Henry BM, Sanna B, Hsieh WC, Saganiak K, Pękala PA, *et al*. A systematic review and meta-analysis of variations in branching patterns of the adult aortic arch. J Vasc Surg 2018;68:298-306.
3. Recto C, Boddi M, Branco JJ, Morucci G, Pacini A, Gulisano M, *et al*. Aortic arch branching pattern variation: Its incidence on a 20030 cases review. Italian J Anat Embryol 2019;124:5-15.
4. Yusuf TE, Levy MJ, Wiersema MJ, Clain JE, Harewood GC, Rajan E, *et al*. Utility of endoscopic ultrasound in the diagnosis of aberrant right subclavian artery. J Gastroenterol Hepatol 2007;22:1717-21.
5. Polguj M, Stefanczyk L, Topol M. The epidemiological, morphological and clinical aspects of the aberrant right subclavian artery (Arteria lusoria). Intech 2016. [doi: 10.5772/64604].
6. Polguj M, Chrzanowski L, Kasprzak JD, Stefanczyk L, Topol M, Majos A. The aberrant right subclavian artery (Arterial lusoria): The morphological and clinical aspects of one of the most important variations – A systematic study of 141 reports. ScientificWorldJournal 2014;2014:292734.
7. Molz G, Burri B. Aberrant subclavian artery (Arteria lusoria): Sex differences in the prevalence of various forms of the malformation. Evaluation of 1378 observations. Virchows Arch A Pathol Anat Histol 1978;380:303-15.
8. Priya S, Thomas R, Nagpal P, Sharma A, Steigner M. Congenital anomalies of the aortic arch. Cardiovasc Diagn Ther 2018;8:S26-44.
9. Haesemeyer SW, Gavant ML. Imaging of acute traumatic aortic tear in patients with an aberrant right subclavian artery. Am J Roentgenol 1999;172:117-20.
10. De Luca L, Bergman JJ, Tytgat GN, Fockens P. EUS imaging of the arteria lusoria: Case series and review. Gastrointest Endosc 2000;52:670-3.
11. Abhaichand RK, Louvard Y, Gobeil JF, Loubeyre C, Lefèvre T, Morice MC. The problem of arteria lusoria in right transradial

coronary angiography and angioplasty. Catheter Cardiovasc Interv 2001;54:196-201.
12. Kelly MD. Endoscopy and the aberrant right subclavian artery. Am Surg 2007;73:1259-61.
13. Nie B, Zhou YJ, Li GZ, Shi DM, Wang JL. Clinical study of arterial anatomic variations for transradial coronary procedure in Chinese population. Chin Med J (Engl) 2009;122:2097-102.
14. Berko NS, Jain VR, Godelman A, Stein EG, Ghosh S, Haramati LB. Variants and anomalies of thoracic vasculature on computed tomographic angiography in adults. J Comput Assist Tomogra 2009;33:523-8.
15. Piyavisetpat N, Thaksinawisut P, Tuinkosit M. Aortic arch branches' variations detected on chest CT. Asian Biomed 2011;5:817-23.
16. Muller M, Schimtz BL, Pauls S, Schick M, Rohrer S, Kappa T, *et al*. Variations of the aortic arch – A study on the most common branching patterns. Acta Radiol 2011;52:738-42.
17. Sunitha V, Narasinga Rao B. A study on the anatomical organization of the aortic arch anomalies. J Clin Diagn Res 2012;6:1127-31.
18. Mata-Escolanto F, Aparicio-Bellver L, Matinez-Sanjuan V, Sanchis-Gimeno JA. Aortic branch variations: An anatomical study in 900 subjects. Sci Res Essays 2012;7:2213-7.
19. Celikyay ZR, Koner AE, Celikyay F, Denız C, Acu B, Firat MM. Frequency and imaging findings of variations in human aortic arch anatomy based on multidetector computed tomography data. Clin Imaging 2013;37:1011-9.
20. Uchino A, Saito N, Okada Y, Kozawa E, Nishi N, Mizukoshi W, *et al*. Variation of the origin of the left common carotid artery diagnosed by CT angiography. Surg Radiol Anat 2013;35:339-42.
21. Shakeri A, Pourisa M, Deldar A, Goldust M. Anatomical variations of aortic arch branches and relationship with diameter of the aortic arch by 64-row CT angiography. Pak J Biol Sci 2013;16:496-500.
22. Basti RS, Kumar S. Evaluation of anatomical variations in the aortic arch branching pattern in south Indian population using computed tomography. Int J Recent Trends Sci Technol 2014;12:280-4.
23. Rea G, Valente T, Iaselli F, Urraro F, Izzo A, Sica G, *et al*. Multi-detector computed tomography in the evaluation of variants and anomalies of aortic arch and its branching pattern. Ital J Anat Embryol 2014;119:180-92.
24. Karacan A, Türkvatan A, Karacan K. Anatomical variations of aortic arch branching: Evaluation with computed tomographic angiography. Cardiol Young 2014;24:485-93.
25. Lale P, Toprak U, Yagiz G, Kaya T, Uyanik SA. Variations in the branching pattern of the aortic arch detected with computerized tomography angiography. Adv Radiol 2014;2014:969728.
26. Boyaci N, Dokumaci DS, Karakas E, Yildiz S, Cece H, Kocarslan A, *et al*. Multidetector computed tomography evaluation of aortic arch and branching variants. Turk Gogus Kalp Dama 2015;23:51-7.
27. Ergun O, Tatar İG, Birgi E, Durmaz HA, Akçalar S, Kurt A, *et al*. Angiographic evaluation of branching pattern and anatomy of the aortic arch. Turk Kardiyol Dern Ars 2015;43:219-26.
28. Tapia GP, Zhu X, Xu J, Liang P, Su G, Liu H, *et al*. Incidence of branching patterns variations of the arch in aortic dissection in Chinese patients. Medicine (Baltimore) 2015;94:e795.
29. Wang L, Zhang J, Xin S. Morphologic features of the aortic arch and its branches in the adult Chinese population. J Vasc Surg 2016;64:1602-80.
30. Jalali Kondori B, Asadi MH, Rahimian E, Tahsini MR. Anatomical variations in aortic arch branching pattern. Arch Iran Med 2016;19:72-4.
31. Sankhe AP, Ukirde V, Gomes CV, Pai S, Kulkarni S. MDCT evaluation of variations in branching patterns of aortic arch: Study of 830 Indian patients. Int J Biomed Adv Res 2016;7:329-36.
32. Skouroumouni G, Panagiotidou D, Lelegianni M, Stratilati S, Tsitouridis I, Thessaloniki GR. Aberrant right subclavian artery as an incidental finding in chest MDCT: Evaluation and imaging features. ECR 2017:C-0983. [doi: 10.1594/ecr2017/C-0983].
33. Krupiński M, Irzyk M, Moczulski Z, Banyś R, Dwojak I, Urbańczyk-Zawadzka M. CT evaluation of aberrant right subclavian artery: Anatomy and clinical implications. Cardiol Young 2019;29:128-32.
34. Choi Y, Chung SB, Kim MS. Prevalence and anatomy of aberrant right subclavian artery evaluated by computed tomographic angiography at a single institution in Korea. J Korean Neurosurg Soc 2019;62:175-82.
35. Krishnan VK, Narayan V, Ibrahim N, Mathew J, James SM. Imaging spectrum and prevalence of variant branching pattern of aortic arch. Int J Res Med Sci 2019;7:1313-8.
36. Natsis K, Didagelos M, Gkiouliava A, Lazaridis N, Vyzas V, Piagkou M. The aberrant right subclavian artery: Cadaveric study and literature review. Surg Radiol Anat 2017;39:559-65.
37. Natsis K, Didagelos M, Gkiouliava A, Lazaridis N, Vyzas V, Piagkou M. Erratum to: The aberrant right subclavian artery: Cadaveric study and literature review. Surg Radiol Anat 2017;39:1181-2.
38. Polednak AP. Prevalence of the aberrant right subclavian artery reported in a published systematic review of cadaveric studies: The impact of an outlier. Clin Anat 2017;30:1024-8.
39. Zapata H, Edwards JE, Titus JL. Aberrant right subclavian artery with left aortic arch: Associated cardiac anomalies. Pediatr Cardiol 1993;14:159-61.
40. Saito T, Tamatsukuri Y, Hitosugi T, Miyakawa K, Shimizu T, Oi Y, *et al*. Three cases of retroesophageal right subclavian artery. J Nippon Med Sch 2005;72:375-82.
41. Nayak SR, Pai MM, Prabhu LV, D'Costa S, Shetty P. Anatomical organization of aortic arch variations in the India: Embryological basis and review. J Vasc Bras 2006;5:95-100.
42. Poonam Jyoti N, Singla RK. Prevalence of retroesophageal right subclavian artery. Int J Biol Med Res 2013;4:3422-25.
43. Chavda H, Varlekar P, Khatri C, Saiyad SS, Bhatt R. Abnormal origin of right subclavian artery – A cadaveric study. Int J Med Sci Public Health 2014;3:85-8.
44. Panchal P, Prasad A, Singh S, Bhadain PP, Kumari R. A study of variations of subclavian artery and its clinical implication. Int J Med Sci Public Health 2017;6:1610-3.
45. Qiu Y, Wu X, Zhuang Z, Li X, Zhu L, Huang C, *et al*. Anatomical variations of the aortic arch branches in a sample of Chinese cadavers: Embryological basis and literature review. Interact Cardiovasc Thorac Surg 2019;28:622-8.
46. Keet K, Gunston G, Alexander R. Variations in the branching pattern of the aortic arch: An African perspective. Eur J Anat 2019;23:91-102.
47. Hanzic N, Cizmarevic U, Lesjak V, Caf P. Aberrant right subclavian artery with a bicarotid trunk: The importance of diagnosing this rare incidental anomaly. Cureus II 2019;11:e6094.
48. Natsis K, Didagelos M, Manoli SM, Papathanasiou E, Sofidis G, Anastasopoulos N. A bicarotid trunk in association with an aberrant right subclavian artery. Report of two cases, clinical impact, and review of the literature. Folia Morphol (Warsz) 2011;70:68-73.
49. Welsh P, Lucacin C, Hockley S. The simultaneous presence of

a bicarotid trunk and a retroesophageal right subclavian artery: A case report with clinical impact. Eur J Anat 2015;19:381-5.
50. Kumar S, Kumar P. Truncus bicaroticus with aberrant right subclavian artery and origin of right vertebral from right common carotid artery. Surg Radiol Anat 2014;36:829-31.
51. Keet K, Gunston G. An unusual case of three branches arising from the aortic arch: Bicarotid trunk, left subclavian artery and aberrant right subclavian artery. Eur J Anat 2018;22:429-32.
52. Gluncic V, Marusic A. Association of the truncus bicaroticus, common trunk of the left subclavian and vertebral arteries and retroesophageal right subclavian artery. Ann Anat 2000;182:281-3.
53. Turkbey B, Hazirolan T, Canyigit M, Peynircioglu B, Cil BE. Coexistence of aberrant right subclavian artery and common carotid trunk: Diagnosis with CT angiography. Eur J Radiol Extra 2007;62:63-4.
54. Granite G, Meshida K, Jones S. Rare case of five branched aortic arch exhibiting a retroesophageal right subclavian artery and an accessory left vertebral artery. Int J Anat Var 2018;11:117-22.
55. Velioglu M, Kaya S, Ertugrul EE. Arteries get confused: An arch variation. JBR-BTR 2014;97:28-9.
56. Tsai IC, Tzeng WS, Lee T, Jan SL, Fu YC, Chen MC, *et al*. Vertebral and carotid artery anomalies in patients with aberrant right subclavian arteries. Pediatr Radiol 2007;37:1007-12.
57. Plotkin A, Ng B, Han SM, Weaver FA, Han SW, Bowdish ME, *et al*. Association of aberrant subclavian arteries with aortic pathology and proposed classification system. J Vasc Surg 2020;7:1534-43.

Original Article

Estimation of Gestational Age by Ultrasound Measurement of Fetal Transcerebellar Diameter

Abstract

Introduction: Transcerebellar diameter (TCD) normogram predicts gestational age (GA) with an accuracy of 94% in the third trimester. The study aims to evaluate the application and accuracy of Transcerebellar diameter in determining the GA of the fetus and Its Correlation. **Material and Methods:** A cross-sectional prospective study conducted to determine the different antenatal ultrasound examinations were performed in 100 normal healthy pregnant with single fetus women having between 25 and 32 weeks of gestation. **Results:** Mothers mean GA on ultrasound was 28.4 ± 0.75 (27–30.2) weeks. The mean fetal biometry parameters including biparietal diameter (BPD) was 73 ± 2.3 mm (67–80), head circumference (HC) was 264 ± 8.7 mm (237.8–311), abdominal circumference (AC) was 244 ± 8.9 mm (226.6–265.9), femur length (FL) was 55 ± 2.1 mm (49.5–59.6), fetal heart rate was 149 ± 8.5 beats (121–175). The mean transcerebellar (TCD) measurement was 31 ± 1.1 mm. The correlation coefficient between the period of gestation and TCD was found to be 0.99 at 27–30 weeks which was statistically significant ($P < 0.001$) ($r > 0.99$). **Discussion and Conclusion:** From the present study, it was observed that the TCD increases linearly with GA. The correlation between GA and the GA by TCD seems to increase from 28 to 30 weeks. There is a good correlation between GA derived from TCD and from established biometric indices like BPD, HC, AC, and femur length.

Keywords: *Biparietal diameter, femur length, gestational age, head circumference, transcerebellar diameter, ultrasound*

Maheswari Cinnusamy[1], Deepti Shastri[2], Josephine Arokia Martina[3]

[1]Department of Anatomy, Vinayaka Missions Research Foundation (Deemed to be University), [2]Department of Anatomy, Vinayaka Missions Kirubananda Variyar Medical College, [3]Arogya Madha Hospital, Salem, Tamil Nadu, India

Introduction

The accurate understanding of gestational age (GA) is a keystone in an obstetrician's ability for antepartum care and management. Failure can result in iatrogenic prematurity which is connected with increased perinatal morbidity and mortality.[1] Ultrasonography of fetal measurements is highly reliable in the first and second trimester of pregnancy, but the reliability of any ultrasound method greatly diminishes as gestation advances. In the third trimester, the reliability of any single ultrasound parameter is poor.[1-3]

Since the last decade, ultrasound parameter transcerebellar diameter (TCD)' is considered a reliable predictor for GA in the third trimester.[4-8] Size of the cerebellum is less affected by deviation in feta growth restriction or growth acceleration.[6-9] The predicted GA by TCD between 22 and 28 weeks is within 0–2 days, between 29 and 36 weeks is within 5 days and at 37 weeks is 9 days of actual gestation. TCD nomogram predicts GA with the accuracy of 94% in the third trimester.[8,9]

TCD is one such nontraditional parameter for estimating GA under study. It is easy to identify and measure. It is strongly correlated to GA. This parameter is particularly useful in the prediction of GA in patients who are unsure of dates or suspected of having intrauterine growth restriction and it is a standard against which other parameters can be compared.

A true estimation of GA plays an important role in quality maternity care such as assessment of fetal growth and to schedule the delivery date. Any inaccurate estimation may lead to perinatal morbidity and mortality due to iatrogenic pre-or post-maturity. About 30% of women forget their accurate LMP or misunderstand early pregnancy bleeding as normal menses. GA can be estimated in the first trimester by ultrasonic measurement of diameter and volume of gestational sac as well as crown-rump length. Furthermore, other biometric indices such as fetal biparietal diameter (BPD), femur length (FL),

How to cite this article: Cinnusamy M, Shastri D, Martina JA. Estimation of gestational age by ultrasound measurement of fetal transcerebellar diameter. J Anat Soc India 2021;70:XX-XX.

Article Info

Received: 13 August 2020
Accepted: 22 February 2021
Available online: ***

Address for correspondence:
Dr. Maheswari Cinnusamy, Department of Anatomy, Vinayaka Missions Research Foundation (Deemed to be University), Ariyanoor, Salem - 636 308, Tamil Nadu, India.
E-mail: ravicra@gmail.com

Access this article online

Website: www.jasi.org.in
DOI: 10.4103/JASI.JASI_142_20
Quick Response Code:

abdominal circumference (AC), foot length, and head circumference (HC) are used for GA estimation at different pregnancy trimesters.

These parameters are limited in late pregnancy and in uncertain dated pregnancies. This was explained by the increasing biologic variability in advancing GA. To determine the abnormal fetal growth, serial ultrasonographic evaluation in the third trimester is required for appropriate fetal surveillance and intervention. The size of the cerebellum or TCD is important because it is a useful biometric parameter in estimating GA in the second and third trimester.

So we aim to establish reference curves for the size of the fetal TCD measured using ultrasound between the 25th and 32 weeks of gestation, determine the accuracy of fetal TCD measurement in the prediction of GA and to evaluate the application and accuracy of TCD in determining the GA of the fetus and Its Correlation.

Material and Methods

A cross-sectional prospective study conducted to determine the different ultrasonographic interpretations concerned. This study was a scan center based one in a hospital that conducted to determine the different parameters of the fetus in normal pregnancies. The study was conducted during the period between 2019 and February 2020. The study was conducted at Arogyamatha hospital in collaboration with the Department of ultrasound Scan center in Gengavally taluk, Salem district of Tamilnadu, India. The subset of antenatal mothers attending the Department of ultrasound scan of the Hospital for assessment of their feto-placental profile during their pregnancy. All the subjects were identified from the antenatal mothers attending the Department of ultrasound scan of the Hospital for assessment of their feto-placental profile along with documented first trimester crown-rump length (CRL) in previous ultrasonography report. Study subjects were selected according to the inclusion and exclusion criteria mentioned in the study protocol.

The data collection was carried throughout the weekdays at the scan center with the previous appointments. The subjects were examined once never repeated for participation in this study. Maintaining the criteria of inclusion and exclusion at all antenatal mothers was approached for this study based on the reviews of previous research papers.

Eligibility of the study population

Inclusion criteria

1. Pregnancy having 25–32 weeks of gestation
2. Having documented 1st-trimester investigations
3. Uneventful pregnancy till date or without any bad obstetric history
4. Given informed consent
5. Pregnant women having single live normal fetus.

Exclusion criteria

1. Having no documented 1st-trimester CRL
2. High-risk pregnancy or in emergency crisis
3. Documented or reported any associated disorders (medical/surgical) of the mother
4. Documented with any fetal anomaly.

Study plan

After obtaining the approval from Ethical committee from the concerned institution, we had visited the center and started the study with the CRF forms. Data were collected from the participants at the time of ultrasonography and transferred to the electronic module. And we were advocated that every participant should visit the center between the 25th and 32 weeks (3rd trimester) of the gestational period.

The patient was asked to come with full bladder as it was difficult to measure the BPD as the head was sagging down in the pelvis. Ultrasound jelly was used to eliminate the air interface between the transducer and the patient skin. If jelly is not used, the presence of air causes hindrances during the examination. Sufficient jelly was spread over the abdomen before the examination. The TCD was mainly measured in the transcerebellar plane. The measurement of TCD was obtained by placing electronic calipers at outer to outer margins of the cerebellum. The landmarks of the thalami, cavum septum pellucidum and third ventricle were identified, thereby slight rotating transducer below the thalamic plane. The posterior fossa was revealed with the characteristic butterfly-like appearance of the cerebellum [as shown in the Figure 1]. In all cases cerebellum was seen as two lobes on either side of the midline in the posterior cranial fossa.

Each patient was subjected to serial ultrasound for fetal biometry and TCD measurement. The BPD, HC, AC, femoral length (FL), fetal heart rate (FHR) were collected along with TCD to assess the GA. For the data collection same machine, same probe and the same observer were maintained throughout the study period.

Statistical analysis

The data were entered on the space scheduled in the master sheet previously made ready. Variables were explored and analyzed using appropriate statistical methods. The data were entered in Excel datasheet and converted to SPSS (SPSS Incorporation Chicago, USA) data sheet and final analysis was done by using the SPSS (Statistical Package for Social Science) 12 versions. The statistical evaluation between fetal TCD and GA was assessed. Various parametric and nonparametric statistical analysis methods used like Descriptive analysis, Regression analysis, and Pearson correlation coefficient "*r*" in the range of (+1, −1) was calculated.[10,11]

Table 1: Descriptive statistics

Variables (*n*=100)	Average	SD	Minimum	Maximum
Mothers' age in years	24	4	17	39
Mothers' height in cm	153	6.5	132	168
Mothers' weight in kg	60	10.5	37	87
GA at third trimester in weeks	28	0.7	27	30
Foetal weight at third trimester	1.3	0.13	1.1	1.6
FHR at third trimester	149	8.5	121	175
BPD - 3rd trimester	73	2.3	67	80
HC - 3rd trimester	264	8.7	237.8	311
AC - 3rd trimester	244	8.9	226.6	265.9
FL - 3rd trimester	55	2.1	49.5	59.6
Transverse cerebellar diameter - 3rd trimester	31	1.1	28.6	33.9

Mean and SD value of GA, TCD with BPD, FL, AC, FHR and HC in third-trimester gestation. SD: Standard deviation, GA: Gestational age, TCD: Transcerebellar, BPD: Biparietal diameter, FL: Femur length, AC: Abdominal circumference, FHR: Fetal heart rate, HC: Head circumference

Results

Summary of the results is tabulated in Table 1. The total number of mothers who participated in this study was 100. The patients mean age was 24 years and mean GA depending on ultrasound was 28 ± 0.7 (27–30) weeks. The mean fetal biometry parameters including BPD of the study population was 73 ± 2.3 mm (67–80), HC was 264 ± 8.7 mm (237.8–311), AC was 244 ± 8.9 mm (226.6–265.9), FL was 55 ± 2.1 mm (49.5–59.6), FHR was 149 ± 8.5 beats (121–175). The mean transcerebellar measurement of the fetus was 31 ± 1.1 mm (range 28.6–33.9 mm) as shown in Figures 2 and 3. Regression and correlation coefficients for correlation between GA with routine fetal biometric parameters and TCD are presented.

Table 2 shows the relationship between TCD with other biometrics and period of gestation in normal pregnancy. The cases were divided into 4 groups. The mean TCD at 27 weeks was 30.073 ± standard deviation (SD) 0.863, at 28 weeks it was 30.838 ± SD 0.727 mm, at 29 weeks it was 31.783 ± SD 0.787 mm and raised up to 32.5 ± SD 0.973 mm at 30 weeks of gestation.

When individual observations of mean TCD in normal pregnancy cases were studied in relation to the period of gestation in weeks, linear relationship seen between the period of gestation and TCD. The mean observations of other standard biometrics are tabulated in Table 2. The correlation coefficient between period of gestation and TCD was found to be 0.99 which was statistically significant ($P < 0.001$) and other standard biometrics were found a better correlation with the GA [Table 3]. Figure 4 shown in the scatter diagram, there is a good linear relationship seen between GA and TCD.

Out of 100 mothers, 57 were primigravida and 43 were multigravida status, and there is no difference between primigravida and multigravida in terms of gestational weeks [Table 4].

Linear regression models for estimation of GA were derived from all the biometric indices (TCD, BPD, FL, and AC).

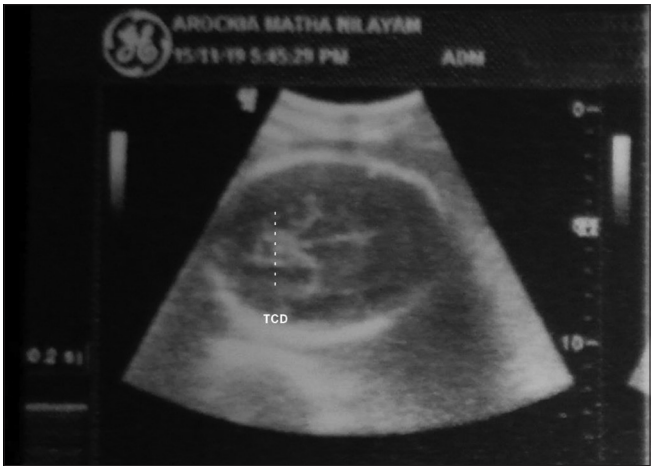

Figure 1: Ultrasonagram showing butterfly shaped cerebellum in the posterior cranial fossa

In addition, stepwise regression models were constructed to determine the best model for the determination of GA between 27 and 30 weeks of gestation. Comparison of the accuracy of these models in the determination of GA showed that TCD has 99% predictive accuracy, with a standard error of 1.6 days. In this study, the regression coefficient of the transcerebral diameter was +0.48 with a standard error of 0.053 and $P < 0.01$ [Table 5]. Figure 5 shown in the scatter diagram, the linear regression seen between GA and TCD.

Discussion

Accurate gestational dating is of paramount importance and the cornerstone for the management of pregnancies; easily reproducible sonographic fetal biometric parameters for gestational dating are clinically important for the best obstetric management of pregnancies. This is especially true in determining the timing of a variety of gestational tests, assessing the adequacy of growth and timing of delivery for the optimal obstetric outcome. Campbell *et al*. demonstrated that 45% of pregnant women are uncertain of menstrual dates as a result of poor recall, irregular cycles,

Table 2: Mean and standard deviation for biparietal diameter, abdominal circumference, head circumference, femoral length, and transcerebellar of gestational age subgroups based on period of gestation

GA in weeks	Number of cases	BPD mean (mm)±SD	AC mean (mm)±SD	HC mean (mm)±SD	FL mean (mm)±SD	TCD mean (mm)±SD
27	11	70.436±1.605 (68.2-73.8)	233.509±3.361 (228.6-238.5)	254.136±6.96 (237.8-262.3)	52.182±1.366 (49.5-54.4)	30.073±0.863 (28.6-31.1)
28	47	71.664±1.557 (67-74.3)	239.911±5.781 (226.6-250.8)	261.325±4.341 (253.3-271.9)	53.777±1.342 (51.2-57)	30.838±0.727 (29.8-32.5)
29	30	73.967±1.445 (71.4-77.7)	248.32±5.761 (235.7-258.3)	266.32±4.852 (257.1-273.7)	55.39±1.616 (49.7-58.6)	31.783±0.787 (30.7-33.5)
30	12	75.95±2.089 (71.3-80)	257.333±7.24 (238.7-265.9)	278.633±11.285 (262.6-311)	57.517±1.602 (54.8-59.6)	32.5±0.973 (30.8-33.9)

SD: Standard deviation, GA: Gestational age, TCD: Transcerebellar, BPD: Biparietal diameter, FL: femur length, AC: Abdominal circumference, HC: Head circumference

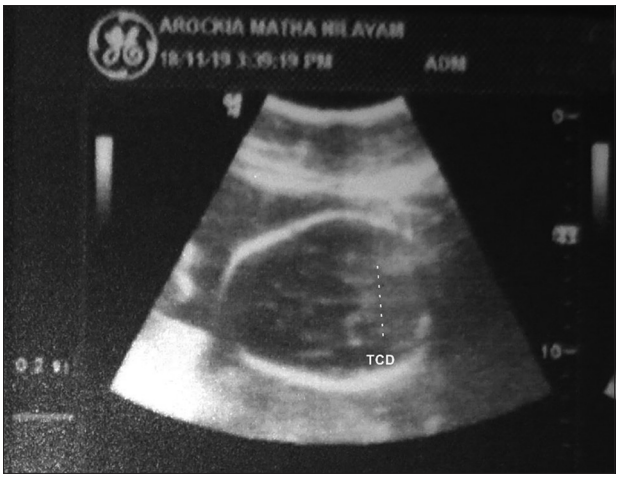

Figure 2: Measurement of transcerebellar diameter of 32.1 mm at 29.1 weeks of gestation

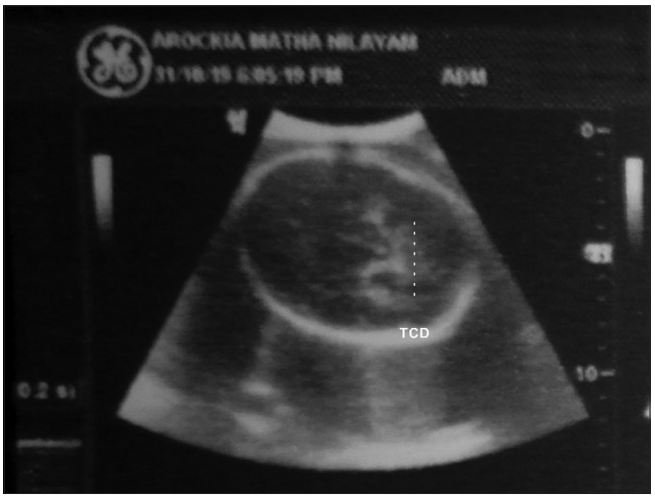

Figure 3: Measurement of transcerebellar diameter of 28.6 mm at 27 weeks of gestation

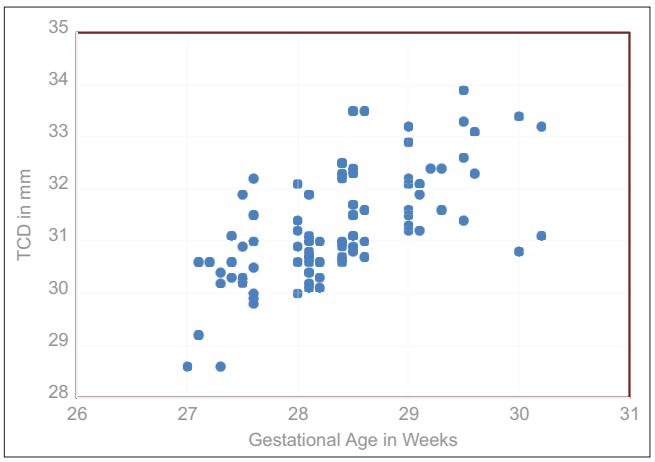

Figure 4: Linear relationship seen between gestational age and transcerebellar diameter -Figure showing the transcerebellar diameter increased linearly against the gestational age increases

bleeding in early pregnancy, or oral contraceptive use within 2 months of conception.

Table 3: Correlation coefficient with third-trimester gestational age

GA in weeks-3rd trimester (*n*=100)	Pearson's correlation coefficient	*P*
FHR/min	0.95	<0.001
BPD	0.99	<0.001
HC	0.97	<0.001
AC	1	<0.001
FL	1	<0.001
Transverse cerebellar diameter	0.99	<0.001

Linear correlation was observed between fetal TCD with other biometrics and GA for the whole sample (correlation coefficient [*r*]=0.99 and *P*<0.001). FHR: Fetal Heart Rate, GA: Gestational age, BPD: Biparietal diameter, FL: femur length, AC: Abdominal circumference, HC: Head circumference

Table 4: Distribution of pregnancy by gravidity versus gestational weeks

Group	Number of cases	Mean GA weeks±SD	95% CI
Primigravida	57	37.9±0.8	37.7-38.1
Multigravida	43	38.0±1.0	37.7-38.3
Combined	100	38.0±0.9	37.8-38.1
P	0.349		

SD: Standard deviation, GA: Gestational age

Table 5: Linear regression coefficient of transcerebellar against gestational age

Variable	Coefficient	SE	*t*	*P*	95% CI	Significant (*P*)
TCD\GA	0.476	0.053	9.04	0	0.371-0.58	<0.01
Constant	13.514	1.645	8.22	0	10.25-16.778	<0.01

TCD: Transcerebellar, GA: Gestational age, CI: Confidence interval, SE: Standard error

The most reliable parameter used in the estimation of the GA in the second and early third trimester is the BPD; femur length (FL) is the most accurate for the late third trimester. The measurement of BPD in the second-trimester routine scan is performed in all good antenatal care centers.

As per ultrasound literature TCD is a unique, reliable parameter for estimating the duration of gestation and is consistently superior in predicting GA in both singleton and twin gestation.[11,12] The TCD has been shown to be a reliable parameter that is significantly correlated with GA by the end of the second trimester.[4]

Prediction of GA in the pregnancies without precise last menstrual period information is a tough task for sonologists, especially in case of growth-restricted pregnancies, although in normal pregnancy fetal biometric parameters are helpful for the estimation of GA as successive growth of these parameters occurs during the course of pregnancy. Hence, the focus of a sonologist is generally on such parameters that can be used independently without being affected by the impaired growth of the fetus. In recent years, several studies revealed that TCD has been identified as a useful growth indicator that stands the growth pattern

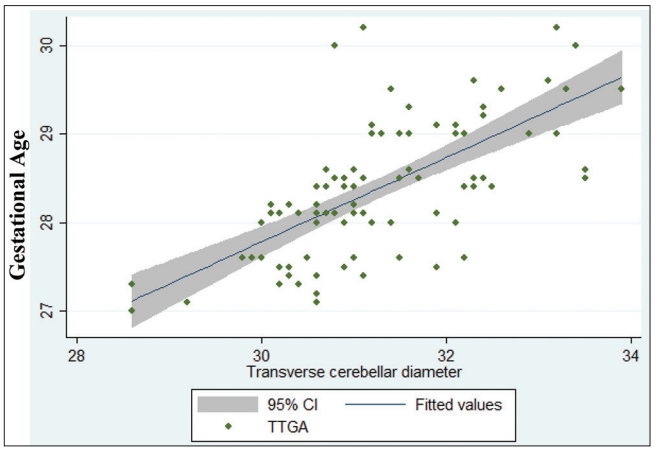

Figure 5: Linear regression of transcerebellar diameter against gestational age-showing in the scatter diagram, the linear regression seen between gestational age and transcerebellar diameter at the 95.0% confidence level

irrespective of the overall growth pattern of pregnancy. Routine biometric parameters for GA assessment such as BPD, HC, AC, and FL have their own limitations like BPD and HC are difficult to measure because of molding of the head in the third trimester. Similarly, femur length is not reliable in cases of achondroplasia.

In a study done on TCD in singleton pregnancies by Gupta AD *et al*[13] from India, the authors observed that the GA of pregnant women not sure of their LMP can be reliably estimated by measuring the TCD which showed good correlation (r = +0.946, r^2 = 89.6% and P < 0.001). The increase in TCD throughout gestation helped in assessing the development of the cerebellum.[14] The present study is an attempt to find whether fetal TCD can be used as an independent parameter to calculate the GA like the other established biometric indices (BPD, HC, FL, AC) and accuracy to which GA can be calculated if TCD is added to the four routine biometric parameters. An often quoted rule of thumb is that "TCD in mm approximates GA in weeks."

The increase in TCD throughout gestation helped in calculating the development of the cerebellum. Guan B[15] found curvilinear relationship between TCD and GA (R2 = 0.99624, P < 0.0005). He inferred that the function of the TCD in the evaluation of fetal growth and development is better than any other biometrics. Mikovic and Markovic *et al*.[16] studied the growth of fetal cerebellum in normal pregnant mothers between 20 and 40 gestational weeks and proposed that TCD can be practically applied in cases where it is difficult or impossible to measure BPD or in cases where it is unsuitable because of the expressed molding of the head.

When individual observation of mean TCD was studied in relation to the period of gestation in weeks [Table 3], the correlation coefficient was found to be 0.99, which was statistically significant (P < 0.001), similar to the findings of Meyer WJ *et al*.,[13] Goel P. *et al*.[17] Furthermore, it was deduced that the other standard biometric values had a

good correlation with GA [Table 2] and established a better correlation coefficient as shown in Table 3.

From the regression analysis, a strong relationship has been observed between fetal TCD and GA. With increasing GA, there was a significant increase in TCD values. The correlation between TCD measurements and GA was strong at 27–30 weeks ($r > 0.99$). Using correlation coefficients, it has been predicted that for every one mm increase in TCD there is an increase of 0.4 weeks in GA, i. e., one day. There is a statistically significant relationship between TCD and GA at the 95.0% confidence level.

Conclusions

This study showed that TCD is an accurate predictor of GA in the third trimester. The correlation between GA and the GA by TCD seems to increase from 28 to 30 weeks. From the present study, it was observed that the TCD increases linearly with GA. There is a good correlation between GA derived from TCD and GA from established biometric indices like BPD, HC, AC, and FL. The TCD in mm, and this parameter alone can predict the GA, TCD can be combined with the other four biometric indices to give a fair estimation of GA. Hopefully, the results will demonstrate its applicability in routine practice.

Consent

Written informed consent was taken from the patients for publication of this research study.

Approval from IRB: Yes

Financial support and sponsorship

Nil.

Conflicts of interest

There are no conflicts of interest.

References

1. Platt LD. Assessment of gestational age. In: QueenanJT, Hobbins JC, Spong CY, editors. Protocols for High Riskpregnancies. Oxford: Wiley-Blackwell; 2005: p. 64-8.
2. American College of Obstetricians and Gynecologists. ACOG Practice Bulletin No. 98: Ultrasonography in pregnancy. Obstet Gynecol 2008;112:1419-44.
3. Shehzad K, Ali M, Zaidi S. Fetal biometry. J Med Sci Pak 2006;22:503-8.
4. Chavez MR, Ananth CV, Smulian JC, Vintzileos AM. Fetal transcerebellar diameter measured for prediction of gestational age at the extremes of fetal growth. J Ultrasound Med 2007;26:1167-71.
5. Araujo EJ, Pires CR, Nardozza LM. Correlation of the fetal cerebellar volume with other fetal growth indices by three dimensionalultrasounds. J Matern Fetal Neonat Med 2007;20:581-7.
6. Chavez MR, Ananth CV, Kaminsky LM, Smulian JC, Yeo L, Vintzileos AM. Fetal transcerebellar diameter measurement forprediction of gestational age in twins. Am J Obstet Gynecol 2006;195:1596-600.
7. Chavez MR, Ananth CV, Smulian JC, Yeo L, Oyelese Y, Vintzileo AM. Fetal transcerebellar diameter measurement with particularemphasis in the third trimester: A reliable predictor of gestationalage. Am J Obstet Gynecol 2004;191:979-84.
8. Benson CB, Doubilet PM. Sonographic prediction of gestational age: Accuracy of second- and third-trimester fetal measurements. AJR Am J Roentgenol 1991;157:1275-7.
9. Kumar K, Beg MR, Ramesh Babu CS, Shrivastava RK. Estimation of fetal gestational age in second & third trimesters from ultrasonographic measurements of different fetal biometric parameters. Indian J Clin Anat Physiol 2015;2:111-6.
10. Laishram D, Senthilnathan S, Anand G, Shastri D. Ultrasound estimation of Gestational Age from Fetal Kidney Length. Natl J Basic Med Sci 2014,5:38-41.
11. Chavez MR, Ananth CV, Smulian JC, Lashley S, Kontopoulos EV, Vintzileos AM. Fetal transcerebellar diameter nomogram in singleton gestations with special emphasis in the third trimester: A comparison with previously published nomograms. Am J Obstet Gynecol 2003;189:1021-5.
12. Meyer WJ, Gauthier DW, Goldenberg B, Santolaya J, Sipos J, Cattledge F. The fetal transverse cerebellar diameter/abdominal circumference ratio: A gestational age-independent method of assessing fetal size. J Ultrasound Med 1993;12:379-82.
13. Gupta AD, Banerjee A, Rammurthy N, Revati P, Jose J. Gestational age estimation using transcerebellar diameter with grading of foetal cerebellar growth. Natl J Clin Anat 2012;1:115-20.
14. Pinar H, Burke SH, Huang CW, Singer DB, Sung CJ. Reference values for transverse cerebellar diameter throughout gestation. Pediatr Dev Pathol 2002;5:489-94.
15. Guan B. Surveillance of fetal growth and fetal cerebellar transverse diameter by ultrasonographic measurement. Zhonghua Yi Xue Za Zhi 1992;72:65-7.
16. Miković Z, Marković A, Dukić M, Pazin V. Growth of the fetal cerebellum in normal pregnancy. Jugosl Ginekol Perinatol 1989;29:157-60.
17. Goel P, Singla M, Ghai R, Jain S, Budhiraja V, Rameshbabu CS. Transeverse cerebellar diameter – A marker for estimation of gestational age. J Anat Soc India 2010;59;158-61.

Original Article

Study of Histological Changes of Placenta in Pregnancy-Induced Hypertension in Poorvanchal Region of Uttar Pradesh, India

Vishram Singh, Kumud Ranjan, S. L. Tewarson[1], Rashi Singh[2], Yogesh Yadav

Department of Anatomy, Santosh Deemed to be University, [2]Department of Paedodontics and Preventive Dentistry, Santosh Dental College, Ghaziabad, [1]Department Pathology, Government Medical College and Superfacility Hospital, Azamgarh, Uttar Pradesh, India

Abstract

Introduction: The placenta is a fetomaternal organ. It is a connection of the fetus with the uterine wall of mother. Through the placenta, exchange of gases and nutrient supply takes place. Through the placenta, fetal blood tissue comes in direct contact with the maternal blood without any rejection. It is a special transient organ of pregnancy. In our study, we carried out the microscopic examination of the placenta in pregnancy-induced hypertension, i.e., syncytial knot, cytotrophoblastic cellular proliferation, fibrinoid necrosis, endothelial proliferation, and calcified villous spot. **Material and Methods:** One hundred and fifty-two placentas of full-term pregnancy were collected from the labor room/operation theater of the Gynecology and Obstetrics Department of the Government Medical College and Superfacility Hospital Azamgarh. Out of one hundred and fifty-two placentas, 76 cases were controls from mothers with no known history of preexisting hypertension and 76 were collected from mothers with pregnancy-induced hypertension. Placentas were kept in 10% formalin for 24 h for fixation. After 24 h, tissues of placentas were passed through a series of the procedures from dehydration and clearing to wax impregnation before being sectioned from automated microtome. Time took for processing was 24 h. Five microns thick tissues sections were cut. Prepared slides were mounted in DPX and covered with the cover slip. Through binocular light, microscope slides were examined at ×10, ×40, and ×100 magnifications. **Results:** Histology in our study revealed that syncytial knots were present in placentas of all 100% of hypertensive and only 32.89% of normotensive mothers. Cytotrophoblastic proliferation was seen in 98.68% and 19.73% placentas of hypertensive and normotensive mothers, respectively. Fibrinoid necrosis of placenta was found in 88.15% of hypertensive and only 28.94% of normotensive mothers. The 100% placentas of the hypertensive mothers had endothelial proliferation as compared to controls. Calcified villous spots were seen in 84.21% and 31.57% of placentas of hypertensive and normotensive mothers, respectively. **Discussion and Conclusion:** Pregnancy-induced hypertension adversely affects the health of the fetus through its harmful effects on the placentas. Syncytial knots, cytotrophoblastic cellular proliferation, fibrinoid necrosis, endothelial proliferation, and the calcified villous spots were present more in the placentas of hypertensive mothers in our study in comparison to the study of other authors. In our research, we found that endothelial proliferations were present in all placentas. If proper treatment is given to the mother in the early stage of pregnancy, it may prevent the death of a fetus. Hence, this study helps the clinician for early diagnosis and treatment of pregnancy-induced hypertension.

Keywords: *Calcified villous spot, hypertensive placenta, normotensive placenta, placental fibrinoid necrosis*

Article Info

Received: 20 December 2020
Accepted: 05 March 2021
Available online: ***

Address for correspondence:
Mr. Kumud Ranjan, Department of Anatomy, Government Medical College and Superfacility Hospital, Azamgarh - 276 128, Uttar Pradesh, India. E-mail: drkumudranjan@gmail.com

Access this article online

Website: www.jasi.org.in
DOI: 10.4103/jasi.jasi_271_20
Quick Response Code:

Introduction

The placenta is a fetomaternal organ. It is a connection of the fetus with the uterine wall of mother.[1] Through the placenta, exchange of gases and nutrient supply and removal of waste takes place. Through the placenta, fetal blood comes in direct contact with the maternal blood without any rejection. It is a special transient organ of pregnancy.[2] The placenta provides an interface for nutrients and oxygen between fetal and maternal circulation for growth and development of the fetus.[3] Hemochorial type of placenta is present in the humans. In this type of placenta, exchange occurs between maternal and fetal blood while maintaining anatomical separation between the circulatory system of fetus and mother. Hypertension is a common complication of pregnancy; significantly, it contributes to perinatal and maternal morbidity and mortality.[4] Pregnancy-induced hypertension is a pregnancy-specific syndrome.[5] In this study, we designed to search the histopathological

How to cite this article: Singh V, Ranjan K, Tewarson SL, Singh R, Yadav Y. Study of histological changes of placenta in pregnancy-induced hypertension in Poorvanchal region of Uttar Pradesh, India. J Anat Soc India 2021;XX:XX-XX.

changes in the placenta due to pregnancy-induced hypertension. Complications of hypertension are reflected in the placenta macroscopically and microscopically.[6] In pregnancy-induced hypertensions due to maternal vasospasm, decreased blood flow occurs in the placenta. Constriction occurs in the fetal arteries these changes seen in the placenta. Pregnancy-induced hypertension affects all organ systems. Maternal vasospasm leads to fetal hypoxia, and it leads to fetal distress and ultimately, fetal death.[7]

The fetus depends on placenta for growth and development.[8] Pathological changes occur in the placenta in pregnancy-induced hypertension, such as infarction, calcification, diffuse placental thrombosis, inflammatory placental vasculopathy, and abnormal trophoblastic proliferation. Reduced blood flow occurs in the placenta due to pathological changes, which lead to uteroplacental insufficiency. 2%–8% maternal death occurs due to hypertension.[9] Cytotrophoblastic cellular proliferation, syncytial knots, and fibrin plaques are present more in the pregnancy-induced hypertensive then in normotensive placentas. In this study, we carried out an analysis of microscopic changes of placenta in pregnancy-induced hypertension; especially syncytial knots, cytotrophoblastic cellular proliferation, fibrinoid necrosis, endothelial proliferation, and calcified villous spots both in placentas of normotensive and hypertensive mothers.

Material and Methods

The one hundred and fifty-two placentas of full-term pregnancy were collected from labor room/operation theater of Gynaecology and Obstetrics, Department of Government Medical College and Superfacility hospital Azamgarh, Uttar Pradesh of Poorvanchal Region India. Out of 152 placentas, 76 were from mothers with no known history of preexisting hypertension as controls and 76 were collected from mothers with hypertension. Subjects included in our research were aged between 20 and 44 years and were from all socioeconomic groups. There were no differences according to race culture or environmental conditions. All placentas were obtained either from a vaginal route or during cesarean section. The collected placentas were weighed on weighing machine graduated in grams after washing in running tap water and dried with blotting paper. We took morphometric examination of placentas. After 24 h for fixation, tissue pieces were passed through a series of procedures, i.e., from dehydration and clearing to wax impregnation before being sectioned by an automated microtome. Time taken for processing was 24 h. The tissues were sectioned at 5 μ by automated microtome. APES-coated glass slides used for sectioned tissues. Before staining slides were placed on a hot metallic plate at 60° for 30 min. Hematoxylin and eosin staining for slide were done. All slides prepare they passed through xylene −1 for 10 min and xylene −2 for next 10 min. Then kept in 100%, 95%, 80%, 70%, alcohol for 5 min each to dehydrate the sections. For staining, slides were placed into the Harris Hematoxylin solution for 5–10 min after that rehydrated with water. Again, tissues were washed with tap water then placed into 1% eosin for approximately 1–2 min. Finally, tissues were dehydrated by passing through increasing concentrations of alcohol and cleared in the solution of xylene for 5 min. The slides were allowed to dry before being mounted in DPX and covered with a cover slip. The prepared slides were examined under light microscope ×10, ×40, and ×100.

Results

The histological examination showed that syncytial knot was present in all (100%) placentas of hypertensive mothers. Whereas it was seen only in 32.89% placentas of normotensive (controls) mothers. Thus, 67.10% placentas of normotensive mothers did not have any syncytial knot [Table 1 and Figures 1, 2a and b]. The 98.68% placentas of hypertensive mothers had cytotrophoblastic cell proliferation, but it was present in 19.73% of placentas of normotensive (control) mothers. It means 80.26% placentas of a normotensive mothers and 1.31% placentas of a hypertensive mothers were free of cytotrophoblastic cell proliferation [Table 1 and Figures 3, 4a and b]. Further, 88.15% of placentas of hypertensive mothers had fibrinoid necrosis. On the other hand, only 28.94% of placentas of normotensive (control) mothers had fibrinoid necrosis. It means that 71.05% placentas of the normotensive (control) mothers had no fibrinoid necrosis but 11.84% placentas of the hypertensive mothers had it [Table 1 and Figures 5, 6a and b]. Placentas of all (100%) hypertensive mothers had endothelial proliferation in comparison to placentas of normotensive mothers in histological examination [Table 1 and Figures 7, 8a and b]. It was seen that 84.21% of placentas of hypertensive mothers had calcified villous spots, whereas only 31.57% placentas of normotensive mothers had it. The 68.42% of normotensive mother's placentas had no calcified villous spots in 15.78% of hypertensive mother's placentas had no calcified villous spots [Table 1 and Figures 9, 10a and b].

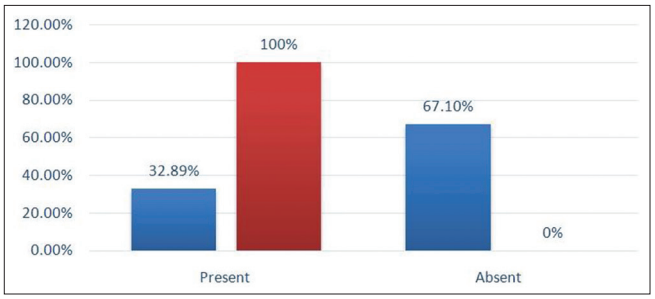

Figure 1: In histological review, there was syncytial knot in 100% placentas of hypertensive mothers. However, there was also a syncytial knot in 32.89% placentas of normotensive (control) mothers and no syncytial knot in 67.10% of placentas of normotensive (control) mothers

Table 1: A comparison of histological changes in normotensive and hypertensive (pregnancy-induced hypertension) placenta

Histological changes	Normotensive (control) (%)	Hypertensive (%)
Syncitial knot		
Present	32.89	100
Absent	67.10	0
Cytotrophoblastic cellular proliferation		
Present	19.73	98.68
Absent	80.26	1.31
Fibrinoid necrosis		
Present	28.94	88.15
Absent	71.05	11.84
Endothelial proliferation		
Present	0	100
Absent	100	0
Calcified villous spot		
Presents	31.57	84.21
Absent	68.42	15.78

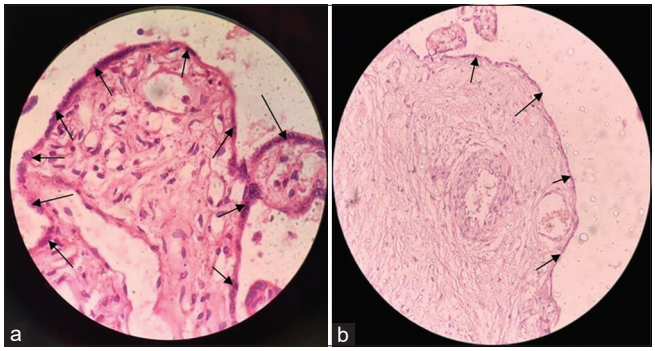

Figure 2: (a) Histological slide of hypertensive placenta – arrows shows syncytial knot (×100). (b) Histological slide of normotensive placenta - Arrow shows syncytial knot (×40)

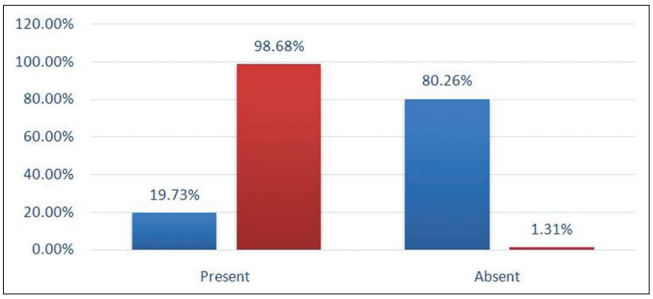

Figure 3: In histological review, 98.68% of placentas of hypertensive mothers hadcytotrophoblastic cell proliferation, but there was also cytotrophoblastic cell proliferation in 19.73% of placentas of normotensive (control) mothers. It means that 80.26% placentas of a normotensive mother and 1.31% placentas of a hypertensive mother do not hadcytotrophoblastic cell proliferation

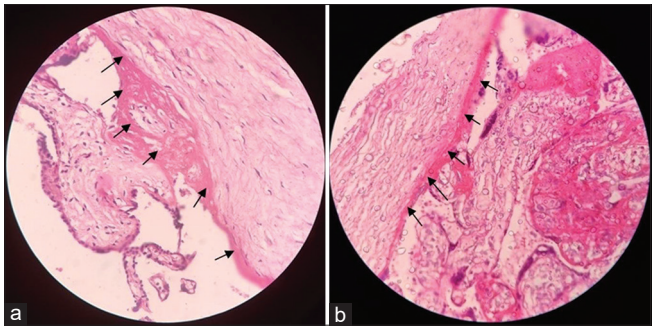

Figure 4: (a) Histological slide of hypertensive placenta - Arrow shows cytotrophoblastic cellular proliferation (×40). (b) Histological slide of normotensive placenta - Arrow shows cytotrophoblast (×40)

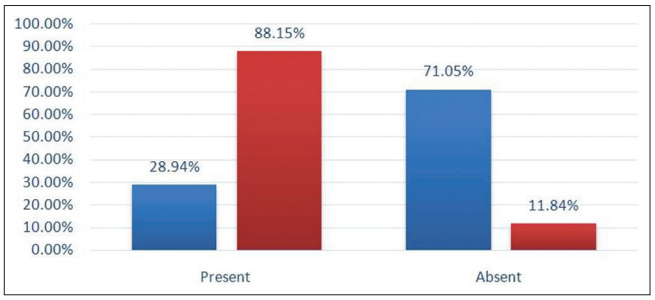

Figure 5: In histological examination, 88.15% of placentas of hypertensive mothers had fibrinoid necrosis, but in 28.94% of placentas of normotensive (control) mothers also had fibrinoid necrosis. It means that 71.05% placentas of the normotensive (control) mothers had no fibrinoid necrosis, but 11.84 placentas of the hypertensive mothers had no fibrinoid necrosis

Discussion

5% to 8% of all maternal deaths are due to hypertension. Prevalence rate of pregnancy-induced hypertension is 5%–10%. Significant histological changes can be seen in placentas of hypertensive mothers with incidence much higher than the normotensive placentas. In histological review, syncytial knots were seen in all (100%) placentas of hypertensive mothers and in 32.89% placentas of normotensive mothers and no syncytial knots in 67.10% of placentas of normotensive mothers [Table 1 and Figures 1, 2a and b]. According to Genset,[10] there was extreme syncytial knots formation and stromal fibrosis in hypertensive mother's placenta. The syncytial knots and stromal fibrosis are responsible

for reducing placental fetal perfusion. The major cause of increased syncytial knots formation was due to disturbance in the hormonal factors that leads to alteration in placental morphology and the effect of this shift in pregnancy-induced hypertension occurs in the mothers and low birth weight fetus is delivered. In extreme pregnancy-induced hypertension, the syncytial knots occur substantially more, i.e., the syncytial knots increase with the severity of hypertension during pregnancy.[11] Similar results were also reported by Majumdar *et al*.[12] and Rath *et al*.[13] 98.68% of placentas of hypertensive mothers had cytotrophoblastic cells proliferation, but only 19.73% of placentas of normotensive (control) mothers had it. It means 80.26% placentas of the normotensive mothers and 1.31% placentas of the hypertensive mothers had no cytotrophoblastic cell proliferation [Table 1 and Figures 3, 4a and b]. Cytotrophoblastic cellular proliferation was present more in hypertensive pregnancies.[14] Decreased blood flow occurs to the placenta due to cytotrophoblastic proliferation, resulting in a decreased blood supply to the fetus and subsequently leading to low birth weight of the fetus. Cytotrophoblastic proliferation of cells occurs more in the hypertensive mother's placenta as compared to controls. These placental alterations are directly proportional to illness and incidence of fetal outcome. Das *et al*.[15] reported similar findings, 88.15% of placentas of hypertensive mothers had fibrinoid necrosis but only 28.94% of placentas of normotensive mothers fibrinoid necrosis as well. It means that 71.05% placentas of normotensive mothers do not have fibrinoid necrosis but only 11.84% of hypertensive mothers were free of fibrinoid necrosis [Table 1 and Figures 5, 6a and b]. Fibrinoid necrosis occurs more in placentas of hypertensive mothers.[15] Endothelial proliferation was seen in all 100% in comparison to controls (normotensive) in histological review [Table 1 and Figures 7, 8a and b]. In other studies, more endothelial proliferation was seen in the hypertensive placentas than in the normotensive placentas. According to Damania *et al*.,[16] less perfusion occurs in the placenta due to endothelial proliferation, resulting in fetal hypoxia, and eventually fetal death. According to Di Salvo *et al*.,[17] tissue perfusion decreases due to endothelial proliferation, and ischemia occurs. Similar observations were also found by Pretorius *et al*.[18] In the histological review, 84.21% of placentas of pregnancy-induced hypertensive mothers had calcified villous spots, but only 31.57% placenta of normotensive mothers. The 68.42% of placentas of a normotensive mother had no villous spots calcified and 15.78% of placentas of a pregnancy-induced hypertensive mother had no villous spots [Table 1 and Figures 9, 10a and b]. Findings of Kofinas *et al*.[19] were in accordance with the findings of the present study. Qureshi *et al*.[20] also reported higher incidence of calcification in hypertensive than in normotensive placentas. According to Salmani *et al*.,[21] underperfusion of tissues occurs in severe pregnancy-induced hypertension. According to the Nahar *et al*.,[22] syncytial knot, fibrinoid

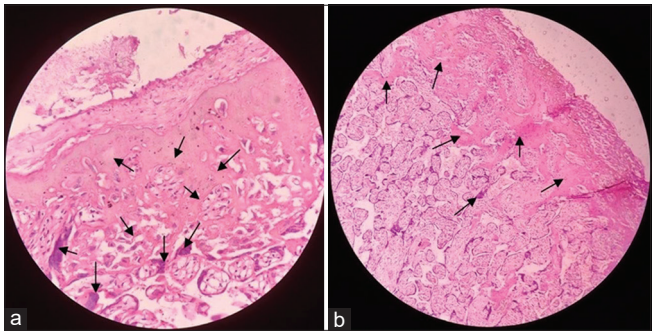

Figure 6: (a) Histological slide of hypertensive placenta-Arrow shows fibrinoid necrosis (×40). (b) Histological slide of normotensive placenta Arrow shows fibrinoid necrosis (×10)

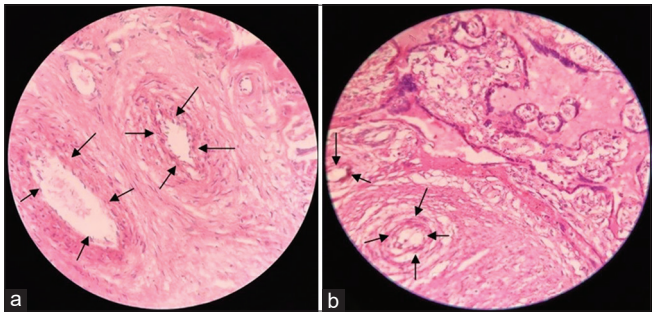

Figure 8: (a) Histological slide of hypertensive placenta arrow shows endothelial proliferation (×40). (b) Histological slide of normotensive placenta-Arrow shows endothelium (×40)

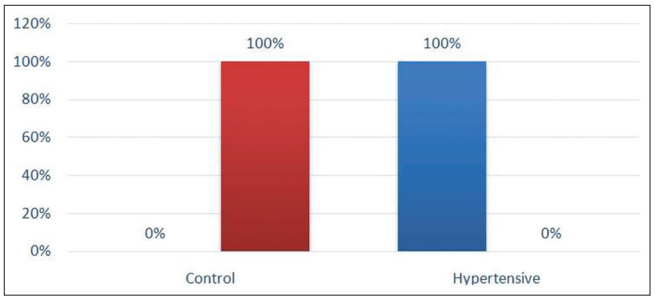

Figure 7: The 100% of placentas of hypertensive mothers had endothelial proliferation in comparison to control (normotensive) in histological examination

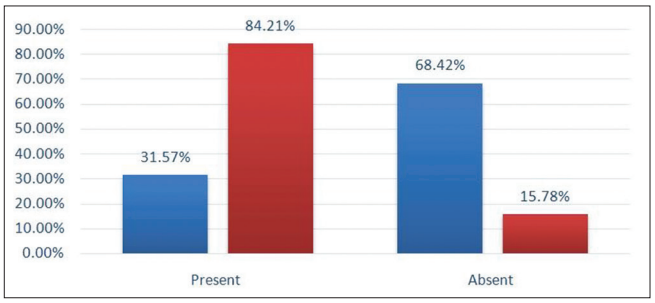

Figure 9: In the histological review, 84.21% of placentas of normotensive mothers had calcified villous spot but also calcified villous spot in 31.57% placenta of normotensive mothers. The 68.42% of normotensive mother's placentas had not calcified villous spot and 15.78% of hypertensive mother's placentas had not calcified villous spot

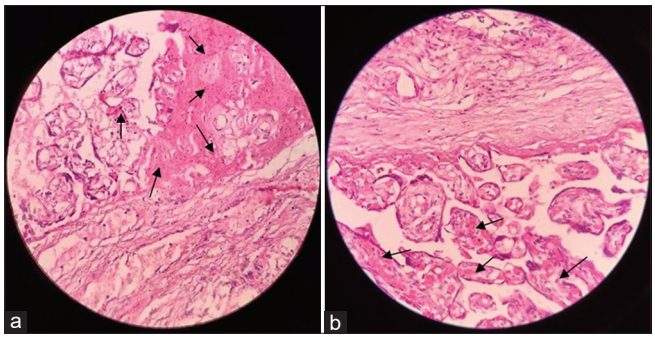

Figure 10: (a) Histological slide of hypertensive placenta – arrow shows calcified villous spot (×40). (b) Histological slide of normotensive placenta – Arrow shows calcified villous spot

necrosis, and calcified villous spots are more in hypertensive placentas. This was similar to our findings. Gibbins *et al*.[23] found excessive syncytial knots was present in hypertensive pregnancies. Rajyalakshmi *et al*.[24] found more syncytial knots, fibrinoid necrosis, and cytotrophoblastic cellular proliferation in hypertensive placentas. Biswa *et al*.[25] found cytotrophoblastic cells proliferation more in hypertensive placentas. Gore *et al*.[26] found more syncytial knots, fibrinoid necrosis, calcified villous spots, and cytotrophoblastic cellular proliferation in comparison to control and this was similar to our findings.

Conclusion

Pregnancy-induced hypertension has an adverse effect on the health of fetus through its harmful effects on the placentas. In our study, syncytial knots, cytotrophoblastic cells proliferation, fibrinoid necrosis, endothelial proliferations, and calcified villous spots, these lesions are more present in the hypertensive mother's placentas in comparison to observations of other authors. In severe pregnancy-induced hypertension, underperfusion of tissues occurs. Proper treatment given to the mothers in early stage of pregnancy prevents complications. Thus, our study helps the clinician for early diagnosis and treatment to lower the mortality rates of mothers and fetuses.

Financial support and sponsorship

Nil.

Conflicts of interest

There are no conflicts of interest.

References

1. Singh V. Textbook of Clinical Embryology. 2nd ed. New Delhi: Elsevier Relx India Pvt. Ltd.; 2017.
2. Sadler TW. Langman's Medical Embryology. 14th ed. New Delhi: Wolters Kluwer (India) Pvt. Ltd.; 2018.
3. Singh I. Human Embryology. 11th ed. New Delhi: Jaypee Brother Medical Publishers Pvt. Ltd.; 2014.
4. Dutta DC. Textbook of Obstetrics. 9th ed. New Delhi: Jaypee Brothers Medical Publishers Pvt. Ltd.; 2018.
5. Ahmad M. Study of placental changes in pregnancy induced hypertension. Int J Repord Contracepts Obstet Gynaecol 2013;2:524-7.
6. Landesmon R, Douglas RG, Holze E, The bulbar conjuctival vascular bed in toxmemias of pregnancies. Am J Obstet Gynaecol 1954;68:170-2.
7. Boyd PA, Scott A. Quantitative structural studies on human placentas associated with preeclampsia, essential hypertension and intrauterine growth retardation. Br J Obstet Gynecol 1985;92:714-21.
8. Brown MA. Pregnancy-induced hypertension: Pathogenesis and management. Aust N Z J Med 1991;21:257-60, 262, 264-73.
9. Roberts JM, Pearson G, Culter J. Summary of the NHLBI working group on research on hypertension during pregnancy. Hypertension 2003;41:437-45.
10. Genest DR. Estimating the time of death in stillborn fetuses: II. Histologic evaluation of the placenta; a study of 71 stillborns. Obstet Gynecol 1992;80:585-92.
11. Kurdukar MD, Deshpande NM, Shete SS, Zawar MP. Placenta in PIH. Indian J Pathol Microbiol 2007;50:493-7.
12. Majumdar S, Dasgupta H, Bhattacharya K. A study of placenta in normal and hypertensive pregnancy. J Anat Soc India 2005;54:1-9.
13. Rath G, Garg K, Sood M. Insertion of umbilical cord to the placenta in hypertensive mothers. J Anat Soc India 2000;49:149-54.
14. Udainia A, Bhagwat SS, Mehta CD. Relation between placental surface area, infarction and fetal distress in pregnancy induced hypertension with its clinical relevance. J Anat Soc India 2004;53:27-30.
15. Das B, Dutta S, Chakraborthy P, Nath P. Placental morphology in hypertensive disorders of pregnancy and its correlation with fetal outcome. J Obstet Gynaecol India 1996;46:40-6.
16. Damania KR, Salvi VS, Ratnaparki SK. The placenta in hypertensive disorder in pregnancy. J Obstet Gynaecol India 1989;39:28-31.
17. Di Salvo DN, Benson CB, Laing FC, Brown DL, Frates MC, Doubilet PM. Sonographic evaluation of the placental cord insertion site. AJR Am J Roentgenol 1998;170:1295-8.
18. Pretorius DH, Chau C, Poeltler DM, Mendoza A, Catanzarite VA, Hollenbach KA. Placental cord insertion visualization with prenatal ultrasonography. J Ultrasound Med 1996;15:585-93.
19. Kofinas AD, Penry M, Swain M, Hatjis CG. Effect of placental laterality on uterine artery resistance and development of preeclampsia and intrauterine growth retardation. Am J Obstet Gynecol 1989;161:1536-9.
20. Qureshi F, Jacques SM, Reyes MP. Placental histopathology in syphilis. Hum Pathol 1993;24:779-84.
21. Salmani D, Purushothaman S, Somashekara SC, Gnanagurudasan E, Sumangaladevi K, Harikishan R, *et al*. Study of structural changes in placenta in pregnancy-induced hypertension. J Nat Sci Biol Med 2014;5:352-5.
22. Nahar L, Nahar K, Hossain MI, Yasmin H, Annur BM. Placental changes in pregnancy induced hypertension and its impacts on fetal outcome. Mymensingh Med J 2015;24:9-17.
23. Gibbins KJ, Silver RM, Pinar H, Reddy UM, Parker CB, Thorsten V, *et al*. Stillbirth, hypertensive disorders of pregnancy, and placental pathology. Placenta 2016;43:61-8.
24. Rajyalakshmi S, Vani BS, Jijiya Bai P. Placental pathology in different degrees of pregnancy induced hypertension. Trop J Pathol Microbiol 2019;5:988-96.
25. Biswa M, Gyanaranjan N, Das SR. Histopathological study of placenta in pregnancy with hypertension in Western Odisha. IOSR J Dent Med Sci 2017;16:100-4.
26. Gore CR, Pandey A, Shetty A, *et al*. A study on histopathological changes in placenta in pre-eclampsia/eclampsia: A case-control study in tertiary care center, Western India. Indian Journal of Pathology and Oncology 2018:5:385-90.

Original Article

Vascular Anatomy of Distal End of Femur and Its Clinical Implications

Deepa Bhat, Sunilkumar Doddaiah[1], Pushpalatha Murugesh, N. B. Pushpa

Departments of Anatomy and [1]Community Medicine, JSS Medical College, JSS Academy of Higher Education and Research, Mysore, Karnataka, India

Abstract

Introduction: The distal end of the femur is a highly vascular tissue with unique features in its blood supply. The outcome of surgical interventions is determined by the interference of corresponding blood supply. The study examines the pattern of blood supply in terms of density, size, and direction of vascular foramina (VF) to the distal end. **Material and Methods:** The lower end of normal adult dry femora (n = 300) was divided into segments. The number, size, and direction of VF in each segment were documented. Wilcoxon signed-rank test identified the statistical difference in the number of VF between various segments and Friedman test compared the difference between segments of two sides. **Results:** The maximum average number of VF was observed in medial condylar surface while minimum in central part of intercondylar region. Condylar medial recorded the highest number of VF of all sizes. The number of VF of >2 mm size was found to be significantly different between right and left in right condylar lateral and right intercondylar posterior regions. Right condylar lateral had considerably large number of VF of >2 mm size with statistical significance (P = 0.000). A Friedman test indicated that segements of two sides rated differently. **Discussion and Conclusion:** The density of VF through which vessels traverse at lower end were not only numerous but also constant and uniformly scattered. Detailed understanding of the arterial anatomy of lower end helps to identify and localize vascular pedicles, thus ensuring vitality of graft as well as donor site.

Keywords: *Condyles, femur, lower end, vascular foramina, vascularity*

Introduction

Femur is the longest and strongest proximal weight-bearing bone of the lower limb. It is composed of an upper end, lower end, and shaft. The distal extremity is large and massive bearing two large condyles, which articulates with the tibia consequently transmitting weight. Anteriorly the condyles are separated by smooth shallow surface, articulating with patella and posteriorly they protrude considerably with the interval between them forming a deep notch, the intercondylar fossa. The lateral condyle is protruberent and is the broader each in its anteroposterior and transverse diameters. When the femur is held perpendicular, the medial condyle is the longer and projects to a lower level.[1] The distal end is of great importance from the anatomical, functional, and clinical point of view. It is exposed to serious morbidity as a consequence of its position, structure, and weight-bearing function.[2]

Femur is a highly vascular with distinctive blood supply.[3] The diseases affecting knee joint or lower end of the femur such as osteoarthritis and fractures are very common. It is additionally utilized for harvesting vascularized bone grafts. The success of surgical interventions undertaken at lower end is determined by interference by means of corresponding blood supply. Increased incidence of ischemic events at medial femoral condyle over lateral necessitates precise understanding of vascular anatomy.[4]

The purpose of this study is to understand the pattern of blood supply to the distal end of femurthrough the density, size, and direction of its vascular foramina (VF). This would facilitate in contemplating surgical procedures at this region.

Material and Methods

The present study was undertaken on 300 dry normal adult femora obtained from the department of anatomy after obtaining the institutional ethical clearance. Among them, 150 belonged to the right side and rest to the left. Specimens were selected according to the following criteria: (1) no significant

How to cite this article: Bhat D, Doddaiah S, Murugesh P, Pushpa NB. Vascular anatomy of distal end of femur and its clinical implications. J Anat Soc India 2021;70:XX-XX.

Article Info

Received: 25 March 2020
Accepted: 31 January 2021
Available online: ***

Address for correspondence:
Dr. Deepa Bhat,
Department of Anatomy, JSS Medical College, JSS Academy of Higher Education and Research, Mysore - 570 015, Karnataka, India.
E-mail: deepabhat@jssuni.edu.in

Access this article online

Website: www.jasi.org.in
DOI: 10.4103/JASI.JASI_34_20
Quick Response Code:

osteoarthritis or morphological changes in the lower end and (2) bone intactness.

Lower end of the femur was divided into following segments: (a) supracondylar–anterior (SCA)/supracondylar–anterior posterior (SCP); (b) condylar–medial (CM)/condylar–lateral (CL); (c) intercondylar-central/intercondylar peripheral (ICP).

The following parameters were worked out.

- The VF was identified by the presence of a well-marked groove and canal on different segments of the bone. The Kirschner (K)-wire of diameter 0.8 mm was probed through each foramen to verify their patency as well as the size. The foramina which easily admitted K-wire of 2-mm gauge was noted as A ≥2 mm, those which did not allow 0.6 mm K-wire were noted as C ≤0.5 mm, and rest as B = 0.5–2 mm [Figure 1].

The distribution of VF in each of these segments was noted. Their number and size were counted and documented photographically.

The direction of the foramina in each segments were noted and were categorized into three types: horizontal, upper oblique, and lower oblique.

The data collected were entered into Microsoft Excel 2010, and the statistical analysis was done using the SPSS version 22. (IBM Corp. Released 2013. IBM SPSS Statistics for Windows, Version 22.0. Armonk, NY: IBM Corp). The bones were analyzed to determine if the distribution of number of VF was normal. A Wilcoxon signed-rank test was applied to find statistical difference in the number of VF between various segments of lower end of the right and left femur. Friedman test was used to compare the significance in number of VF between segments of two sides. A $P < 0.05$ was taken statistically significant.

Results

A total of 300 (150 right-sided and 150 left-sided) bones were evaluated in this anatomical study.

The average number of VF recorded in different segments at the lower end is shown in Figure 2 and of different sizes in Figure 3.

In the lower end, the maximum average number of VF was observed in medial condylar surface (right - 12.38, left - 12.67) and minimum in the central part of intercondylar region (right 3.23, left - 3.31).

Large-sized VF (>2 mm) was recorded in the left SCP, both left and right CM surfaces. CM recorded the highest number of VF of all sizes.

The direction of VF in the lower end documented was: horizontal - 37.89%; upper oblique - 35.77%; and lower oblique - 26.34%.

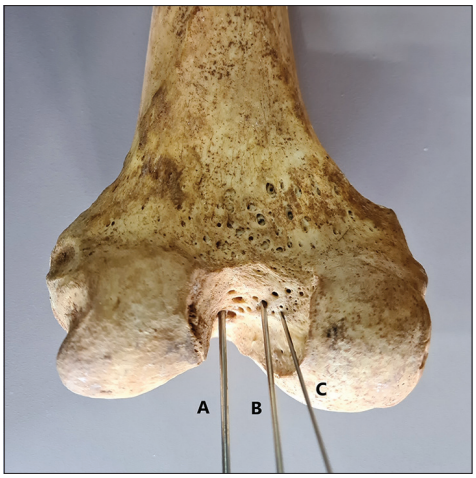

Figure 1: Measurement of VF: A = Vascular foramina easily admitting 2 mm K-wire, B = Admitting 1 mm K-wire, and C = Not admitting 0.6 mm K-wire

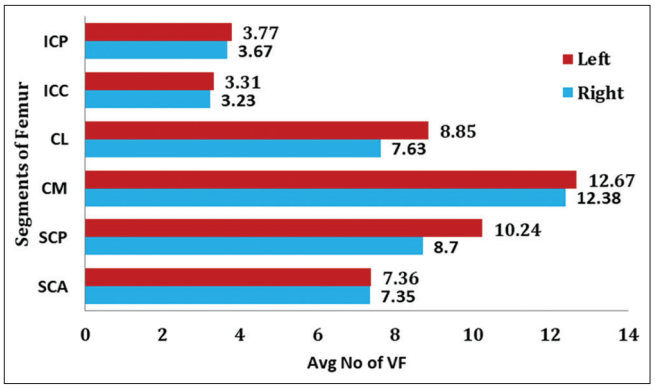

Figure 2: Average number of vascular foramina in different segments of lower end of the femur

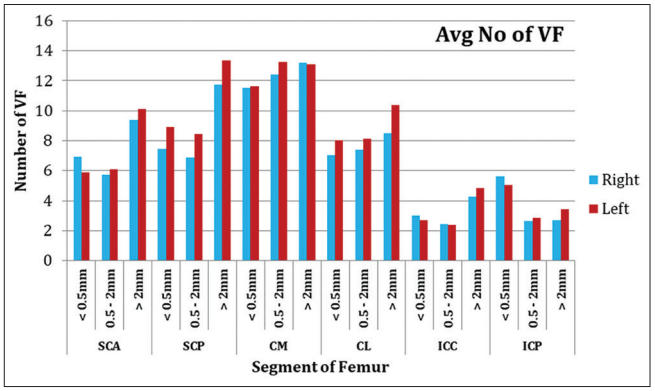

Figure 3: Vascular foramina of various sizes in different segments of lower end of the femur

The VF on various segements of lower end are depicted in Figures 4-8 (A ≥2 mm, B = 0.5–2 mm, and C ≤0.5 mm.

The Shapiro–Wilk test confirmed that the data show a nonnormal distribution of the number of VF ($P = 0.000$). Hence, Wilcoxon signed-rank test was applied to find statistical difference between various segments of lower end of the right and left femur. The segments between which significant difference was noted are described in Table 1.

Table 1: Statistical comparison of vascular foramina between various segments of right and left side

Segments of right and left bones with size	*Z* score	*P*
RSCP<0.5 mm (mean rank=73.56) was rated more favorably than the LSCP<0.5 mm (mean rank=59.67)	−3.009	0.003
RSCP 0.5-2 mm (mean rank=72.15) was rated more favorably than the LSCP 0.5-2 mm (mean rank=61.16)	−3.238	0.001
RSCP>2 mm (mean rank=79.16) was rated more favorably than the LSCP>2 mm (mean rank=63.44)	−2.695	0.007
RCL>2 mm (mean rank=86.68) was rated more favorably than the LCL>2 mm (mean rank=56.62)	−3.737	0.000
RICP>2 mm (mean rank=73.12) was rated more favorably than the LICP>2 mm (mean rank=56.46)	−2.681	0.007

RSCP: Right supracondylar posterior, LSCP: Left supracondylar posterior, RCL: Right condylar lateral, LCL: Left condylar lateral, RICP: Right intercondylar peripheral, LICP: Left intercondylar peripheral

Table 2: Comparison of the number of vascular foramina between segments of two sides

Segment	Side	Mean rank (mm)		
		<0.5	0.5-2	>2
SCA	Left	9.82	8.18	12.66
	Right	7.59	8.27	12.81
SCP	Left	10.24	9.67	13.85
	Right	11.40	10.68	14.88
CM	Left	13.89	14.39	14.74
	Right	13.73	14.48	14.82
CL	Left	9.93	10.43	11.63
	Right	10.46	10.75	12.69
ICC	Left	4.63	3.84	6.42
	Right	3.64	3.26	6.24
ICP	Left	8.34	4.16	4.17
	Right	6.92	3.90	4.48

SCA: Supracondylar anterior, SCP: Supracondylar posterior, CM: Condylar medial, CL: Condylar lateral, ICC: Intercondylar central, ICP: Intercondylar peripheral

Figure 4: Large, prominent vascular foramina in the intercondylar region

Right supracondylar posterior region had statistically significant difference in the number of VF of all the sizes than left. Only the number of VF of >2 mm size was found to be significantly different between right and left in the right condylar lateral and right ICP regions. Right lateral condyle had considerably large number of VF of >2 mm size with statistical significance (P = 0.000).

Friedman test test was used to compare the number of VF between segments of two sides. The results are depicted in Table 2.

A Friedman test indicated that right and left lower end of the femur segments were rated differently: Chi-square (2) = 1236.490, P = 0.000 and Chi-square (2) = 1503.857, P = 0.000, respectively.

Discussion

The distal end of the femur is abundantly nourished by the branches of popliteal artery. The medial condyle is supplied by deep branch of descending genicular artery (DGA) and medial superior genicular artery (MSGA) and lateral condyle by lateral superior genicular artery (LSGA). The arteries to supracondylar region are derived from DGA, MSGA, LSGA, and intercondylar region are from middle genicular artery. Due to generous vascularity, necrosis consequent to fractures seems to be implausible. The studies associated to VF of the femur are meager and scanty literature has been added in the previous 80 years. The density of VF through which the vessels traverse at lower end were not only numerous but also constant and uniformly scattered. The findings are comparable to research by Rogers in 1953.[5] The amplitude of blood supply to the distal end compared to proximal end of the bone has direct implications on the frequency of fractures and other traumatic injuries.[6] Earlier study through resin injection technique has demonstrated that the vessels supplying lower end were of sufficient size to allow microvascular anastomosis (41 mm).[7]

While harvesting the condyles for grafting, vascularity has to be taken into consideration to avoid the donor site complications. The topographic knowledge of larger VF of lower end which admits bigger vessel entry, would help the surgeon to be vigilant during graft preparation, instrumentation, and its fixation.[8]

Distinguishing the vascular pattern around the knee from the perspective of osteotomies is critical, when considering potential complications. Zone of risk has to be precisely considered (zone of high-risk vessels <5 mm from the cut, between 5 mm and 10 mm as moderate, and more than 10 mm as no risk).[9]

MC segment of both sides presented with the highest number of VF of all sizes and density. MC as donor site presents

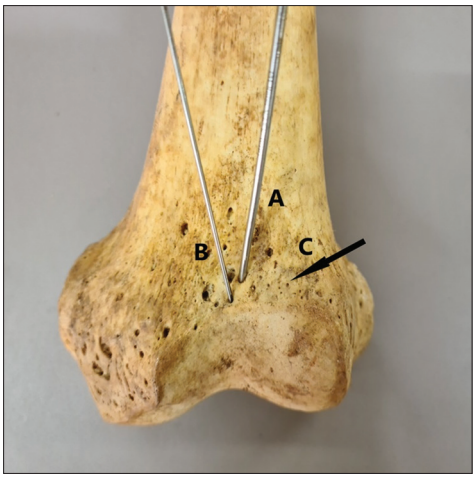

Figure 5: Few vascular foramina on supracondylar anterior surface

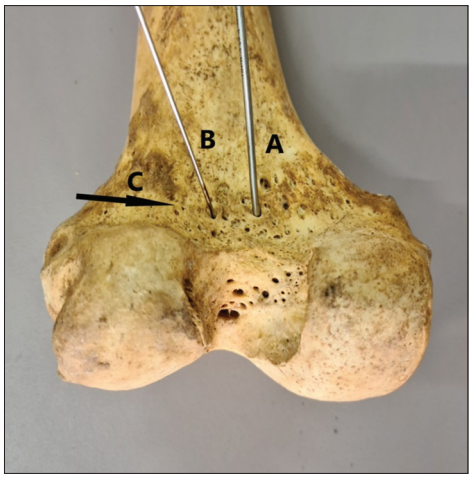

Figure 6: Prominent but few vascular foramina on supracondylar posterior surface

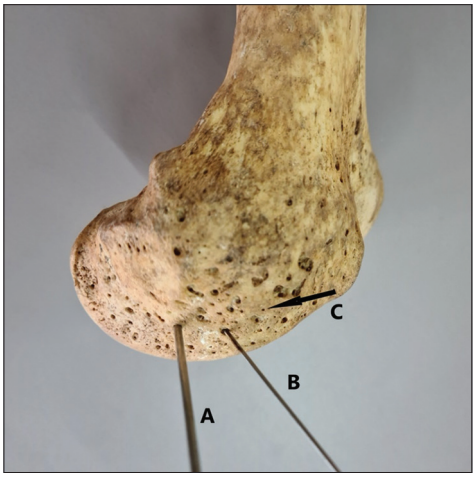

Figure 7: Larger density and prominent vascular foramina on lateral surface of medial condyle

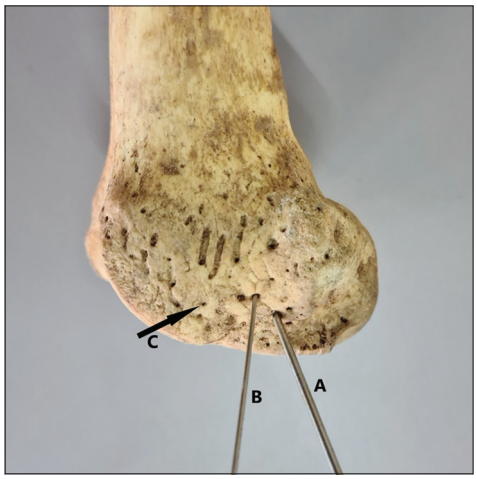

Figure 8: Prominent vascular foramina on lateral surface of lateral condyle

several exceptional features sch as length of pedicle and its diameter that is advantageous for microsurgical transfers. The compound flap at this region offers nutrition to its bony and skin portions separately, permitting various allowing multifold spatial positioning. Martin *et al*. demonstrated the vascular anatomy in 36 cadaveric dissections and found that the pedicle with a diameter of 1.5–3.5 mm at its origin.[10]

Consistent scattering of VF and their larger size provides plentiful periosteal blood supply to MC allowing adequate corticocancellous bone flap harvest without jeopardizing the nutrition.[11] The high osteogenic potential of cambium layer and density of VF makes this area an exemplary choice to combat resistant bony nonunions, irrespective of site and size. Thus, the MC is a preferred donor site for vascularized bone grafts. Being a nonweight-bearing portion with its superficial location provides a broad area of graft that can be harvested without affecting the articulation or strength of femur shaft. No donor site morbidities have been reported in any of the studies till date.[12] In contrast, the clinico pathological studies by Ahuja and Bullough and Ashok and Robert have reported that osteonecrosis of the distal femur occurs more often in the MC than in the LC. This contradicts the assumption of safe utility of MC in graft procedures. Suitability of MC as donor site must be thoroughly evaluated for osteonecrosis due to osteoarthritis or rheumatoid arthritis, etc.[13,14]

CL had average distribution of VF of all sizes with slightly higher number of VF of >2 mm size. This is contrary to the findings of Morsy et al. on wet specimens with the VF of average diameter 1.3 mm (range 0.9–1.7 mm) and 1.2 mm (range 0.7–1.9 mm), from superficial (patellar) branch and a deep (condylar) branch, respectively. The right side showed statistically significant difference in average number of VF than left.[15] A potentially significant difference exists between the intraosseous and extraosseous blood supply to the medial and lateral femoral condyles that may explain the higher frequency of ischemic events occurring in the MC. The intraosseous supply to the LC was shown to consist of an arcade of vessels providing multiple branches to the subchondral bone with no obvious "watershed" region of limited vascularity. The intraosseous supply to the MC

is by a single nutrient vessel nourishing the subchondral bone with an obvious watershed area of limited supply. Furthermore, the proximity of the extraosseous vessels to the MC and the standard femoral tunnel used during posterior cruciate ligament reconstruction may account for the occurrence of avascular necrosis after this procedure.[4]

Rogers' study showed that usually there are 10–15 large foramina and great numbers of smaller foramina (about 20) found in the SCA region. This number is almost similar to foramina on SCP. A few small scattered foramina were observed on the lateral and medial supracondylar region. This is similar to our study except >2 mm sized VF being denser on the right. The utility of this region is clinically correlated by the study of Doi and Sakai, who demonstrated that free vascularized thin corticoperiosteal grafts and small periosteal supracondylar grafts might be readily harvested from this region without disturbing the vascularity. This is due to better osteogenic potential and its compliance to the recipient bed configuration.[16]

Intercondylar area exhibited VF ranging from 3 to 9 in number. The central zone had VF of larger sizes, but periphery had more of <0.5 mm size. This is different from the distribution pattern of Rogers' study that had uniform distribution of 15–25 foramina of sizes ranging from 3 to 8 mm in 22% of bones. Distinct fovea [larger VF ranging from 3 to 8 mm] were observed in the anterior inferior portion of intercondylar fossa between the attachments of cruciate ligaments in 78% of bones. Each fovea had an opening of 5–15 large foramina that extended deeper than smaller and medium-sized VF.

In addition, the density of VF at ICP associated with medial condyle is largely reduced. This could be causative cofactor for osteochondrosis dissecans. Hence, the region adjacent to the femoral insertion of the posterior cruciate ligament is the most frequent site for osteochondrosis dissecans in the knee joint.[17] Osteotomies of the distal femur, for realigning a varus or valgus leg alignment, bleed substantially. The periosteal feeders or larger vessels near the bone cuts should be safeguarded during the procedure.[18]

The limitations of the study would be possible damage to the VF due to prodding by students or while procuring the bone and cleaning, which could alter the dimension of the opening. The combination of cadaveric observational study with intervention through latex injection and analysis through radiographic techniques would further enhance the credibility of these findings.[9]

Conclusion

Several attempts have been made to correlate vascular patterns with the outcome of clinical interventions at the lower end. Detailed understanding of the arterial anatomy of bones utilized for harvesting vascularized bone flaps allows identification of portions at risk. The pattern of distribution of VF at different segments of lower end affirms the nonoccurrence of osteonecrosis at the distal end. However, localization of vascular pedicles of larger size will ensure the vitality of graft as well as donor site.

Financial support and sponsorship

Nil.

Conflicts of interest

There are no conflicts of interest.

References

1. Standring S. Gray's Anatomy: The Anatomical Basis of Clinical Practice. 41st ed. London: Elsevier; 2016. p. 1348-50.
2. Raghu KJ, Anaberu P, Oswal VM. Minimally invasive plate osteosynthesis of lower end of femur fractures using locking compression plating: A prospective study. Int J Res Orthop 2017;3:1043-50.
3. Laroche M. Intraosseous circulation from physiology to disease. Joint Bone Spine 2002;69:262-9.
4. Reddy AS, Frederick RW. Evaluation of the intraosseous and extraosseous blood supply to the distal femoral condyles. Am J Sports Med 1998;26:415-9.
5. Rogers WM, Gladstone H. Vascular foramina and arterial supply of the distal end of femur. J Bone Joint Surg 1953;32:867-74.
6. Liang PG. The blood supply of the femoral shaft: Anatomical study. J Bone Joint Surg Am 1953;35-B: 462.
7. Yamamoto H, Jones Jr., DB, Moran SL, Bishop AT, Shin AY. The arterial anatomy of the medial femoral condyle and its clinical implications. J Hand Surg Eur 2010;35:569-74.
8. Rogers WM, Gladstone H. Vascular foramina and arterial supply of the distal end of the femur. J Bone Joint Surg Am 1950;32:867-74.
9. Bisicchia S, Rosso F, Pizzimenti MA, Rungprai C, Goetz JE, Amendola A. Injury risk to extraosseous knee vasculature during osteotomies: A cadaveric study with CT and dissection analysis. Clin Orthop Relat Res 2015;473:1030-9.
10. Martin D, Bitonti-Grillo C, DeBiscop J, Schott H, Mondie JM, Baudet J, *et al*. Mandibular reconstruction using a free vascularized osteocutaneous flap from the internal condyle of the femur. Br J Plast Surg 1991;44:397-402.
11. Rysz M, Grabczan W, Mazurek MJ, Krajewski R, Grzelecki D, Ciszek B. Vasculature of a medial femoral condyle free flap in intact and osteotomized flaps. Plast Reconstr Surg 2017;139:992-7.
12. Kumta S, Warrier S, Jain L, Ummal R, Menezes M, Purohit S. Medial femoral condyle vascularised corticoperiosteal graft: A suitable choice for scaphoid non-union. Indian J Plast Surg 2017;50:138.
13. Ahuja SC, Bullough PG. Osteonecrosis of the knee. A clinicopathological study in twenty-eight patients. J Bone Joint Surg Am 1978;60:191-7.
14. Ashok SR, Robert WF. Evaluation of the intraosseous and extraosseous blood supply to the distal femoral condyles. Am J Sports Med 1998;26:415-19.
15. Morsy M, Sur YJ, Akdag O, Eisa A, El-Gammal TA, Lachman N, *et al*. Anatomic and high-resolution computed tomographic angiography study of the lateral femoral condyle flap: Implications for surgical dissection. J Plast Reconstr Aesthet Surg 2018;71:33-43.
16. Doi K, Sakai K. Vascularized periosteal bone graft from the supracondylar region of the femur. Microsurgery 1994;15:305-15.
17. Lankes M, Petersen W, Hassenpflug J. Arterial supply of the femoral condyles. Z Orthop Ihre Grenzgeb 2000;138:174-80.
18. Van der Woude JA, van Heerwaarden RJ, Bleys RL. Periosteal vascularization of the distal femur in relation to distal femoral osteotomies: A cadaveric study. J Exp Orthop 2016;3:6.

Original Article

Sheath of Distal Tendon of Semimembranosus Muscle and it's Functional Significance

Subhash D. Joshi, Sharda S. Joshi, Namrata Valimbe

Department of Anatomy, Sri Aurobindo Medical College and Post Graduate Institute, Indore, Madhya Pradesh, India

Abstract

Introduction: Semimembranosus (SM) muscle is important in maintaining the stability of knee joint, and the distal end of it's tendon is not only complex but has been described differently in the available literature, which is quite perplexing. How a muscle with such divergent attachments can efficiently perform it's functions? Hence a detailed study of the distal semimembranosus tendon unit was undertaken. **Material and Methods:** One hundred lower limbs (Rt-50; lt.-50) were utilized for the present study. The posterior surface of SM was exposed and as the main tendon could not be traced to its insertion hence a vertical incision was made on the posterior surface of this tendon and this lead to the splitting of the tendon-sheath which exposed the thick shining distal tendon of SM. **Results:** Surprisingly, it was found that the main tendon of the SM (SMT) was surrounded by a fibrous sheath which was derived from the main muscle mass in the lower part of the thigh and in the majority of cases it was separated from it by a synovial space. Traced inferiorly it was observed that it is the sheath that spreads out to various divergent destinations described in the literature, whereas the main tendon gets attached to the groove on the posterior aspect of the medial condyle of tibia and a rough triangular area below the groove. **Discussion and Conclusion:** It is the nature's ingenuity that a single muscle with such divergent distal attachments can still efficiently perform its functions due to the formation of a sheath of distal tendon of SM.

Keywords: *Distal tendon, expansions of SM, semimembranosus, sheath of SMT*

Introduction

The posterior aspect of the knee, due to the clinical relevance of its musculoskeletal system is very important and the anatomists must have a definitive and precise understanding of the morphology of this region.

Semimembranosus muscle (SM) is a key component of the complex anatomy of the posteromedial aspect of knee joint. The distal tendon of semimembranosus has always attracted the curiosity and attention of orthopedic surgeons, radiologists, biomechanists, physical therapists and anatomists, but there is no clearly defined uniformity in the description of termination of the tendon of insertion of semimembranosus and it's nomenclature. A variable number of expansions of the distal tendon of SM have been described.

It had always been very intriguing to be convinced by the idea that in spite of so many divergent expansions and attachments of the distal tendon of SM muscle at its insertion, how can it so efficiently perform the movement of flexion at the knee joint? Why the pull of the contracting muscle should be lost or wasted by diverging to such attachments as oblique popliteal ligament (OPL), Fascia over the popliteus muscle, medial collateral ligament (MCL) of the knee joint, menisci, etc., and it's main tendon of insertion on the medial condyle of tibia?

The literature search revealed significantly inconsistent morphology of the distal semimembranosus tendon unit (SMTU). This prompted us to undertake a detailed study of SM muscle.

Material and Methods

One hundred lower limbs (Rt. 50, Lt. 50), which were used for the routine dissection by students over a period of few years were utilized for the present study. Hamstrings were traced towards the popliteal fossa. On the medial side, the tendon of semitendinosus was identified and reflected inferiorly exposing the posterior surface of

How to cite this article: Joshi SD, Joshi SS, Valimbe N. Sheath of distal tendon of semimembranosus muscle and it's functional significance. J Anat Soc India 2021;XX:XX-XX.

Article Info

Received: 04 October 2020
Accepted: 22 February 2021
Available online: ***

Address for correspondence:
Dr. Subhash D. Joshi, Department of Anatomy, Sri Aurobindo Medical College and Post Graduate Institute, Indore, Madhya Pradesh, India. E-mail: sdjoshi_2003@hotmail.com

Access this article online

Website: www.jasi.org.in
DOI: 10.4103/jasi.jasi_206_20
Quick Response Code:

the semimembranosus muscle. The neuro-vascular bundle present in the popliteal fossa was cleaned and removed to expose the posterior surface of the fibrous capsule of knee joint and the OPL, the fascia covering the popliteus muscle and in the upper medial part the Posterior Oblique Ligament (POL), MCL was also cleaned and exposed.

Having done this the thick tendon of SM was identified; but the main tendon that has to insert on tibia could not be seen. Hence, a vertical incision was made on the posterior surface of this tendon and this lead to the splitting of the tendon-sheath which exposed the thick shining distal tendon of SM [Figure 1]. After extending the incision inferiorly on the tendon sheath the main tendon could be traced inferiorly where it was found to continue: (a) as a thick tendon that bent at right angle to pass anteriorly deep to MCL in the groove on the posterior surface of medial condyle of tibia, and (b) the rest of it continued inferiorly and expanded to be attached to the rough triangular area below the Medial condyle of tibia [Figure 2].

Tendon sheath of SM was carefully traced distally where it was found to diverge to be continuous with: (a) OPL, (b) fascia covering the posterior surface of popliteus muscle [Figures 3 and 4], (c) merging with the posterior edge of the MCL and some fibres passing deep to it to be attached to the upper part of medial border of tibia (POL). Details were noted and Photographs were taken at various stages of dissection.

The posterior surface of the upper end of dry tibia were examined for the presence of groove on the posterior surface of the medial condyle and the rough triangular area below the groove.

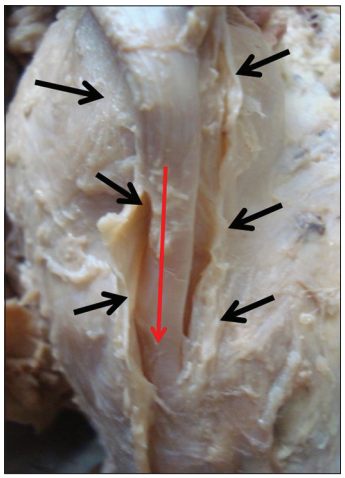

Figure 1: Dissection of the posterior aspect of right knee showing the Thick tendon of SM (red arrow) seen after splitting the sheath (cut edges shown with black arrows) which extends well above the joint line of the knee

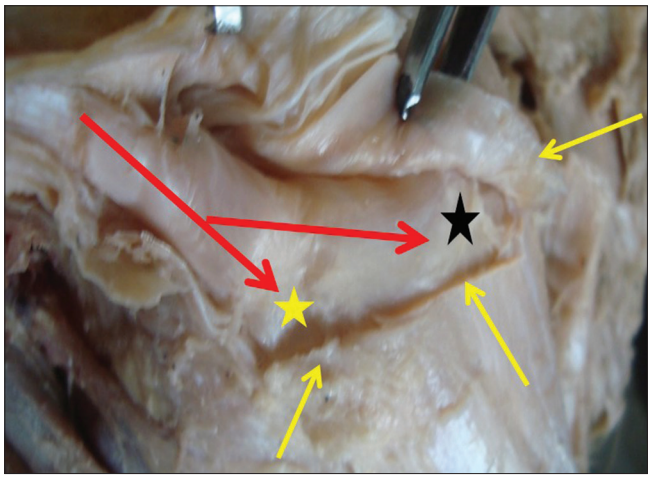

Figure 2: The main tendon of SM (red arrow) to bifurcate into two after crossing the knee joint. One part (black star) passes deep to the medial collateral ligament (cut edges of which are shown by yellow arrows) and gets attached to the groove on the posterior surface of medial condyle of tibia. The other part (yellow star) gets attached to the rough triangular area below the groove

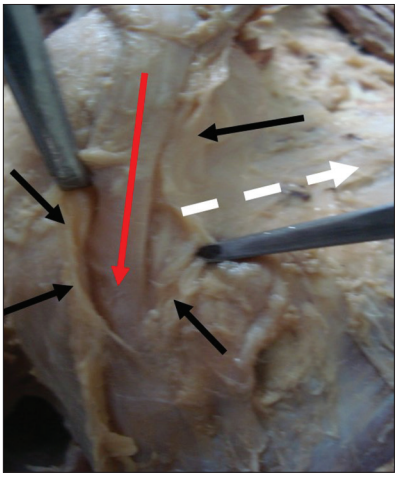

Figure 3: Main tendon (red arrow); cut edge of the sheath indicated by black arrows. Oblique popliteal ligament shown by white interrupted arrow which is seen to be continuous with sheath of SM

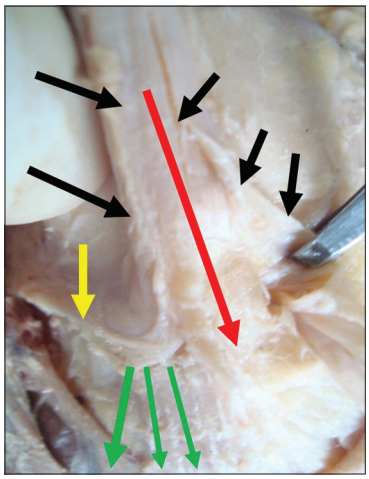

Figure 4: Posterior surface of left SM main tendon shown by red arrow. Edges of the split sheath shown by black arrows. Oblique popliteal ligament (yellow arrow) is seen to be continuous with the sheath. Green arrows indicate the fascia covering the popliteus muscle

Results

When the tendon of Semitendinosus is reflected downwards behind the knee then the grooved posterior surface of SM was clearly visualized. Slightly above the knee joint, the fleshy fibres are replaced by the thick strong tendon [Figure 1]. A vertical incision was made on the posterior surface of this tendon which opened up a sheath surrounding the main tendon which lies within it [Figures 5 and 6]. In the majority of cases, there was a shining synovial sheath surrounding the tendon [Figure 7]. In other cases, where the lining synovial membrane between the tendon and sheath was absent, the tendinous sheath was found to be adherent to the main tendon. One part of the main tendon passed almost at right angles deep to the MCL to be attached to the groove on the posterior surface of the medial condyle of tibia [Figure 8]. The other part of the tendon was found to be attached to the triangular area on the posterior surface of the medial condyle of tibia just below the groove [Figure 2]. Posterior surface of upper end of dry tibia were examined and it was found that in the majority there was prominent rough triangular area below the groove on the posterior surface of medial condyle. It showed prominent vertical ridges and also a large number of vascular foramina [Figure 9a-c]. The tendon sheath when dissected and traced distally was found to spread out to various destinations to form: (a) POL, (b) fascia over the popliteus muscle, (c) OPL and to merge with MCL [Figures 3 and 4]. At the level of the middle of thigh: on the anterior surface of the SM muscle fleshy fibers were observed, which when traced inferiorly were found to be flanking on either side of the centrally placed muscle mass and led to the formation of the sheath of SM, and the central part continued as the main tendon of the muscle [Figures 10 and 11].

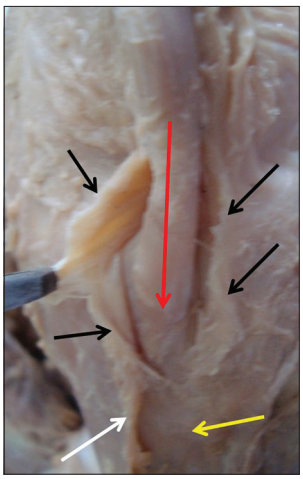

Figure 5: Dissection of the posterior aspect of right knee showing the Thick tendon of SM (red arrow) exposed after splitting the sheath (black arrows). Fascia over the popliteus muscle (yellow arrow) and the medial ligament of knee (white arrow) are also seen

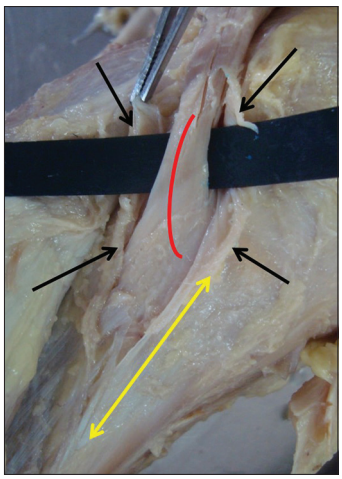

Figure 6: Dissection of the posterior aspect of left knee showing tendon of SM (red line) and cut edges of sheath (black arrows). Medial collateral ligament (yellow arrow)

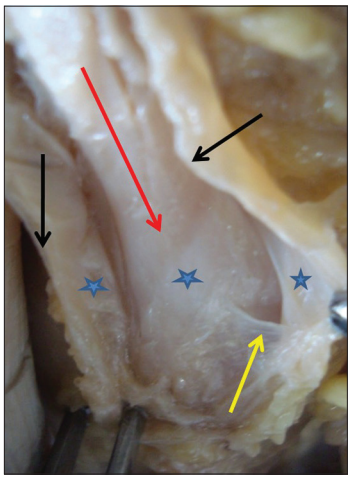

Figure 7: Dissection of the posterior aspect of left knee showing the SM tendon (red arrow) seen after splitting the sheath of the tendon (black arrows); delicate synovial membrane (yellow arrow) seen. This is also seen to wrap the tendon and its sheath (blue stars

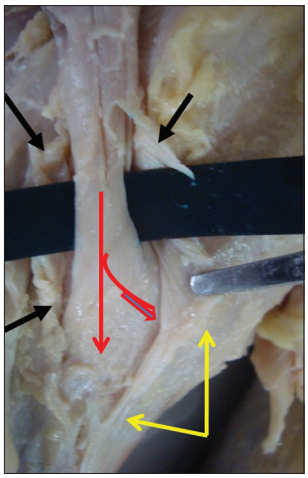

Figure 8: Dissection of the posterior aspect of left knee showing tendon of SM seen to divide into two: One part passes deep to medial collateral ligament (yellow arrows) of knee and the other proceeds in a straight line (red arrow) to posterior surface of tibia below the medial condyle. Cut edges of the sheath shown by black arrows. Black strip is placed deep to the tendon, between it and the sheath

Discussion

In the present study, the main tendon of SM after crossing the knee joint was seen to divide into two parts: One part of the tendon passed almost at right angles deep to the MCL to be attached to the groove on the posterior surface of the medial condyle of tibia [Figure 2]. This is in agreement with the description by Gardner *et al*.,[1] Sinnatamby,[2] Standring *et al*.[3] Snell,[4] and Benninger and Delamarter.[5]

The other part of the main tendon was getting attached to the triangular area on the posterior surface of the medial condyle of tibia just below the groove [Figures 2 and 12]. It has been mentioned that the main tendon is attached to a tubercle on the posterior aspect of medial tibial condyle;[3] and others have also mentioned that from the deep part of the tendon a short slip is attached to a tubercle below the groove,[1] which in the present study was found to be in the form of a rough triangular area [Figure 9a-c] below the medial condyle of tibia. This is quite a prominent area of insertion on the posterior surface of tibia below the groove on the medial condyle of tibia, giving attachment to SM tendon, which has been shown in illustrations in books.[3,4,6]

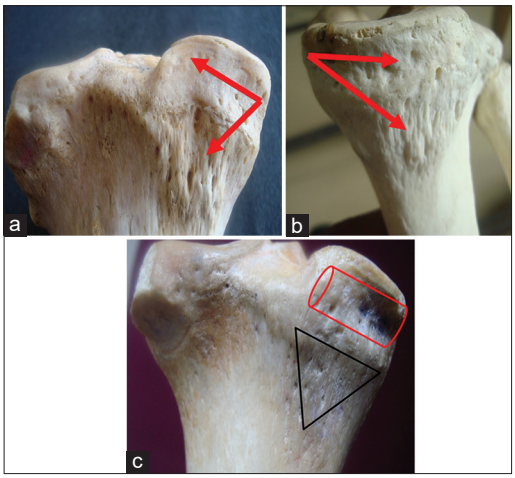

Figure 9: (a) Posterior surface of upper end of left tibia showing the insertion of SM by red arrow in the groove on the posterior surface of medial condyle of tibia and the rough triangular area below the groove. (b) Posterior surface of right tibia showing the insertion of SM by red arrows in the groove on the posterior aspect of medial condyle and the rough triangular area below it. (c) The groove on the posterior aspect of medial condyle of tibia marked by red and rough triangular area indicated by black triangle

Expansions of distal tendon of SM

While reviewing the literature we find that various workers have described the number of expansions of distal attachment of SM varying from three to eight, and the nomenclature of these expansions is also variable and confusing.

Moore stated that SMT divides distally into *three parts*.[7]

Sinnatamby stated that the insertion of SMT diverges into three expansions: (1) passes forwards along the medial

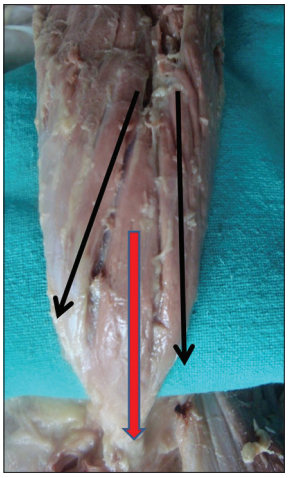

Figure 10: Central part of SM (red arrow) continues inferiorly as the main tendon, and the flanking part of the muscle on either side (black arrows) when traced inferiorly leads to the formation of the sheath of the SM tendon

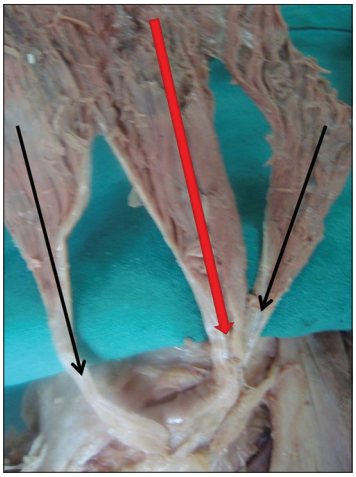

Figure 11: The central part of SM (red arrow) is seen to continue as a strong tendon and the muscle mass flanking on either side continues inferiorly as tendon sheath of SM

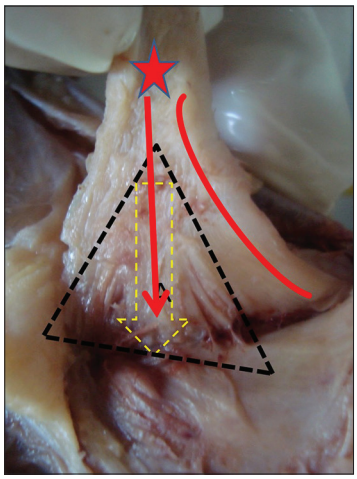

Figure 12: Posterior surface of left SM main tendon (red star) diverting into two limbs (red arrows)- the right curved one is lodged in the groove on the posterior surface of medial condyle and the vertical component continues inferiorly and expands to be attached to the rough area below the groove

surface of the condyle deep to tibial collateral ligament, (2) expansion passes obliquely upwards to the lateral femoral condyle as OPL, and (3) forms a strong fascia over popliteus and reaches the soleal line of tibia.[2]

In a comprehensive review article, Benninger and Delamarter[5] have quoted the works of some authors[3,8,9] who have described a total of five expansions of SM.

Moncayo *et al*. have also described that there are five tendinous expansions in the meniscocapsular complex of distal SM insertions.[10]

Maeseneer *et al*. have stated that the anatomy of the distal SMT is complex and six different insertions can be identified on routine proton density and FE sequences at 3 T.[11]

Kim *et al*. have described a tendinous branch of SM inserting into posterior horn of lateral meniscus in 43.2% of knees dissected, This is in addition to 5 already known insertional branches i.e., six attachments.[12]

Beltran *et al*. described five tendinous insertions and additionally two more attachments to the posterior horns of medial and lateral meniscus, i.e., a total of seven attachments; and have further stated that the different tendinous arms of SM complex are intimately related to the POL and the arcuate ligament. The POL (Ligament of Winslow) originates from the adductor tubercle of the femur.[13]

Turman *et al*. have mentioned eight consistent insertions of SM, distal to the main common tendon. They have stated that as the insertion of SM tendon is extra capsular, it is not typically visualized during arthroscopy.[14]

LaPrade *et al*. described SMTU and have stated that there are eight consistent posterior attachments of the SM distal to the main common tendon at the knee.[15]

In the present study, we found that the fleshy fibres commenced at the level of the middle of the thigh. This is in agreement with the observation wherein it has been stated that the muscle fibres of SM commence about the middle of the thigh.[2] Whereas other authors have stated that the tendon of SM becomes muscular in the upper part of the thigh and the tendon of insertion begins about the middle of the thigh.[1,7]

In the present study, it was observed that the fleshy fibres, that were present on the anterior surface of the muscle, when traced inferiorly were seen to be flanking on either side of the centrally placed muscle mass [Figure 10] and led to the *formation of the sheath of SM*. The centrally placed muscle fibres continued as the main tendon of the muscle [Figure 11] in the lower part of the thigh.

Gardner, Gray and O'Rhahilly have not described the sheath of SM but mentioned that it consists of a Superficial part which turns upwards and laterally as the OPL of the knee joint; the remainder forms the fascia of popliteus and is attached to the medial border and soleal line of tibia.[1]

In the literature reviewed, we found only Warren and Marshal who described the SMTU as having two main insertions and a tendon sheath. The division between the tendon fibres going directly to the bone and the fibres of the sheath splaying out into the posteromedial part of the capsule is usually clear.[16]

Loredo *et al*. who have studied the postero-medial aspect of the knee with MR imaging and correlated it with gross anatomy and concluded that there are: five arms of insertions, the third arm is derived mainly from the tendon sheath and blends with the posteromedial capsule.[17]

In the present study, we have observed that the main tendon gets attached to the groove on the posterior surface of medial condyle of tibia and the rough triangular area below it. All the expansions were seen to be derived from the tendon sheath of SM rather than the main tendon as is described by different workers. The sheath was seen to be spreading out in various directions to their destination viz. POL. MCL, popliteal fascia and OPL.

Kim *et al*. are of the opinion that the multiple insertions of SM at the knee contribute to the medial stability of the knee specially in flexion, and when combined with the action of popliteus muscle they contribute together to maintain the posterior stability.[12]

Beltran *et al*. discussing the biomechanics have mentioned that the intricate distal insertion of SM in the posteromedial aspect of the knee and biceps in the posterolateral aspect of the knee allow these two muscles to become very important stabilizing structures during knee flexion. The dynamic synergy of the SM complex and the biceps femoris also provides controlled stability of the flexed knee during internal and external rotation. Conceptualization of SM and biceps femoris complexes as horse reins attached to the medial and lateral aspect of the capsule adds to the understanding of these functions.[13]

SM stabilizes the posterior capsule through OPL and acts synergistically with the popliteus muscle through the fibrous extension. It contributes to the stability of posteromedial aspect of the joint through its intertwining with POL They further mention that the different structures of the SM complex act as a suction cup placed over the posteromedial aspect of the knee as seen from inside the joint with the knee in flexion.[13]

Kim *et al*. state that SM actively pulls the posterior horns of the medial and lateral meniscus, protecting them from being crushed between femoral condyles and the medial and lateral tibial plateau during knee flexion.[12]

Maeseneer *et al*. mention that in knee extension the SMT prevent valgus, whereas in knee flexion it prevents external rotation.[11]

Schache *et al*. discussing the biomechanics of the Human Hamstring Muscles during Sprinting mention that as peak musculotendon force and strain for long head of Biceps femoris, Semitendinosus and SM occurred around the same time during terminal swing phase, the biarticular hamstrings are at greatest risk of injury. SM produced the highest peak force, absorbs and generates the most power and performs the largest amount of positive and negative work.[18]

Conclusion

After a detailed study, it can be stated that nature has with its ingenuity provided an excellent solution to this complexity of distal attachment of SM muscle by allowing the main tendon of insertion to pass through a sheath, which is also derived from the same muscle (and is mostly separated by a synovial space), that the sheath spreads out to their various destinations. The main tendon passes (a) deep to the MCL to be attached to a groove on the posterior surface of the medial condyle of tibia and (b) to a rough triangular area at the upper end of the posterior surface of the shaft of tibia below this groove.

The sheath gets wide purchase over all these areas of attachment of the distal tendon of SM and probably has a stabilizing effect on the central tendon to exert its unhindered pull over its insertion to bring about flexion at the knee joint as well as provide stability to the joint.

Thus it makes it amply clear that the architecture of the muscle can be resolved into a sheath of SM that spreads out to various divergent attachments and surrounds the main tendon that can work independently on the tibia during the movements at the knee joint.

Thus SM besides providing strength to the posteromedial part of the knee joint can also function unhindered due to the presence of it's sheath to produce the flexion at the knee joint and medial rotation of leg.

Financial support and sponsorship

Nil.

Conflicts of interest

There are no conflicts of interest.

References

1. Gardner E, Gray DJ, O'Rahilly R. Anatomy: Regional Study of Human Structure. 4th ed. London: W B Saunders Co.; 1975. p.186, 213.
2. Sinnatamby CS. In: Last's Anatomy, Regional and Applied. 10th Edition. Churchill Livingstone. Edinburgh; 1999. p. 126,166.
3. Standring C. In: Gray's Anatomy. The Anatomical Basis of Clinical Practice. 40th Edition. Churchill Livingstone; Edinburgh 2008. p. 1414, 1377.
4. Snell RS. Clinical Anatomy by Regions. 8th Edition: Wolters Kluwer, Lippincott Williams and Wilkins; Philadelphia 2008. p. 595.
5. Benninger B, Delamarter T. Distal Semimembranosus muscle tendon unit Review: Morphology, accurate terminology and clinical relevance. Folia Morphol 2013;72:1-9.
6. Augur AM, Dalley AF. In: Grant's Atlas of Anatomy. 14th Edition. Wolters Kluwer, South Asian Ed; 2017. p. 503.
7. Moore KL, Dalley AF, Augur AM. In: Moore Clinically Oriented Anatomy. 7th Edition. Wolters Kluwer, Lippincott Williams and Wilkins; Philadelphia. 2014. p. 572.
8. Woodburne RT. In: Essentials of Human Anatomy. Editors Benninger B, Delamarter T, Oxford: University Press; 1978.
9. Hollinshead WH. The back and limbs. In: Benninger B, Delamarter T, editors. Anatomy for Surgeons. Vol. 3. New York: Hoeber- Harper; 1961.
10. Moncayo VM, Carpenter WA, Pierre-Jerome C, Smitson RD, Terk MR. Congenital absence of the semimembranosus muscle: Case report. Surg Radiol Anat 2010;32:519-23.
11. Maeseneer MD, Shahabpour M, Lenchik L, Ridder MA, May JD, Cattrysse E. Distal insertion of Semimembranosus tendon: MR imaging with anatomic correlation. Skeletal Radiol 2014;43:781-91.
12. Kim YC, Yoo WK, Chung IH, Seo JS, Tanaka S. Tendinous insertion of semimembranosus muscle into the lateral meniscus. Surg Radiol Anat 1997;19:365-9.
13. Beltran J, Matityahu A, Hwang K, Jbara M, Maimon R, Padron M, *et al*. The distal semimembranosus complex: Normal MR anatomy, variants, biomechanics and pathology. Skeletal Radiol 2003;32:435-45.
14. Turman K, Miller CD, Miller MD. Semimembranosus tendon viewed through an isolated medial meniscus capsular avulsion: A case report. Knee Surg Sports Traumatol Arthrosc 2010;18:760-2.
15. LaPrade RF, Morgan PM, Wentorf FA, Johansen S, Engebretsen L. The anatomy of the posterior aspect of the knee. An anatomic study. J Bone Joint Surg Am 2007;89:758-64.
16. Warren LF, Marshall JL. The supporting structures and layers on the medial side of the knee: An anatomical analysis. J Bone Joint Surg Am 1979;61:56-62.
17. Loredo R, Hodler J, Pedowitz R, Yeh LR, Trudell D, Resnick D. Posteromedial corner of the knee: MR imaging with gross anatomic correlation. Skeletal Radiol 1999;28:305-11.
18. Schache AG, Dorn TW, Blanch PD, Brown NA, Pandy MG. Mechanics of the human hamstring muscles during sprinting. Med Sci Sports Exerc 2012;44:647-58.

Original Article

Evaluation of Morphometric and Volumetric Measurements of Temporomandibular Joint Structures on Patients with Disc Displacement

Melike Başaran, Esin Bozdemir[1], Şehnaz Evrimler[2]

Department of Dentomaxillofacial Radiology, Faculty of Dentistry, Kutahya Health Sciences University, Kutahya, [1]Department of Dentomaxillofacial Radiology, Faculty of Dentistry, Suleyman Demirel University, [2]Department of Radiology, Faculty of Medicine, Suleyman Demirel University, Isparta, Turkey

Abstract

Introduction: To evaluate the morphometric and volumetric measurements of the temporomandibular joint (TMJ) structures, of healthy, anterior disc displacement with reduction (ADDWR) and anterior disc displacement without reduction (ADDWoR) joints using magnetic resonance imaging (MRI). **Material and Methods:** Fifty-two TMJs of 38 patients with TMJ disorders and 26 TMJs of 13 healthy patients were evaluated on MRI images. The disc length and volume, the condylar height, width and volume, and the height and inclination of the articular eminence were measured on MRI. A one-way analysis of variance was used to establish the differences between the values with regard to the ADDWR, ADDWoR, and control groups. The differences in the disc volumes of each group with respect to open and closed mouth position statuses were evaluated using the Bonferroni test. **Results:** The articular disc mean volume was larger in the control group than the other two groups for both the closed and open mouth positions ($P < 0.05$). There were statistically significant differences between the control group and the other two groups in terms of the condylar width and disc length ($P = 0.00$ and $P = 0.001$, respectively). The mean articular eminence inclination was the lowest in the ADDWoR group and the highest in the control group ($P = 0.02$). **Discussion and Conclusion:** Measurements of the disc volume, disc length, condylar width, and articular eminence inclination are associated with disc displacement (DD). Degenerative changes that may cause morphometric and volumetric changes in TMJ structures may be a marker of TMJ DD.

Keywords: *Magnetic resonance imaging, mandibular condyle, temporomandibular joint disc, temporomandibular joint disorders*

Introduction

The temporomandibular joint (TMJ) is an articulation between the mandibular condyle and the mandibular fossa and articular eminence.[1] The articular disc is positioned between the condyle and the temporal bone components, and it has a biconcave shape with a thick anterior band, thicker posterior band and thin middle part. In normal disc-condyle relationship, the posterior band is located above the condyle near the 12 o'clock position. In the open mouth position, the thin intermediate zone lies between the condylar head and the articular eminence.[2] TMJ disc displacement (DD) is one of the most commonly seen pathologies in the internal derangement (ID) of the TMJ, and it is defined as an abnormally positioned or displaced disc.[3] The disc can become displaced in any direction but anterior DD is most common type of DD.[2,4] Magnetic resonance imaging (MRI), which is a radiation-free, noninvasive imaging modality with high tissue contrast, is currently the best imaging method for evaluating the disc and diagnosing DD.[4-6] Many authors have assessed the morphometric characteristics of the TMJ, and they have suggested that DD could lead to changes in the morphology and morphometric characteristics of TMJ.[1,4,7-9] Although there have been studies evaluating the morphometric and volumetric measurements of the TMJ in patients with DD,[1,9-11] there have been few studies that have determined the relationship between the disc volume and DD in the literature.[12,13] Therefore, the purpose of this study was to evaluate the morphometric and volumetric features of the TMJ structures of healthy, anterior DD with reduction (ADDWR), and anterior DD without reduction (ADDWoR) joints using MRI.

How to cite this article: Basaran M, Bozdemir E, Evrimler S. Evaluation of morphometric and volumetric measurements of temporomandibular joint structures on patients with disc displacement. J Anat Soc India 2021;70:XX-XX.

Article Info

Received: 29 April 2020
Accepted: 15 February 2021
Available online: ***

Address for correspondence:
Dr. Melike Başaran, Department of Dentomaxillofacial Radiology, Faculty of Dentistry, Kutahya Health Sciences University, Kutahya, Turkey.
E-mail: basarannm@gmail.com

Access this article online

Website: www.jasi.org.in
DOI: 10.4103/JASI.JASI_77_20
Quick Response Code:

Material and Methods

Sample selection

This prospective study was approved by the 98,227 project number by the clinical research ethics committee of the university hospital, and the participants signed approved consent forms. Fifty-two TMJs of 38 patients (6 males and 32 females) with Temporomandibular disorders (TMD) and 26 TMJs of 13 healthy patients (7 males and 6 females) were evaluated in the present study. All patients included in this study were clinically examined according to the Research diagnostic criteria for TMD axis I protocol. As a result of clinical examination, patients between 18 and 40 years' old who presented at least two positive clinical TMD symptoms underwent MRI examinations and then patients who detected anterior DD on MRI images included in the TMD group. Patients who had no clinical TMD symptom and normal disc-condyle relationship on MRI images were included in the control group. The exclusion criteria were as follows: Systemic or inflammatory joint diseases, congenital deformities or syndromes, trauma, maxillofacial bone fractures, or surgeries in the TMJ area.

Magnetic resonance imaging examination

The MRI examinations were performed using a 1.5 T MRI scanner (Siemens Magnetom Avanto; Siemens Medical Systems, Erlangen, Germany). Each subject was placed in a supine position, with the sagittal plane perpendicular to the horizontal plane and the Frankfort plane parallel to the scanner gantry. A bite block (Dental Mouth Prop Bite Block; Shangai Carejoy Medical Co., Guangzhou, China) was used to stabilize the maximal mouth opening and minimize motion artefacts in the open mouth position. The osseous structures of the TMJ were evaluated using a 0.9-mm section thickness 3D flash T1-weighted sequence (repetition time [TR]: 21 ms, echo time [TE]: 4.95 ms, matrix: 224 × 156 pixels, voxel size: 0.9 mm × 0.9 mm × 0.9 mm, field of view: 200 mm). The articular disc was evaluated using a 1.2-mm section thickness three-dimensional proton-density (PD) weighted sequence (TR: 1200 ms, TE: 39 ms, matrix: 256 × 228 pixels, voxel size: 0.6 mm × 0.6 mm × 1.3 mm, field of view: 165 mm). OsiriX MD v. 7.5.1 software (2016; PixmeoSarl, Bernex, Switzerland) was used for the diagnostic evaluation and the linear and volumetric measurements. MRI images were examined by a radiologist with 10 years' experience, and the patients divided into three groups: ADDWR, ADDWoR, and control. ADDWR was considered the posterior band of the disc was located anteriorly to the condylar head in the closed mouth position and have normal position during the mouth opening. ADDWoR was diagnosed the disc was positioned anteriorly to the condyle both in the closed and in open mouth positions.[2-4] Control group was accepted normal disc position to the condyle in the closed and open mouth position. All measurement was made by a dentomaxillofacial radiologist with 5 years' experience.

Linear measurements

Disc length and disc volume

The most anterior (A) and most posterior (B) points of the disc and the midpoint of the intermediate zone (C) were noted on the sagittal PD-weighted images. The disc length was calculated as the sum of the AC and BC distances.[14] The disc volume was measured for 5 consecutive sequences by drawing the borders of the disc in the open and closed mouth positions on the sagittal PD-weighted images [Figure 1].

Condylar height, condylar width and condylar volume

Two circles were drawn internally in order to determine the condylar long axis on the sagittal T1-weighted images. O_1 was a tangent circle that was drawn between the condylar neck and the condylar head. O_2 was a tangent circle that was drawn on the narrowest region of the condylar neck. γ was the axis of the condylar neck passing through the center of the two circles. A line was drawn perpendicular to the γ, which passed from the lowest part of the sigmoid notch as the horizontal axis (x), and the line parallel to the x and tangent to the top of the condylar head was designated x'. The condylar height was calculated as the distance between x and x' (H).[4] The condylar width was calculated by measuring the distance between the most medial and lateral points of the condyle, where the condyle was widest on the coronal T1-weighted images.[9] The condylar volume was measured from the sigmoid notch to the top of the condyle, while drawing the borders of the condyle on the axial T1-weighted images [Figure 2].

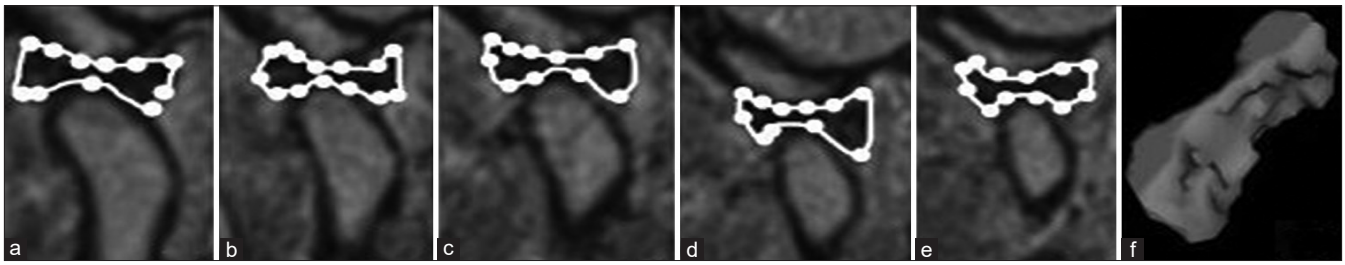

Figure 1: Drawing of the disc borders on five consecutive sagittal magnetic resonance imaging sections on the open mouth position (a-e) and three-dimensional image of the disc (f)

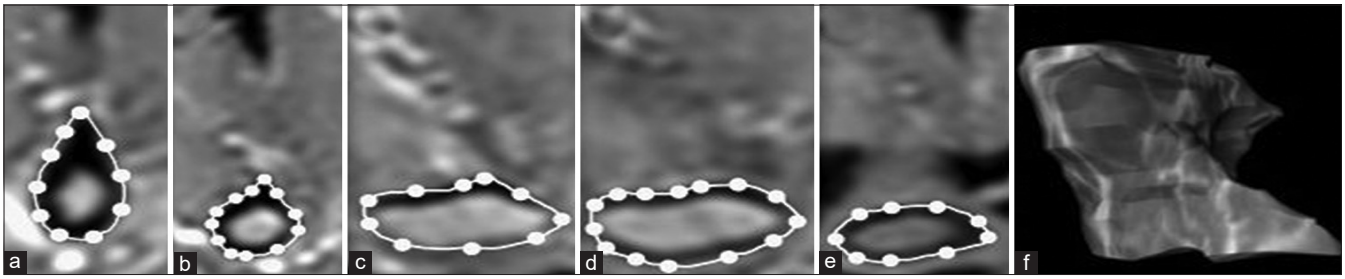

Figure 2: Drawing of the condyle borders on axial magnetic resonance imaging sections (a-e) and three-dimensional image of the condyle (f)

Articular eminence height and articular eminence inclination

The articular eminence height was measured as the perpendicular distance between the lowest point of the articular eminence and the highest point of the fossa on the sagittal T1-weighted images.[15] The articular eminence inclination was measured by using the top-roof line method that was the angle between the Frankfort horizontal plane and the plane passing through the highest point in the roof of the glenoid fossa and the lowest point at the crest of the articular eminence on the sagittal T1-weighted images.[15,16]

Statistical analysis

The Statistical Package for the Social Sciences (SPSS 17.0 for Windows; SPSS Inc., Chicago, IL, USA) was used for the statistical analyses, and a $P < 0.05$ was considered to be statistically significant. According to the statistical power analysis, when considering the ratios in the ADDWR, ADDWoR, and control groups, with 95% power, at least 9 observations were required from each of these three groups. A one-way analysis of variance was used to establish the differences in the disc length, condylar height, width and volume and the articular eminence inclination, and height values with respect to the ADDWR, ADDWoR, and control groups. The differences in the disc volumes in each group with respect to the open and closed mouth position statuses were tested using the Bonferroni test. All measurements were repeated after a month, and the intraclass correlation coefficients were calculated for the intra-observer agreement. The values were interpreted as poor (<0.40), moderate (0.40–0.59), good (0.60–0.74), and excellent (≥0.75).

Results

Fifty-two TMJs with DD and 26 healthy TMJs were evaluated in this study. Most of the participants were women (84.2%), and the mean age was 26.7 ± 7 years. In the TMJs with DD, the disc volume (both in the open mouth and closed mouth positions), disc length, condylar width, and articular eminence inclination were statistically different than those values in the healthy TMJs ($P < 0.05$) [Table 1]. There was an association between the control group and the other two groups in terms of the disc length and condylar width ($P = 0.00$ and $P = 0.001$, respectively). In addition, there was a statistical difference between articular eminence inclination of the control and the ADDWoR group ($P = 0.02$) [Table 2].

Table 1: The means of morphometric and volumetric measurements of temporomandibular joint structures in with disc displacement and healthy temporomandibular joints

	Mean±SD		*P*
	TMJs with DD	Healthy TMJs	
Disc			
Length	7.44±1.51	9.89±1.05	0.00*
Volume in closed mouth position	0.08±0.02	0.11±0.22	0.00*
Volume in open mouth position	0.1±0.03	0.15±0.02	0.00*
Condyle			
Width	1.68±0.27	1.93±0.24	0.00*
Height	2±0.35	2.04±0.19	0.52
Volume	1.24±0.42	1.44±0.42	0.05
Articular eminence			
Height	6.05±1.5	6.66±1.28	0.81
Inclination	31.6±5.81	35.97±7.31	0.00*

*P<0.05. TMJ: Temporomandibular joint, DD: Disc displacement, SD: Standart deviation

The mean disc volume was greater in the control group both in the open and closed mouth positions. Moreover, the mean disc volume was greater in the open mouth position than closed mouth position in all the groups [Table 3]. There was a statistical association between disc volume and the control group and the other two groups in the closed mouth position and among the three groups in the open mouth position [Table 4].

The intra-observer agreement was high when evaluating the reliability of the morphometric and volumetric measurements. The intraclass correlation coefficient was the highest (0.98) in the condylar volume measurements, and it was the lowest (0.92) in the disc volume measurements in the closed mouth position.

Discussion

An accurate description of the TMJ morphometry is critical to better understand the structure and function of the TMJ for the evaluation, diagnosis, and treatment of TMD.[17] The morphometric parameters of the condyle, articular eminence

Table 2: Comparison of the morphometric and volumetric measurements of temporomandibular joint structures among the groups

Variables	Mean±SD		
	ADDWR	ADDWoR	Control
Disc length	7.35±0.24 B	7.6±0.38 B	9.89±0.2 A
Condylar width	1.69±0.06 B	1.68±0.04 B	1.93±0.04 A
Condylar height	1.99±0.06	2.01±0.08	2.04±0.04
Condylar volume	1.19±0.08	1.32±0.09	1.44±0.08
Articular eminence height	6.23±0.29	5.79±0.29	6.66±0.25
Articular eminence inclination	32.07±6.5 AB	31.05±4.5 B	35.97±7.3 A

Different uppercase letters in table data indicate statistical differences. SD: Standart deviation, ADDWR: Anterior disc displacement with reduction, ADDWoR: Anterior disc displacement without reduction

Table 3: The disc volume means in closed and open mouth position in the three groups

	Mean±SD	
	Closed mouth position	Open mouth position
ADDWR	0.08±0.003	0.12±0.006
ADDWoR	0.07±0.004	0.08±0.004
Control	0.11±0.022	0.15±0.005

ADDWR: Anterior disc displacement with reduction, ADDWoR: Anterior disc displacement without reduction, SD: Standart deviation

and disc, have been investigated in many studies using the different types of imaging techniques. In this study, the disc volume and length of the articular disc and condyle, height and inclination of articular eminence were measured in the patients with and without DD.

MRI is an imaging technique that best shows the articular disc. However, the detection of TMJ osseous abnormalities using MRI has exhibited contradictory results. Some authors have concluded that MRI is limited in the detection of osseous changes,[18,19] there are also studies that demonstrated high sensitivity and specificity in detecting.[20,21] MRI may be considered an adequate examination for the assessment of bone so that further examinations (e.g., computed tomography) that may expose patients to ionizing radiation are not required.[10]

TMD is more common in females, but there is no consensus on the reason why. It has been found that women seek TMD treatment four to seven times more often than men, and that there may be gender or psychosocial differences in the appropriateness of seeking assistance for pain problems.[22] Krogstad *et al*.[23] reported no gender differences in the somatic complaints or anxiety in patients with TMD. Endogenous female reproductive hormones, such as estrogen, may potentially contribute to the TMD etiology.[24] Moreover, in this study, the number of female participants was more, as in many other TMJ studies.[1,2,4,10,25]

Both the progression and severity of degenerative bone changes in the mandibular condyle and fossa increase with age.[25] Manfredini *et al*.[26] reported a mean age of 32.7 years in patients with DD without degenerative changes, whereas the mean age of the patients with inflammatory/degenerative changes was 52.4 years. Therefore, patients aged between 18 and 40 years old were included in this study to minimize the effects of age-related degenerative changes in the bones.

Deformation of the disc increases and the disc loses its normal position with increased severity in DD.[1,8,27] Cai *et al*.[14] followed patients with anterior DD without treatment and the disc was more anteriorly displaced and became shorter after the follow-up. Furthermore, it was reported that the discs tended to become shorter in the ADDWoR group than in the ADDWR group.[28] In accordance with previous studies, the highest mean disc length was found in the control group in this study, and there was a significant association between the control group and the other two groups.

Based on the studies reporting that there could be changes in the TMJ with DD, the hypothesis of this study, there may be a relationship between DD and the disc volume. Consequently, the mean disc volume was the highest in the control group and the lowest in ADDWoR group in both mouth positions. Moreover, the mean disc volume was increased in all the groups in the open mouth position when compared with the closed mouth position. Barbieri *et al*.[12] found statistically significant differences between migraine patients and controls regarding the articular disc volume; however, they detected higher disc volume in DD groups than normal disc group. While the disc was expanding between the articular eminence and the condyle in the open mouth position in the ADDWR and control groups, the disc maintained its position anterior to the condyle in the ADDWoR group. Because the disc was located anterior to the condyle, the disc morphology maintained its form in the open mouth position in the ADDWoR group. The lesser disc length and disc position at the anterior of the condyle may have been the reason for the lowest disc volume in the ADDWoR group.

Degenerative changes in the condyle and articular eminence can be observed in patients with ID progression, and these changes are an indication that the ID has progressed.[4,8,14] Cai *et al*. and Hu *et al*.[4,14] found that the condylar height

Table 4: Comparison of disc volume means among the groups in closed and open mouth position

	Closed mouth position		Open mouth position	
	Mean of disc volume (mean±SD)	*P*	Mean of disc volume (mean±SD)	*P*
ADDWR				
ADDWoR	0.007±0.005	0.63	0.03±0.008	0.001*
Control	−0.03±0.005	0.00*	−0.03±0.008	0.00*
ADDWoR				
ADDWR	−0.007±0.005	0.63	−0.03±0.008	0.001*
Control	−0.04±0.006	0.00*	−0.06±0.008	0.00*
Control				
ADDWR	0.03±0.005	0.00*	0.03±0.008	0.00*
ADDWoR	0.04±0.006	0.00*	0.06±0.008	0.00*

*$P<0.05$. ADDWR: Anterior disc displacement with reduction, ADDWoR: Anterior disc displacement without reduction, SD: Standart deviation

is decreased in joints with ADDWoR and DD might be accompanied by degenerative changes in the condyle. Although it was observed that the condylar height changed with DD in this study, there was no association between condylar height and among the groups. These differences may have occurred due to the different sample sizes among the studies. The lowest mean condylar width was found in the ADDWoR group in this study, which was similar to the findings of previous studies that examined the relationships between the morphometric features of the mandibular condyle and DD showed that DD was associated with narrower condyles.[9,10] At a late stage of DD, disc deterioration may occur more frequently, and also bone degeneration, facial skeletal changes as the result of condylar bone loss and diminished mandibular growth secondary to DD have been reported.[9,10] Therefore, our results are consistent with those reported previously, which confirm that DD can cause condylar degenerative changes.

The condylar volume may be affected by the remodelling and flattening of the condyle that can occur with DD progression because DD is commonly occur with osteoarthritis. During the course of osteoarthritis, progressive bony erosion and remodelling in the bone occur repeatedly. The repetitive condition between osseous remodelling and degenerative changes tend to change size of the condyle.[11,29] In accordance with the mentioned condition, the lowest condylar volume was found in the ADDWoR group in this study, but there were no significant differences among the groups. Ahn *et al*.[11] also established that the lowest condylar volume in the ADDWoR group, as well as significant differences in both the total condylar and trabecular volumes on computed tomography images. The causes of differences between the results may have been the different sample sizes and volumetric analysis programs between the studies.

The top-roof line and best-fit line methods are two different methods used to measure the articular eminence inclination and the best-fit line method is used to establish the actual condylar path; whereas the top-roof line method better shows the morphology of the articular eminence. Similar to this study, there were statistical differences with regard to the articular eminence inclination in the studies that used the top-roof line method.[7,30] There is no consensus among the authors on the relationship between the articular eminence morphometry and TMD. While some authors have suggested that the inclination and flattening of the articular eminence was related to TMD,[7,31,32] others have reported that the articular eminence inclination has no association.[16,33] Sümbüllü *et al*.[15] reported that the articular eminence height was higher in the TMD group, but there was no association. Similar to previous study, the mean articular eminence height was the lowest in ADDWoR group, and there was no statistical difference among the groups in this study. The articular eminence steepness has been examined in several studies, and the results of these studies have been controversial. Several studies have reported that a steeper articular eminence should cause ID,[30,33] while others have suggested that the articular eminence steepness decreased in the progressive ID cases.[7,32] The articular eminence inclination mean was the highest in the control group and the lowest in the ADDWoR group in this study. According to these results, similar to the condyle, flattening and decreased inclination of the articular eminence might occur because of the modifications of osseous components during the osteoarthritis and during the adaptation of those components to DD progression.[11,34] These discrepancies among the studies may be attributed to the different measurement methods, imaging modalities, and sample sizes.

Conclusion

The greatest limitation in this study was the low sample size. However, based on the results of this study, DD is effective in changing the morphometric and volumetric features of the condyle, articular disc, and articular eminence.

Acknowledgment

The authors kindly thank to Dr. Özgür Koşkan for assistance in the statistical analysis.

Financial support and sponsorship

This study was supported by Scientific Research Center of Suleyman Demirel University (4991-DUI-17).

Conflicts of interest

There are no conflicts of interest.

References

1. de Farias JF, Melo SL, Bento PM, Oliveira LS, Campos PS, de Melo DP. Correlation between temporomandibular joint morphology and disc displacement by MRI. Dentomaxillofac Radiol 2015;44:1-7.
2. Koh KJ, Park HN, Kim KA. Relationship between anterior disc displacement with/without reduction and effusion in temporomandibular disorder patients using magnetic resonance imaging. Imaging Sci Dent 2013;43:245-51.
3. Perschbacher S. Temporomandibular joint abnormalities. In: White SC, Pharoah MJ, editors. Oral Radiology: Principles and Interpretation. St Louis: Elsevier Health Sciences; 2014. p. 492-521.
4. Hu YK, Yang C, Cai XY, Xie QY. Does condylar height decrease more in temporomandibular joint nonreducing disc displacement than reducing disc displacement? A magnetic resonance imaging retrospective study. Medicine (Baltimore) 2016;95:1-7.
5. White SC. Other imaging modalities. In: White SC, Pharoah MJ, editors. Oral Radiology: Principles and Interpretation. St Louis: Elsevier Health Sciences; 2014.p. 229-54.
6. Manfredini D. Current Concepts on Temporomandibular Disorders. 1st ed. Berlin: Quintessence; 2010.
7. Çağlayan F, Sümbüllü MA, Akgül HM. Associations between the articular eminence inclination and condylar bone changes, condylar movements, and condyle and fossa shapes. Oral Radiol 2014;30:84-91.
8. Taşkaya-Yilmaz N, Oğütcen-Toller M. Magnetic resonance imaging evaluation of temporomandibular joint disc deformities in relation to type of disc displacement. J Oral Maxillofac Surg 2001;59:860-5.
9. Torres MG, Crusoé-Rebello IM, Rosário M, Albuquerque MC, Campos PS. Morphometric features of the mandibular condyle and association with disk abnormalities. Oral Surg Oral Med Oral Pathol Oral Radiol 2016;121:566-72.
10. Vieira-Queiroz I, Gomes Torres MG, de Oliveira-Santos C, Flores Campos PS, Crusoé-Rebello IM. Biometric parameters of the temporomandibular joint and association with disc displacement and pain: A magnetic resonance imaging study. Int J Oral Maxillofac Surg 2013;42:765-70.
11. Chang MS, Choi JH, Yang IH, An JS, Heo MS, Ahn SJ. Relationships between temporomandibular joint disk displacements and condylar volume. Oral Surg Oral Med Oral Pathol Oral Radiol 2018;125:192-8.
12. Barbieri AA, Costa AL, Perez Gomes JP, Ricardo AL, Braz-Silva PH, Lopes SL. Association of volume and voxel intensity of the articular disc and lateral pterygoid muscle in migraine patients: A study with magnetic resonance imaging. Acta Odontol Scand 2020;78:189-95.
13. He YM, Wang HY, Feng YP, Li HM, Fang W, Ke J, *et al*. A preliminary study on the registration of MRI and cone beam CT images of temporomandibular joint disc. Zhonghua Kou Qiang Yi Xue Za Zhi 2020;55:772-7.
14. Cai XY, Jin JM, Yang C. Changes in disc position, disc length, and condylar height in the temporomandibular joint with anterior disc displacement: A longitudinal retrospective magnetic resonance imaging study. J Oral Maxillofac Surg 2011;69:e340-6.
15. Sümbüllü MA, Cağlayan F, Akgül HM, Yilmaz AB. Radiological examination of the articular eminence morphology using cone beam CT. Dentomaxillofac Radiol 2012;41:234-40.
16. Shahidi S, Vojdani M, Paknahad M. Correlation between articular eminence steepness measured with cone-beam computed tomography and clinical dysfunction index in patients with temporomandibular joint dysfunction. Oral Surg Oral Med Oral Pathol Oral Radiol 2013;116:91-7.
17. Zhang Y, Xu X, Liu Z. Comparison of morphologic parameters of temporomandibular joint for asymptomatic subjects using the two-dimensional and three-dimensional measuring methods. J Healthc Eng 2017;2017:1-8.
18. Alkhader M, Ohbayashi N, Tetsumura A, Nakamura S, Okochi K, Momin MA, *et al*. Diagnostic performance of magnetic resonance imaging for detecting osseous abnormalities of the temporomandibular joint and its correlation with cone beam computed tomography. Dentomaxillofac Radiol 2010;39:270-6.
19. Yura S, Harada S, Kobayashi K. Diagnostic accuracy on magnetic resonance imaging for the diagnosis of osteoarthritis of the temporomandibular joint. J Clin Diagn Res 2015;9:ZC95-7.
20. Hansson L, Westesson P, Katzberg RW, Tallents R, Kurita K, Holtas S, *et al*. MR imaging of the temporomandibular joint: Comparison of images of autopsy specimens made at 0.3 T and 1.5 T with anatomic cryosections. Am J Roentgenol 1989;152:1241-4.
21. Tasaki MM, Westesson PL. Temporomandibular joint: Diagnostic accuracy with sagittal and coronal MR imaging. Radiology 1993;186:723-9.
22. Rollman GB, Gillespie JM. The role of psychosocial factors in temporomandibular disorders. Curr Rev Pain 2000;4:71-81.
23. Krogstad BS, Jokstad A, Dahl BL, Vassend O. The reporting of pain, somatic complaints, and anxiety in a group of patients with TMD before and 2 years after treatment: Sex differences. J Orofac Pain 1996;10:263-9.
24. Landi N, Lombardi I, Manfredini D, Casarosa E, Biondi K, Gabbanini M, *et al*. Sexual hormone serum levels and temporomandibular disorders. A preliminary study. Gynecol Endocrinol 2005;20:99-103.
25. Alexiou KE, Stamatakis HC, Tsiklakis K. Evaluation of the severity of temporomandibular joint osteoarthritic changes related to age using cone beam computed tomography. Dentomaxillofac Radiol 2009;38:141-7.
26. Manfredini D, Piccotti F, Ferronato G, Guarda Nardini L. Age peaks of different RDC/TMD diagnoses in a patient population. J Dent 2010;38:392-9.
27. Vogl TJ, Lauer HC, Lehnert T, Naguib NN, Ottl P, Filmann N, *et al*. The value of MRI in patients with temporomandibular joint dysfunction: Correlation of MRI and clinical findings. Eur J Radiol 2016;85:714-9.
28. Hu YK, Yang C, Xie QY. Changes in disc status in the reducing and nonreducing anterior disc displacement of temporomandibular joint: A longitudinal retrospective study. Sci Rep 2016;6:1-11.
29. Zhuo Z, Cai X, Xie Q. Is anterior disc displacement without reduction associated with temporomandibular joint condylar height in juvenile patients younger than 20 years? J Oral Maxillofac Surg 2015;73:843-9.
30. Paknahad M, Shahidi S, Akhlaghian M, Abolvardi M. Is mandibular fossa morphology and articular eminence inclination associated with temporomandibular dysfunction? J Dent (Shiraz) 2016;17:134-41.
31. Kurita H, Ohtsuka A, Kobayashi H, Kurashina K. Flattening of the articular eminence correlates with progressive internal

derangement of the temporomandibular joint. Dentomaxillofac Radiol 2000;29:277-9.

32. Ren YF, Isberg A, Westesson PL. Steepness of the articular eminence in the temporomandibular joint. Tomographic comparison between asymptomatic volunteers with normal disk position and patients with disk displacement. Oral Surg Oral Med Oral Pathol Oral Radiol Endod 1995;80:258-66.
33. Sülün T, Cemgil T, Duc JM, Rammelsberg P, Jäger L, Gernet W. Morphology of the mandibular fossa and inclination of the articular eminence in patients with internal derangement and in symptom-free volunteers. Oral Surg Oral Med Oral Pathol Oral Radiol Endod 2001;92:98-107.
34. Rabelo KA, Sousa Melo SL, Torres MG, Campos PS, Bento PM, Melo DP. Condyle excursion angle, articular eminence inclination, and temporomandibular joint morphologic relations with disc displacement. J Oral Maxillofac Surg 2017;75:938.e1-10.

Original Article

Analysis of Vertical Forces in Children with Down's Syndrome by Using emed® Capacitance-Based Pressure Platform

Abstract

Introduction: This study aimed to analyze the vertical forces functioning under the plantar surface of the feet in children with and without Down's syndrome (DS) during walking using a capacitance-based pressure platform (emed®). **Material and Methods:** This is an observational study on 10 individuals with DS, (Group I) and 10 children without DS (Group II), aged 8–15 years. Both the groups were evaluated while standing on a capacitance-based pressure platform. Maximum force, peak pressure, contact time, and contact area parameters were assessed for both right and left foot. In this study, we assessed and compared these parameters in both the groups. **Results:** The results showed that the foot-ground interaction forces varied between the two groups. In particular, parameters such as maximum force, peak pressure, and contact area were statistically significant, where no significant difference was found concerning the contact time parameter. **Discussion and Conclusion:** The capacitance-based pressure platform (emed®) must be considered an essential evaluation tool for assessing vertical forces associated with children with DS. Thus, organizing regular monitoring of foot-ground reaction forces during the early years in DS children is suggested to prevent potential complications associated and decrease the probability of mobility impairments in adulthood.

Keywords: *Capacitance-based pressure platform (emed®), Down syndrome, vertical forces*

Venkata Nagaraj Kakaraparthi, Vamsi Krishna Gannamaneni[1], Lalitha Kakaraparthi[2]

Department of Medical Rehabilitation Sciences, College of Applied Medical Sciences, King Khalid University, Abha, [1]Department of Medical Rehabilitation Sciences, College of Applied Medical Sciences, Hail University, Hail, Saudi Arabia, [2]Department of Physiotherapy, Parul University, Vadodara, Gujarat, India

Introduction

Down syndrome (DS) is a chromosomal disorder mainly produced by full trisomy of chromosome 21.[1] In DS, an increased occurrence of musculoskeletal problems were seen. The most common problems are of less severity. They commonly involve the lower extremities, such as hip disorders, patellofemoral instability, hallux valgus, metatarsus primus varus (MPV), and pes planus/flat foot.[2,3] These insignificant musculoskeletal problems are frequently misjudged and neglected due to the mere presence of more serious associated pathologies in DS. Early diagnosis of these problems by proper clinical evaluation, radiographic evaluation, podiatric evaluation with barometric evaluation is necessary to measure the extent of the deformity.[3,4] These evaluation procedures provide information about the functional limitations of activities of daily living in children with DS. Furthermore, it has been noticed that children with DS demonstrate impaired balance, weight bearing functions, and a distinctive foot ground contact pattern, which has been characterized by larger midfoot and decreased forefoot interaction areas and enhanced contact pressure areas in the midfoot and the forefoot.[5]

The necessity for careful examination and assessment of foot pressures during childhood may help to decrease the risk of impaired mobility in adulthood and minimize the potential effects in DS.[6] Only a limited studies has been done in children with DS, to evaluate the foot-ground interaction forces. Concolino *et al*. evaluated the plantar pressure patterns during DS children's static and dynamic conditions and revealed a substantially altered foot function and altered rearfoot–forefoot surface ratio values.[3] Pau *et al*. evaluated the foot-ground parameters in children with DS. They demonstrated the high prevalence of flat feet in these children, which has been associated with the existence of more significant contact pressures in midfoot and forefoot.[5] Galli *et al*. focused on foot rotation graph using pressure-sensitive mat, and suggested that the existence of flatfoot in children with

How to cite this article: Kakaraparthi VN, Gannamaneni VK, Kakaraparthi L. Analysis of vertical forces in children with down's syndrome by using emed® capacitance-based pressure platform. J Anat Soc India 2020;XX:XX-XX.

Article Info

Received: 04 August 2020
Accepted: 30 November 2020
Available online: ***

Address for correspondence:
Dr. Venkata Nagaraj Kakaraparthi, Department of Medical Rehabilitation (Physical Therapy), College of Applied Medical Sciences, King Khalid University, C/3/139, Abha, Guraiger Campus, Saudi Arabia.
E-mail: kvnagaraj13@yahoo.com

Access this article online

Website: www.jasi.org.in
DOI: 10.4103/JASI.JASI_148_20
Quick Response Code:

DS may cause more extra rotation of their feet than the children devoid of flat foot.[7] Prasher *et al*. explored the foot pressure points by using Harris mat technique, in children with DS and found high pressure points, specifically at the areas of callus formation and verrucae.[8] However, the absence of early identification methods can cause severe biomechanical and postural problems in children with DS.

Hence, the present study aimed to evaluate the vertical forces acting under the plantar surface of the feet in children with and without DS during walking and to assess the progress of contact area and pressure distribution by using capacitance-based pressure platform (emed®). We strongly believe these findings can enhance the current approaches and treatment protocols to podiatric management of children with DS.

Material and Methods

Participants

Three schools (one special and two public) in the Hail region of Kingdom of Saudi Arabia have participated in the study. Ten children with DS, with a mean age of 10.1 ± 1.6 years (age range 8–14 years) who were characterized by abnormality in trisomy 21 chromosome were assigned in Group I. Inclusion criteria in this group (1) age 8–14 years, (2) low-medium intelligence quotient, (3) no history of surgery. Exclusion criteria (1) children who were unable to understand the researcher's instructions to complete the procedure. Additionally, to compare the data obtained, a control group consists of ten children without DS, with a mean age of 10.3 ± 1.8 years (age range 8–14 years) was allocated to Group II. Inclusion criteria in this group (1) age 8–14 years (2) to complete the procedure without any assistance. Exclusion criteria (1) children known to the researchers (2) history of spine, upper limb, or lower-limb surgeries (3) history of musculoskeletal or cardiovascular disorders. Data were assessed for both right and left limbs. All the required permissions were taken from the schools for performing the study. Before executing the evaluation, the examiner described this research's procedure and purpose of this research to all the children. The study was approved by the ethical committee of the institute and informed consent was attained from the parents of the children enrolled in the study.

Procedures

Demographic data (age, gender) and anthropometric measures, which include height (meters), weight (kg), and body mass index (BMI) (kg/m^2), were evaluated for all children with a standard procedure. All the children underwent a general examination of the feet and podiatric assessment and evaluation by using the emed analysis system.

General observation of feet

Clinical examination includes appearance of both the feet-hallux valgus, hallux varus, abnormalities of toes – MPV, syndactyly, clinodactyly of fifth toe, rotation of feet – abduction/adduction or plantar flexion/dorsiflexion of feet and presence of any abnormal arches of the feet.

Podiatric assessment

Podiatric examination and evaluation were assessed by one of the researchers. The emed® analysis is a user-friendly device (emed® q100, 100 Hz, 4 sensors/cm^2-resolution, 475 mm × 320 mm-sensor area, pressure range - 10–1270 kPa, pressure threshold-10kPa) used in this study to evaluate the pressure distribution under the feet during walking.[9] It has pressure plates having calibrated capacitive sensors and two electrically conducting surfaces that were separated by rubber. It starts recording the data automatically when the children's foot contact the platform and[10] It also demonstrated good test-retest reliability (interclass coefficient >0.8) during walking on the platform.[11] Studies also showed less error within sessions and between days and measures the foot pressure accurately during walking.[9,12]

After a brief demonstration of the procedure, the children were asked to walk barefoot on the emed® analysis platform at an average walking speed. Ten trails were performed for the affected foot. To minimize the fatigue in children, a rest period of 5 min was given for every attempt. All the participants were asked to take four to five steps before starting on the platform. The children

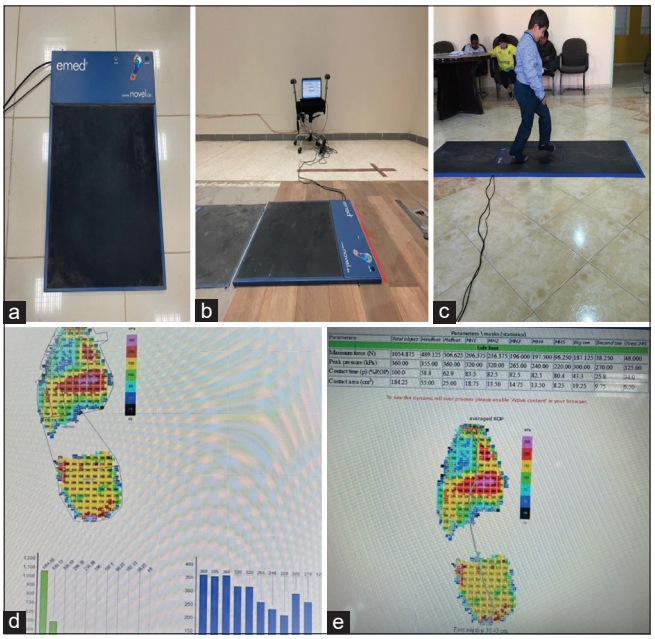

Figure 1: Vertical forces analysis by using emed capacitance-based pressure platform. a) Emed Pressure platform. b) Pressure platform connected system. c) Subject walking on the Pressure platform. d) Vertical forces recorded for the study. e) Maximum forces, Peak pressure, contact time, and contact area recorded for the study

were instructed to mainly focus on the rounded sticker attached in both directions during walking. The researcher recorded the mean of ten trails for further evaluation. Trials fluctuating ≤10% in time were believed to be acceptable. If any child foot is placed near to or on the pressure platform's edges the trail was repeated Figure 1.[13]

Data analysis

In the present study, we utilized Novel's project software (Novel, Munich, Germany) to examine the foot plantar pressure data by applying a twelve-region mask under the foot. For analysis and to compare with the normal foot, the foot was divided into ten regions-hindfoot, midfoot, 1st metatarsal, 2nd metatarsal, 3rd metatarsal, 4th metatarsal, 5th metatarsal, 1st toe, 2nd toe and 3rd, 4th and 5th toes (as one region). We also assessed the Hallux angle and arch index for all children. The following plantar pressure factors were calculated: Maximum force (N), peak pressure (kPa), contact time (% range of pressure (ROP)), and contact area (cm^2). All these parameters were computed from the maximum pressure throughout the stance phase plot for the entire foot contact region (total) and the 10 regions of the foot in children with and without DS.[14]

SPSS software (version 21.0 for Windows; SPSS, Inc., Chicago, IL, USA) was used to perform the statistical analyses. Descriptive statistics of the mean ± standard deviation for each plantar pressure parameter for all ten regions were evaluated. To compare the variances in maximum force, peak pressure, contact time, and contact area between two groups, an independent *t*-test was used.

Results

The anthropometric characteristics for all subjects are presented in Table 1, with a mean height of 1.27 ± 1.66 m for Group I and 1.47±0.077 m for Group II, a mean weight of 34.73 ± 11.97 kg for Group I and 44.55 ± 10.34 kg for Group II, and mean BMI of 20.89 ± 4.62 kg/m^2 for Group I and 20.44 ± 3.59 kg/m^2 for Group II. No significant differences were found in age, height, and BMI, except for weight ($P < 0.001$).

Supplementary Tables 1a and b summarizes the amount of maximum force concerning to right and left foot in both groups. However, regarding maximum force, the right foot group ($P = 0.009$) showed a nonsignificant effect, while the left foot group showed a significant ($P < 0.001$) effect in the study.

Supplementary Tables 2a and b summarizes the peak pressure concerning right and left foot in both groups. Both the foot groups exhibited ($P < 0.001$) a significant effect in the study about peak pressure. In contrast, the DS group showed more peak pressure in all ten regions than the non-DS group.

Supplementary Tables 3a and b summarizes the contact time in relation to right and left foot in both groups. However, regarding contact time, the right foot group ($P = 0.58$) showed a nonsignificant effect, while the left foot group showed a statistically significant ($P < 0.001$) effect in the study. The DS group exhibited more contact time values than the non-DS group in this study.

Supplementary Tables 4a and b summarizes the contact area in relation to right and left foot in both groups. However, about the contact area, both the foot groups exhibited ($P < 0.001$) a substantial statistical effect in the study.

Table 1: Anthropometric data for the overall sample

Anthropometrics	Mean±SD		*P*
	Group I with DS (*n*=10)	Group II without DS (*n*=10)	
Age (years)	10.1±1.66	10.3±1.82	0.64
Height (m)	1.27±0.111	1.47±0.077	0.03
Weight (kg)	34.73±11.97	44.55±10.34	<0.001
BMI (kg/m^2)	20.89±4.62	20.44±3.59	0.86

SD: Standard deviation, BMI: Body mass index, DS: Down's syndrome

Discussion

This study aimed to assess the vertical forces functioning under the plantar surface among the children with and without DS during walking by using capacitance-based pressure platform (emed®).

This study also demonstrated a variance in maximum force, peak pressure, contact time, and contact area among children with DS compared with non-DS children. These results emphasize the need to examine the foot pressure in children with DS more carefully and prevent further complications. Our study reported an increased amount of forces and peak pressures in DS children, particularly in the mid-foot;[15-17] these observations agree with those of previous studies.

In comparison to normal children, most DS children showed orthopedic abnormalities that mostly involve the lower extremities. The negligence of the anomalies adversely affects the motor skills of these children.[8] For this purpose, we firmly believe that during the assessment of children with DS, a proper podiatric assessment can diagnose such problems and improve the quality of life in these children.

However, to our expertise, no study has assessed both the force and contact parameters in children with DS. Concerning maximum force (N), the force applied on the pressure platform by normal children was more than the children with DS, in relative to peak pressure (kPa), more pressure displayed by children with DS, in relation to contact time, no significant differences were found between these two groups of children, and lastly, concerning contact area (cm^2), children with DS showed less amount of contact

areas when compared to normal children. The differences in these parameters were supported by variances in DS children's gait parameters compared to typical children.[18,19]

In the present study, a significant ($P < 0.001$) difference was observed in weight between the children with and without DS and considered one of the factors that explain the variance in these parameters, which further affect the gait parameters in children with DS.[20-22]

The present study has some limitations. First, it was conducted only on small sample size. Second, our results only apply to dynamic foot assessment using a capacitance-based pressure platform (emed®), because other clinical measures with dynamic foot evaluation during walking were not considered. Third, these tests can be done with different age groups in children with and without DS. Besides, more studies were recommended to overcome all these limitations.

Conclusion

The present study found exclusive findings in relation to maximum force, peak pressure, contact time, and contact area in DS children. This study also emphasizes the need for podiatrists and practitioners engaged with care of DS children. Although the variances were found in these parameters, further studies with a larger sample are essential to replicate the current findings.

Acknowledgment

The authors declare that they have no conflict of interest.

Financial support and sponsorship

Nil.

Conflicts of interest

There are no conflicts of interest.

References

1. Mégarbané A, Ravel A, Mircher C, Sturtz F, Grattau Y, Rethoré MO, *et al*. The 50th anniversary of the discovery of trisomy 21: The past, present, and future of research and treatment of Down syndrome. Genet Med 2009;11:611-6.
2. Mik G, Gholve PA, Scher DM, Widmann RF, Green DW. Down syndrome: Orthopedic issues. Curr Opin Pediatr 2008;20:30-6.
3. Concolino D, Pasquzzi A, Capalbo G, Sinopoli S, Strisciuglio P. Early detection of podiatric anomalies in children with Down syndrome. Acta Paediatr 2006;95:17-20.
4. Smith MD. Orthopedic aspects of cervical spine disorders in children and adolescents. Curr Opin Pediatr 1993;5:374-8.
5. Pau M, Galli M, Crivellini M, Albertini G. Foot-ground interaction during upright standing in children with Down syndrome. Res Dev Disabil 2012;33:1881-7.
6. Mahan KT, Diamond E, Brown D. Podiatric profile of the Down's syndrome individual. J Am Podiatry Assoc 1983;73:173-9.
7. Galli M, Cimolin V, Rigoldi C, Pau M, Costici P, Albertini G. The effects of low arched feet on foot rotation during gait in children with Down syndrome. J Intellect Disabil Res 2014;58:758-64.
8. Prasher VP, Robinson L, Krishnan VH, Chung MC. Podiatric disorders among children with Down syndrome and learning disability. Dev Med Child Neurol 1995;37:131-4.
9. Putti A, Arnold G, Cochrane L, Abboud R. Normal pressure values and repeatability of the Emed® ST4 system. Gait Posture 2008;27:501-5.
10. Rosenbaum D, Becker HP. Plantar pressure distribution measurements. Technical background and clinical applications. Foot Ankle Surg 1997;3:1-14.
11. Akins JS, Keenan KA, Sell TC, Abt JP, Lephart SM. Test–retest reliability and descriptive statistics of geometric measurements based on plantar pressure measurements in a healthy population during gait. Gait Posture 2012;35:167-9.
12. Hughes J, Pratt L, Linge K, Clark P, Klenerman L. Reliability of pressure measurements: The EM ED F system. Clin Biomech (Bristol, Avon) 1991;6:14-8.
13. Khallaf ME, Gabr AM, Fayed EE. Effect of Task Specific Exercises, Gait Training, and Visual Biofeedback on Equinovarus Gait among Individuals with Stroke: Randomized Controlled Study. Neurol Res Int 2014;2014:1-9.
14. Hafer JF, Lenhoff MW, Song J, Jordan JM, Hannan MT, Hillstrom HJ. Reliability of plantar pressure platforms. Gait Posture 2013;38:544-8.
15. Mickle KJ, Steele JR, Munro BJ. Does excess mass affect plantar pressure in young children? Int J Pediatr Obes 2006;1:183-8.
16. Dowling AM, Steele JR, Baur LA. What are the effects of obesity in children on plantar pressure distributions? Int J Obes Relat Metab Disord 2004;28:1514-9.
17. Pau M, Galli M, Crivellini M, Albertini G. Relationship between obesity and plantar pressure distribution in youths with Down syndrome. Am J Phys Med Rehabil 2013;92:889-97.
18. Naito M, Aoki S, Kamide A, Miyamura K, Honda M, Nagai A, *et al*. Gait analysis in Down syndrome pediatric patients using a sheet-type gait analyzer: Pilot study. Pediatr Int 2015;57:860-3.
19. Sutherland DH, Olshen R, Cooper L, Woo SL. The development of mature gait. J Bone Joint Surg Am 1980;62:336-53.
20. Beck RJ, Andriacchi TP, Kuo KN, Fermier RW, Galante JO. Changes in the gait patterns of growing children. J Bone Joint Surg Am 1981;63:1452-7.
21. Hausdorff JM, Zemany L, Peng C, Goldberger AL. Maturation of gait dynamics: Stride-to-stride variability and its temporal organization in children. J Appl Physiol (1985) 1999;86:1040-7.
22. Hof AL. Scaling gait data to body size. Gait Posture 1996;3:222-3.

Supplementary Table 1a: Maximum force (*n*) in children with and without down's syndrome (right foot)

Hindfoot		Midfoot		MH1		MH2		MH3		MH4	
RTHFDS	RTHFN	RTMFDS	RTMFN	RTHFDS	RTHFN	RTHFDS	RTHFN	RTHFDS	RTHFN	RTHFDS	RTHFN
122.3±49.8	251.0±117.5	68.7±26.1	204.4±13.1	85.4±29.9	96.6±13.9	36.3±10.9	105.5±17.4	51.2±22.5	92.3±15.5	42±10.2	71.2±14.4
199.3±69.8	357.8±62.9	135.2±27	146±48.2	43.1±16	135.3±30.4	43.5±6.7	130.4±14	76.8±16.7	118±14.6	55.6±16.2	74.6±16
277.3±58.4	279.7±11.3	226.7±33.3	80.2±7.6	143.8±80.8	80.3±12.7	85±16.9	62.1±6.5	112.7±24.1	76.9±5.9	93.8±34	47±5
106.7±16.6	308.9±16.3	141.9±14.5	201.9±41.9	17.5±10.7	125.7±24.2	15.9±4.7	120.2±14.8	35.3±7.1	121.6±7.5	47.9±11.9	83.6±19.1
112.7±20.1	287±34.6	218.7±16.8	58.2±15.5	52.1±13.9	95.3±15.7	53.9±5.4	68.1±7.6	77.5±8.2	62.3±7.9	53.3±5.8	61.3±8.3
274.6±286	244.4±26	270±133.4	319.4±15.5	82±7	108.5±5.4	147.4±5.7	147.3±12.2	116.3±76.7	156.1±15.1	61.8±1.2	115.6±9
223.8±47.6	392.2±24.7	218.4±32.3	113.1±22	92.9±19.6	138.5±26.2	48±6.4	111±4.3	75.2±17.4	116.9±6.7	60.8±16.6	92±12.1
260.1±29.5	350.1±37.7	196.7±7.7	114±17.5	97.6±24.2	57.1±12.5	70.9±6.9	66.8±6.1	110.9±7.5	107.4±17.3	106.5±5	74.6±8.8
222.4±23.2	232.9±28.1	139.8±22.5	19.3±11.5	24.4±17.8	100.2±12.5	33.2±7.3	61.3±2.6	84.1±12.6	52±6.5	64.8±6.8	39.3±15.6
358.4±41.7	399.1±48.5	174±9.9	307±28.1	220.4±35.2	134±39.6	124.9±6.6	97.6±4.9	116±5.9	134.8±21.9	92.1±9.2	107.5±22.3

MH5		Big toe		2nd toe		Toes345		Hallux angle (°)		Arch index	
RTHFDS	RTHFN	RTHFDS	RTHFN	RTHFDS	RTHFN	RTHFDS	RTHFN	RTHFDS	RTHFN	RTHFDS	RTHFN
13±1.9	36.7±9.1	42±39	138.1±42.9	5.5±5	39.9±4.2	6±8.9	45.1±17.7	7.1±5.6	3.9±1.4	0.29±0.03	0.35±0.03
27±9.1	7±1.2	70.2±20.7	508	23.8±6.9	255±3.5	8.4±5.2	89±7.3	9±5.4	4.8±5.5	0.34±0.02	0.23±0.01
44±21.6	19.2±3.4	205.2±14.5	82.8±6.9	27.1±5.6	21.5±3.6	29.6±8.3	19.5±11.8	4.5±5.8	2.7±1.9	0.29±0.01	0.26±0.02
31.4±8.8	30±11.1	33.8±9.7	49.5±9	6±1.5	8.5±7.1	5.3±2	6.2±5.2	10.6±11.4	10±1.4	0.37±0.02	0.29±0.01
20.7±3.2	41.3±6.6	42.2±15.1	140.1±28.8	27.8±6.2	20.7±4.3	8.1±2.7	17.4±3.1	6.8±5.6	7.8±6.8	0.37±0.02	0.23±0.01
19.6±10.9	55.5±5.3	0.9±1.3	106.4±10.5	1.9±2.7	27.5±1.6	1±1.4	32.2±5.7	0	1.6±0.9	0.33±0.01	0.3±0.01
18.6±3.2	58.8±12.1	8±2.2	100.1±12.1	22.4±1.2	16.9±4.3	7±4.5	21.5±5.8	6.5±6	1.7±1.7	0.35±0.01	0.24±0.01
51.5±1.2	32.1±8.1	8±1.1	149.1±39	40±2.1	27.2±2.7	1.7±3.6	30.4±3.9	1.2±1.4	1.9±2.8	0.3±0.01	0.24±0.01
0	26±16.9	74±4.4	57.2±3.4	244±2.7	32±4.5	53±6.2	39.9±7.6	10.3±3.2	3.3±1.4	0.36±0.02	0.10±0.05
25.8±3.3	38.8±9	96±2.7	74±68.8	62±3.4	10.5±12.2	8±0.6	9±9.8	7.3±7.3	4.5±1.5	0.31±0.01	0.31±0.02

MH1: Metatarsal head 1, MH2: Metatarsal head 2, MH3: Metatarsal head 3, MH4: Metatarsal head 4, MH5: Metatarsal head 5, RDS: Right side children with down's syndrome, RN: Right side normal children

Supplementary Table 1b: Maximum force (*n*) in children with and without down's syndrome (left foot)

Hindfoot		Midfoot		MH1		MH2		MH3		MH4	
LTHFDS	LTHFN	LTHFDS	LTHFN	LTHFDS	LTHFN	LTHFDS	LTHFN	LTHFDS	LTHFN	LTHFDS	LTHFN
384.3±35.1	363.8±50.2	281.7±17.5	175.1±14.3	152±12.2	97.3±17.5	145.1±8.8	96.9±13.2	152.6±9.3	86.4±22.5	100.4±5.1	54±20.3
133.8±68.4	457.4±46.2	75.1±3	118±17.8	82.7±20.8	117.9±17.8	34.2±4.2	124.3±8.8	60.4±11.2	125.2±19.5	39.7±7.6	78.2±11.4
283.3±51.5	280.1±30.3	230.4±37	58.9±8.3	146±37.8	62.7±13.9	77.5±8.8	56.5±10.07	105.2±15.8	66.1±8.1	71.5±13.4	49.2±6.6
147.3±24.4	386.7±17.8	119±11.1	152.6±8.9	32.8±11.6	123.7±14.6	22.8±3.2	127.3±8.6	45.5±4.1	117.2±9.4	45.8±7.5	90.1±7.7
195.6±36.4	288.8±39.7	176.2±11.4	85.8±10.6	73.2±26.8	81.6±12.6	43.4±7.3	74.5±4.2	57±18.8	86.8±3.9	46.3±16.9	69.8±3.9
324.8±113.6	384.3±35.1	314.1±54.8	281.7±17.5	36.4±17.6	152±12.2	41.1±11.8	145.1±8.8	85.8±37.3	152.6±9.3	77.7±23.6	100.4±5.1
227±86.6	401.6±10.8	182.8±17.5	101.9±11.3	78.7±16.9	130.4±25.6	32.6±1.06	116.5±4.9	69.8±4.6	134.6±11.4	60.8±3.7	94±100.9
275.5±65.7	380.2±64.4	322.7±24.8	78.4±13.8	197.5±22.5	73.6±13.4	69.3±6.2	81.7±13.2	71.6±9.4	117.8±13.7	49.2±5.5	72.6±15.6
198.7±68.4	211.7±44.3	139.8±27.9	11.5±2.5	47.1±39.5	122.3±4.4	32.4±7.3	66±16.8	55.5±17.4	41.1±8.2	47.5±11	22.9±3.9
284.5±51.3	415.2±28	265.7±105.9	264±25.3	216.2±49.4	70.6±19.5	139.4±37.4	87.5±15.02	130.3±16.5	172±21.8	98.5±14.3	133.5±16.2

MH5		Big toe		2nd toe		Toes 345		Hallux angle (°)		Arch index	
LTHFDS	LTHFN	LTHFDS	LTHFN	LTHFDS	LTHFN	LTHFDS	LTHFN	LTHFDS	LTHFN	LTHFDS	LTHFN
40.8±4.3	23±8.7	106.4±4.3	161.9±49.7	15.9±1.1	36.6±6.5	13.8±13.4	39.8±18.4	4.6±6.6	4.8±2.7	0.25±0.03	0.33±0.01
17.9±2.4	33.9±7.9	69.6±9.2	172.7±36.4	24.1±6.9	36.5±1.08	9.3±5.2	40.3±9.3	1.0±3.5	8.6±1.7	0.31±0.02	0.24±0.01
28.5±10.5	19.5±3.8	189.7±26.6	110.5±12.3	45±6.8	26.1±8	24.8±8.6	20±10.2	1.1±1.8	7.6±2.6	0.35±0.01	0.23±0.01
23.4±3.9	48.9±10.8	34.8±9.7	39±10.4	6.4±2.2	17.1±7.9	9.8±1.9	26.5±9.8	1.2±3	6.1±1.5	0.36±0.02	0.27±0.01
19.8±8.3	48.8±4.5	51.1±21.7	101.8±19.7	24.7±7.4	25.7±4.1	18±8.5	22.2±3.7	10.9±4.3	3.3±2.5	0.37±0.01	0.26±0.01
26.2±5.3	40.8±4.3	41.7±35	106.4±4.39	32.2±2.8	23.8±5.05	51.2±69.1	12.7±6.9	1.7±5.3	4.9±1.5	0.37±0.02	0.29±0.01
32.6±4.4	42.8±7.8	41.5±16.8	92±26.9	15.1±11.7	12±6.01	13.8±16.5	5±6.5	4.4±5.4	1.3±1.6	0.34±0.01	0.25±0.01
16.2±3.2	29.6±9.3	94.2±22.9	129±12.3	17.4±4.1	16.5±1.06	9.4±3.9	24.9±1.6	6.1±2.1	1.7±1.7	0.38±0.01	0.19±0.02
25.9±6.4	9.6±1.5	66.4±14.8	95.8±2.4	20.1±10.8	16.4±7.2	32.3±7.2	11.9±6.6	10.1±2.6	13±5.1	0.33±0.01	0.07±0.01
25.2±2.3	43±8.6	27.2±26.2	93.5±17.4	1.9±3.3	16.5±3.3	0.25±0.43	11.3±3.1	7.7±2.2	9.2±5.9	0.32±0.01	0.29±0.01

MH1: Metatarsal head 1, MH2: Metatarsal head 2, MH3: Metatarsal head 3, MH4: Metatarsal head 4, MH5: Metatarsal head 5, LDS: Left side children with down's syndrome, LN: Left side normal children

Supplementary Table 2a: Peak pressure (kPa) in children with and without down's syndrome (right foot)

Hindfoot		Midfoot		MH1		MH2		MH3		MH4	
RTHFDS	RTHFN	RTMFDS	RTMFN	RTHFDS	RTHFN	RTHFDS	RTHFN	RTHFDS	RTHFN	RTHFDS	RTHFN
149±73.2	266±166.9	90±22.36	123±40.8	253±74.1	159±20.4	169±56.8	323±71.6	144±60.4	265±44.1	113±51.1	155±23.7
224±107.3	254±58.9	106.5±27.6	138±46.9	185.5±119.5	188±33.09	198±70.9	299±19.8	215.5±62.9	297±24.9	165.5±49.5	188±35.1
218±58.3	276±12.9	198±36.1	88±10.3	397±240.8	248±42.5	213±55.07	193±6.71	223±53.9	203±5.70	176±47.3	148±16.4
115±28.9	306±30.7	138±22.5	161±65.8	58±29.92	221±24.08	69±17.4	311±45.6	113±29.7	290±36.2	161±43.6	220±19.3
115±23.4	253±50.5	105±8.66	71±11.9	95±29.58	261±49.3	142.8±20.3	200±25.7	152.8±20.7	168±24.6	132.1±20.3	171±29.03
642.5±576.2	135±16.9	207.5±109.6	174±2.2	385±7.07	187±15.2	537.5±74.2	384±33.05	475±494.9	346±21.6	302.5±258	232±32.1
271.2±27.5	276±15.9	108.7±16.5	100±14.5	268.7±85.7	210±38.2	178.7±51.3	193±7.58	198.7±88.4	190±9.35	158.7±38.6	183±13.04
229±42.1	214±31.5	163±29.5	149±24.6	476±129.9	97±23.6	211±29.2	242±16.05	217±35.8	248±24.9	227±34.9	211±30.2
332±92.5	248±69.1	159±17.1	57±7.58	52±35.46	202±28.4	130±32.7	171±23.02	192±36.8	128±8.37	202±35.1	103±26.1
267.5±40.09	265±39.6	172.5±21.1	162±8.37	533.3±95.4	199±71.2	275±19.4	212±29.2	217.5±16.3	239±31.9	193.3±15.7	205±17.3

MH5		Big toe		2nd toe		Toes345		Hallux angle (°)		Arch index	
RTHFDS	RTHFN	RTHFDS	RTHFN	RTHFDS	RTHFN	RTHFDS	RTHFN	RTHFDS	RTHFN	RTHFDS	RTHFN
83±37.01	133±37.8	159±47.4	317±96.4	51±47.4	246±4.05	46±53.2	182±73.1	7.1±5.6	3.9±1.4	0.29±0.03	0.35±0.03
122.5±43.1	124±32.8	228.5±82.2	337±41.9	202.5±56.1	543±122.2	72.5±49.9	376±67.1	9±5.4	4.8±5.5	0.34±0.02	0.23±0.01
136±55.9	77±10.3	646±101.8	287±14.4	227±7.6	265±7	83±19.5	110±40.4	4.5±5.8	2.7±1.9	0.29±0.01	0.26±0.02
205±67.1	134±46.5	150±9.35	154±17.8	56±11.4	72±44.6	41±6.52	62±43.6	10.6±11.4	10±1.4	0.37±0.02	0.29±0.01
82.8±9.5	272±58.05	129.2±54.1	454±94.5	152.8±29.2	151±25.8	62.1±8.5	92±13.5	6.8±5.6	7.8±6.8	0.37±0.02	0.23±0.01
100±21.2	204±23.5	0	272±36.1	22.5±31.8	306±35.7	17.5±24.7	179±43.7	0	1.6±0.9	0.33±0.01	0.3±0.01
92.5±21.7	279±108	161.2±15.4	234±25.8	150±73.2	143±36.3	152.5±37.9	92±28.4	6.5±6	1.7±1.7	0.35±0.01	0.24±0.01
208±27.2	94±21.04	87±10.37	550±201	67±18.2	182±2.5	27±17.8	130±18.3	1.2±1.4	1.9±2.8	0.3±0.01	0.24±0.01
107±31.7	113±71.2	679±111.2	201±31.9	367±59.1	246±8.22	98±19.2	142±25.1	10.3±3.2	3.3±1.4	0.36±0.02	0.10±0.05
92.5±13.6	140±35.7	97.5±37.5	180±171	43.3±27.8	89±85.4	5.83±14.2	74±77.9	7.3±7.3	4.5±1.5	0.31±0.01	0.31±0.02

MH1: Metatarsal head 1, MH2: Metatarsal head 2, MH3: Metatarsal head 3, MH4: Metatarsal head 4, MH5: Metatarsal head 5, RDS: Right side children with down's syndrome, RN: Right side normal children

Supplementary Table 2b: Peak pressure (kPa) in children with and without down's syndrome (left foot)

Hindfoot		Midfoot		MH1		MH2		MH3		MH4	
LTHFDS	LTHFN	LTHFDS	LTHFN	LTHFDS	LTHFN	LTHFDS	LTHFN	LTHFDS	LTHFN	LTHFDS	LTHFN
229±24.3	416±136.8	161±20.1	131±14.7	227±12	161±23	299±5.48	305±17.6	302±4.4	270±31.6	245±16.9	147±55.4
195±175.4	405±31.6	75±28.50	117.5±21.6	354±146	148.3±22.5	154±40.5	330±18.4	181±63.3	283.3±20.6	127±27.5	170.8±32.6
215.8±29.4	287±86.7	177.5±45.2	71±6.52	388.3±117	177±47.3	208.3±37.3	154±25.1	221.6±35.1	151±27.7	153.3±26.5	125±24.2
213.3±66.9	382±13.5	118.3±26.9	114±10.8	98.3±33.2	233±20.1	100±13.4	334±19.4	128.3±14.7	316±22.1	139.1±18.8	223±10.9
200±51.6	249±41.1	104±21.3	89±11.94	154±82.04	171±31.5	109±31.5	221±14.7	121±47.3	208±9.08	111±43.2	206±14.3
488.4±273.8	229±24.3	207.3±71.2	161±20.1	98.8±60.4	227±12.04	135.7±51.5	299±5.4	232.3±106.2	302±4.4	245±115.3	245±16.9
301.2±117	302±13.5	112.5±9.57	107±9.75	298.7±74.9	208±42.8	131.2±4.7	213±9.7	157.5±8.6	223±11.5	152.5±15	214±17.8
260±81.92	262±86.3	135±17.95	165±29.5	753±120	132±20.1	214.5±53.1	264±17.1	165±28.1	266±16.3	115.5±13.4	241±20.4
268±114.6	229±88.1	153±47.3	48±6.71	120±97.1	347±81.9	113±25.8	206±100.1	119±48.01	116±22.1	118±46	72±13.5
281.6±125.8	292±35.1	258.3±211	164±11.4	371.6±49	105±16.5	268.3±10.4	257±42.8	230±55.6	365±44.3	191.6±58.3	289±38.7

MH5		Big toe		2nd toe		Toes345		Hallux angle (°)		Arch index	
LTHFDS	LTHFN	LTHFDS	LTHFN	LTHFDS	LTHFN	LTHFDS	LTHFN	LTHFDS	LTHFN	LTHFDS	LTHFN
135±7.07	79±31.9	248±13	553±265	108.5±6.8	220±3.8	115±15.7	148±43.1	4.6±6.6	4.8±2.7	0.25±0.03	0.33±0.01
84±18.8	118.3±26.7	235±33.3	441.6±146	193±50.5	355.8±109	80±23.4	259.1±64.3	1.0±3.5	8.6±1.7	0.31±0.02	0.24±0.01
100±30.6	73±9.08	976.7±213	465±122	365±67.1	392±95.4	170±34	116±33	1.1±1.8	7.6±2.6	0.35±0.01	0.23±0.01
131.6±23.2	174±16.3	108.3±26.3	131±30.7	60±10.4	139±41.2	55±15.1	166±54.4	1.2±3	6.1±1.5	0.36±0.02	0.27±0.01
72±25.1	324±60.1	179±76.9	254±54.8	177±55.8	226±49.8	71±18.1	106±15.5	10.9±4.3	3.3±2.5	0.37±0.01	0.26±0.01
126.5±18.9	135±7.07	41.7±35	248±13	32.2±28.6	227±54.8	51.2±69.1	88±34.3	1.7±5.3	4.9±1.5	0.37±0.02	0.29±0.01
191.2±13.7	133±28.8	110±36.7	217±58.5	97.5±75.4	116±79	95±76.9	45±33.1	4.4±5.4	1.3±1.6	0.34±0.01	0.25±0.01
66.5±12.03	93±33.2	249±68	625±195	141±42.6	114±6.5	60±19.5	118±6.7183±30.1	6.1±2.1	1.7±1.7	0.38±0.01	0.19±0.02
84±17.8	42±9.08	573±182	507±61.6	205±107.4	170±66.4	126±14.3	83±30.1	10.1±2.6	13±5.1	0.33±0.01	0.07±0.01
115±26.4	167±38.01	27.2±26.2	223±45.3	1.91±3.3	147±33.2	0.25±0.43	80±15.41	7.7±2.2	9.2±5.9	0.32±0.01	0.29±0.01

MH1: Metatarsal head 1, MH2: Metatarsal head 2, MH3: Metatarsal head 3, MH4: Metatarsal head 4, MH5: Metatarsal head 5, LDS: Left side children with down's syndrome, LN: Left side normal children

Supplementary Table 3a: Contact time (p) (% ROP) in children with and without down's syndrome (right foot)

Hindfoot		Midfoot		MH1		MH2		MH3		MH4	
RTHFDS	RTHFN	RTMFDS	RTMFN	RTHFDS	RTHFN	RTHFDS	RTHFN	RTHFDS	RTHFN	RTHFDS	RTHFN
48.8±30.2	49.7±19.1	53.7±21.1	66.6±1.6	88.8±8.2	78.4±13.6	87.3±9.5	79.5±14	87.8±7.1	78±15.9	84.7±5.6	78±13.1
36.8±15.2	49.1±11.9	65.1±14.7	65.6±2.7	78±11.7	81.7±5.7	70.7±9.3	85.4±4.7	79.1±9.5	88±4.7	80.8±9.6	88±5.3
115±28.9	47.4±8.1	65.4±15.2	59.2±3.6	88±6.1	80.4±0.9	86±5.2	6.4±0.45	87.2±4.7	79±2.1	88.7±3.8	77.7±2.2
56.5±23.1	58.5±3.8	83.5±8.3	69.3±3.2	56.1±16.7	57.9±5.4	72.7±7.6	62.6±5.5	84±10.5	74.8±2.5	87.3±8.5	80.1±4.8
34.1±4.6	59.9±10.1	74.4±2.7	64.9±3.6	74.9±4.7	79.9±3.9	80.5±2	78.9±3.8	79.1±2	81.9±3.1	78.6±2.6	80.9±3.4
38.1±5.4	37.6±2.1	51.6±26.4	66.7±3.7	85±1.8	89.2±3.8	89.1±0.1	90.7±3.4	85.7±6.6	92.4±2.5	81±13.3	90.9±2.2
31±16	61.5±1	58.4±15.7	67.1±2.1	83±6.4	74.9±2.6	80.6±5.3	77.1±0.9	80.6±2.7	79.3±1.6	79.2±6.7	78.8±1.4
49.6±10	37.2±2.2	84.4±3	53.6±7.3	96.4±2.4	81.4±4.3	97.4±1.2	86.1±2.4	99.1±0.9	88.2±3	98.6±1.5	89.5±2.8
46.1±15.6	58.8±5.4	57±13.6	53.1±6.1	33.1±25.3	78.9±2.9	70.8±13.5	78.2±3.3	79±8.5	82±4	81.3±8.2	79±3.8
66.1±19.4	45.2±8.7	80.3±1.4	68.9±2.2	95.7±3.3	79.3±4.9	94.3±1.9	79.7±4	93.5±2.5	79.5±2.4	92.4±2	78.6±4.1

MH5		Big toe		2nd toe		Toes345		Hallux angle (°)		Arch index	
RTHFDS	RTHFN	RTHFDS	RTHFN	RTHFDS	RTHFN	RTHFDS	RTHFN	RTHFDS	RTHFN	RTHFDS	RTHFN
75.9±6.4	68.2±14.6	54.4±49.9	69.3±24	40.6±43.9	67.6±22.9	39.9±45.3	56.4±28.8	7.1±5.6	3.9±1.4	0.29±0.03	0.35±0.03
76.1±14.1	80±3.5	75.3±17.5	78.4±10.7	63.9±14.9	62.8±9.3	52.2±23.3	57.7±8.1	9±5.4	4.8±5.5	0.34±0.02	0.23±0.01
85.3±5.5	68.2±5.5	86.1±5.1	52.2±7.2	65.2±16.5	49.2±8.8	56.9±26.8	34.3±15.9	4.5±5.8	2.7±1.9	0.29±0.01	0.26±0.02
84.8±7.6	76.3±3	74.9±23.2	42.9±5.8	37.5±33.1	22.6±12	57.5±26.9	19.1±10.8	10.6±11.4	10±1.4	0.37±0.02	0.29±0.01
74.6±3.3	77.6±3.3	77.8±13.8	83.2±3.6	48.7±10.4	40.8±11	36.1±12.6	49.9±13.5	6.8±5.6	7.8±6.8	0.37±0.02	0.23±0.01
42.1±16.9	84.5±1.8	0	69±11.6	18.2±25.8	79.3±5.6	13.5±19.1	75.2±8.4	0	1.6±0.9	0.33±0.01	0.3±0.01
61.6±13.6	73.5±1.2	77.7±11.9	55.9±3.4	66.7±12.7	49.9±4.7	72±8.5	31.9±11.4	6.5±6	1.7±1.7	0.35±0.01	0.24±0.01
95.7±2.6	78.7±4	94.6±4.3	85.4±3.9	47.5±12	65.3±5.9	10.8±9.1	78.7±2.2	1.2±1.4	1.9±2.8	0.3±0.01	0.24±0.01
77.3±9	71.3±3.6	86.8±6.7	76.2±12.3	67.6±5.3	65.5±13.3	63.9±15	42.7±7.5	10.3±3.2	3.3±1.4	0.36±0.02	0.10±0.05
88.4±2.5	69.2±7	88.3±6.1	40.1±37.1	18.8±14.3	31.1±28.6s	1.7±4.1	32±29.9	7.3±7.3	4.5±1.5	0.31±0.01	0.31±0.02

MH1: Metatarsal head 1, MH2: Metatarsal head 2, MH3: Metatarsal head 3, MH4: Metatarsal head 4, MH5: Metatarsal head 5, RDS: Right side children with down's syndrome, RN: Right side normal children

Supplementary Table 3b: Contact time (p) (%ROP) in children with and without down's syndrome (left foot)

Hindfoot		Midfoot		MH1		MH2		MH3		MH4	
LTHFDS	LTHFN	LTHFDS	LTHFN	LTHFDS	LTHFN	LTHFDS	LTHFN	LTHFDS	LTHFN	LTHFDS	LTHFN
48.4±5.6	56.5±7.5	66.6±3.9	62.9±12.6	82.2±1.1	70.5±11.6	82.9±1.6	76.7±12.2	85.5±1.1	77±12.1	86.2±2	76.6±11.1
38.6±21	60.8±3.7	49.7±17.5	66.2±9	79±18.9	67.1±11.3	73.1±16.5	74.3±10.1	75.3±15.1	80.6±6.9	72±13.8	80.8±6
54.6±10.2	56.3±10.2	71.3±9	56.3±4.9	88.5±3.4	73.2±3.2	86.4±5.6	71.2±4	87±5.8	77.6±2.4	85.5±9.6	73.6±1.6
64±6.9	54.2±8.4	80.7±4.1	63.1±4.4	75.9±11	72.2±6	75.7±7.6	77.1±4.1	85.3±5.7	80.4±4	86.8±4.8	81.3±3.2
58.1±12.4	56±6.5	81.7±3.4	70.6±4	81±18.5	66.9±12.6	86.7±8.2	71.6±10.5	87.8±7.3	81.8±6.2	88.8±5.2	79.8±4.4
39.4±15.3	48.4±5.6	70.1±8.5	66.6±3.9	68.4±11	82.2±1.1	74.3±8.6	82.9±1.6	79.2±6.1	85.5±1.1	75.7±8.7	86.2±2
41.1±7.2	64.4±4.4	65.9±6	67.6±3.7	81.8±3.3	79.8±3.6	76.5±8.9	81.2±2.3	82.2±6.6	82.4±1.4	83.4±4.8	78.9±0.9
42.9±10.8	42.6±7.9	72.2±6.6	52.3±11.8	95.1±1.7	81.3±3.7	91.2±4.4	83.9±3.4	82.9±8.8	85.1±3	78±8.4	84.1±2.9
48.2±22.3	53.9±12.2	62.5±12.9	41.3±10.7	74.9±19.7	86.5±4.5	75.9±16.9	87.9±4.8	84.5±3.5	84.8±4	83.3±4	70.4±3.6
71.2±22.1	45.8±8.7	85.5±9.8	65.9±2.7	87.1±14.7	74.7±1.8	87.1±13.1	78.7±3.5	88.1±11	80.4±3.9	87.6±9.1	79.9±3.7

MH5		Big toe		2nd toe		Toes345		Hallux angle (°)		Arch index	
LTHFDS	LTHFN	LTHFDS	LTHFN	LTHFDS	LTHFN	LTHFDS	LTHFN	LTHFDS	LTHFN	LTHFDS	LTHFN
79.2±1.7	64.4±15.3	52.2±6.6	60.4±5.8	50.5±35.7	54.7±7.3	50.7±35.4	47.8±8.4	7.1±5.6	3.9±1.4	0.29±0.03	0.35±0.03
59±10.1	74.1±9.2	79.9±21.9	63.7±12.9	80.2±19.4	48.7±5.2	55.1±24.7	49.4±5.4	9±5.4	4.8±5.5	0.34±0.02	0.23±0.01
79±13.5	65±6.3	71.2±15.6	52.3±10.7	71.2±15.6	50.2±11.3	65.4±18.9	39.1±13.4	4.5±5.8	2.7±1.9	0.29±0.01	0.26±0.02
83.9±4.6	74.7±2.9	24.1±3.5	30.5±2.2	24.1±3.5	43.7±11.9	42±23.7	45.8±11.9	10.6±11.4	10±1.4	0.37±0.02	0.29±0.01
86.4±5.2	77.8±4.3	62.1±30.2	59.9±9.4	52.8±26.2	52.7±7.7	66.1±38.2	53.6±11.9	6.8±5.6	7.8±6.8	0.37±0.02	0.23±0.01
72.6±11.6	79.2±1.7	52.2±36.6	52.2±6.6	55.4±32	63±6.7	63.3±29.9	68.7±5.9	0	1.6±0.9	0.33±0.01	0.3±0.01
77.2±4	70.1±3	70.6±20.8	49.5±7.3	34.7±22.9	37.4±3.9	32.5±26.9	18.2±9.5	6.5±6	1.7±1.7	0.35±0.01	0.24±0.01
64.3±11.7	71.1±6.6	86.4±15.3	82.1±6.2	60±18.2	56.7±13.8	42.1±18.5	74.4±8.2	1.2±1.4	1.9±2.8	0.3±0.01	0.24±0.01
61.5±21.1	54.6±22.1	88.9±7	74.9±21.4	70±24.6	57.5±19.9	78.8±19.5	44.5±19	10.3±3.2	3.3±1.4	0.36±0.02	0.10±0.05
84.4±2.5	70.2±5.9	57.4±49.8	58.7±4.2	7.8±13.6	48.5±1.7	3.9±6.8	41.5±9.3	7.3±7.3	4.5±1.5	0.31±0.01	0.31±0.02

MH1: Metatarsal head 1, MH2: Metatarsal head 2, MH3: Metatarsal head 3, MH4: Metatarsal head 4, MH5: Metatarsal head 5, LDS: Left side children with down's syndrome, LN: Left side normal children

Supplementary Table 4a: Contact area (cm^2) in children with and without down's syndrome (right foot)

Hindfoot		Midfoot		MH1		MH2		MH3		MH4	
RTHFDS	RTHFN	RTMFDS	RTMFN	RTHFDS	RTHFN	RTHFDS	RTHFN	RTHFDS	RTHFN	RTHFDS	RTHFN
18.35±1.1	25±3.3	17±2.2	39.4±1.5	8.7±2.3	13.3±1.5	6.2±2.3	10.8±1.1	7.5±2	10.1±1.4	6.4±1.5	8.1±0.9
20.02±1.5	27.2±0.6	28±2.1	22.4±1.5	8.1±1.06	12.7±0.5	7.5±0.5	9.6±0.4	7.9±0.7	10.8±0.6	6.5±1.09	8.8±0.4
27.2±1.1	23.8±0.5	30.5±2.3	21.1±1.4	10±1.7	8.6±0.2	9.9±0.7	6.4±0.4	11.1±0.7	8.8±0.1	9.3±0.5	7.7±0.3
17.4±1.2	25.9±1.02	24.3±2.6	29.6±2.6	5.05±1.9	11.8±1.2	4.1±1.2	9.9±1.1	5.9±0.4	10.2±0.3	5.3±0.4	8.7±0.1
21.5±0.9	25.3±0.9	35.7±3.2	17.6±1.1	10.7±1.2	9±0.56	8.7±1.2	6.55±0.4	8.7±0.6	7.6±0.2	6.5±0.4	6.6±0.3
18.1±5.1	28.1±1.4	30.5±5.3	32.6±0.9	10.5±0.1	12.1±0.2	11.3±4.07	10.6±0.5	9.6±1.2	11.4±0.4	8.5±0.7	9±0.1
21.4±0.7	31.1±0.2	32.1±1.01	24.9±1.6	12.2±1.3	12.3±0.5	8.2±0.74	9.7±0.1	7.9±0.3	10.6±0.5	6.6±0.5	8.6±0.4
26.1±0.7	28.4±0.9	28.8±1.6	22.2±0.9	9.3±0.4	8.9±0.6	7.6±0.55	7.6±0.6	9.5±0.5	9.4±0.4	8±0.48	8.9±0.4
22.4±1.1	22.9±0.7	31.9±1.1	6.35±3.9	7.1±4.2	8.8±0.4	6.8±1.4	6.3±0.5	9.6±1.1	7±0.47	7.4±0.7	6±0.95
28.7±0.58	28.1±0.9	33±1.4	38.1±1.4	13.4±0.8	16.9±5.2s	10.1±0.13	12.9±1.8	10±0.33	12.3±1.9	8.3±0.2	9.9±1.3

MH5		Big toe		2nd toe		Toes345		Hallux angle (°)		Arch index	
RTHFDS	RTHFN	RTHFDS	RTHFN	RTHFDS	RTHFN	RTHFDS	RTHFN	RTHFDS	RTHFN	RTHFDS	RTHFN
3.4±0.6	4.7±0.9	4.3±4	9.9±1.1	1.3±1.2	4±0.47	1.6±1.9	7.3±1.5	7.1±5.6	3.9±1.4	0.29±0.03	0.35±0.03
3.9±0.5	5.1±0.5	7.3±1.2	10.2±0.7	3.2±0.6	3.7±0.1	2.6±1.1	6.9±0.6	9±5.4	4.8±5.5	0.34±0.02	0.23±0.01
5.1±0.7	4.4±0.3	11.4±0.9	7±0.66	3.3±0.1	2.1±0.3	6.9±0.8	4±1.9	4.5±5.8	2.7±1.9	0.29±0.01	0.26±0.02
3.1±0.5	5.3±0.4	5.9±1.2	7±0.59	1.7±0.4	1.7±1.1	2.3±0.4	1.5±1.1	10.6±11.4	10±1.4	0.37±0.02	0.29±0.01
3.7±0.5	3.8±0.3	7.8±1.3	9.9±0.68	3.9±0.4	2.9±0.6	2±0.53	4.2±0.3	6.8±5.6	7.8±6.8	0.37±0.02	0.23±0.01
4.1±3.3	5.6±0.5	0	8.6±0.5	0.7±1.06	2.9±0.5	0.5±0.7	5.9±0.3	0	1.6±0.9	0.33±0.01	0.3±0.01
3.1±0.3	5.6±0.31	8.2±0.68	9.5±0.41	3.1±1.1	3.5±0.2	4.8±1.03	6.1±0.8	6.5±6	1.7±1.7	0.35±0.01	0.24±0.01
5.1±0.3	5±0.50	6.6±0.5	8.4±0.3	2.2±0.6	3.1±0.1	0.7±0.4	6.2±0.6	1.2±1.4	1.9±2.8	0.3±0.01	0.24±0.01
4.4±0.8	4±0.5	7.1±0.7	7.6±0.3	3.8±0.4	3.2±0.3	5.5±0.6	6.1±0.7	10.3±3.2	3.3±1.4	0.36±0.02	0.10±0.05
4.3±0.2	5.5±0.82	6.7±0.8	6.1±5.6	1.1±0.8	1.5±1.57	0.1±0.31	2.4±2.3	7.3±7.3	4.5±1.5	0.31±0.01	0.31±0.02

MH1: Metatarsal head 1, MH2: Metatarsal head 2, MH3: Metatarsal head 3, MH4: Metatarsal head 4, MH5: Metatarsal head 5, RDS: Right side children with down's syndrome, RN: Right side normal children

Supplementary Table 4b: Contact area (cm^2) in children with and without down's syndrome (left foot)

Hindfoot		Midfoot		MH1		MH2		MH3		MH4	
LTHFDS	LTHFN	LTHFDS	LTHFN	LTHFDS	LTHFN	LTHFDS	LTHFN	LTHFDS	LTHFN	LTHFDS	LTHFN
32.6±0.8	26.9±1.4	33.8±0.6	36.2±1.1	12.4±0.3	12.3±0.9	11.8±0.5	10.8±0.4	11.7±0.4	10.6±0.4	9.7±0.2	8.8±0.5
17.2±2.6	28.5±1.7	22.7±1.6	24±1.3	8.7±1.06	11.8±0.4	6.9±0.3	9.7±0.4	7.7±0.9	11.1±0.2	6.4±0.3	9.2±0.3
28.2±0.97	24.3±0.8	39.6±2.1	18±0.94	12.2±1.7	8.3±0.4	9.7±0.7	6.7±0.3	9.9±1	8.6±0.22	8.3±0.4	7.7±0.2
19±0.5	27.2±0.8	26.9±3.1	26.7±1.2	7.9±1.1	10.6±0.7	5.8±0.9	8.3±0.3	6.3±0.74	9.9±0.4	5.1±0.3	8.9±0.2
22.3±2.1	25.3±0.6	34.5±1.08	20±0.6	10.7±1.4	9.3±0.4	7.7±0.8	7±0.4	7.5±1.22	8.5±0.4	6.5±0.4	6.3±0.2
24±1.9	32.6±0.8	37.2±3.2	33.8±0.6	10.5±1.8	12.4±0.3	8.7±1.2	11.8±0.5	8.8±3.08	11.7±0.4	6.9±2.3	9.7±0.2
20.8±0.6	32.5±0.7	29.6±1.8	26±1.33	10.2±0.7	12±0.5	8.1±0.2	9.6±0.5	8.6±0.6	11±0.41	6.2±0.3	8.7±0.4
27.1±1.7	28.4±0.4	41.8±0.9	16.9±2.7	13.3±0.7	9.95±0.5	8.8±0.5	8±0.8	8.3±0.44	9.1±0.5	6.9±0.2	8.8±0.4
21.9±0.7	22.6±0.9	28.2±2.9	3.9±0.5	7.5±1.05	8.7±1.2	7.2±1.7	6.1±0.5	9±0.47	5.5±1.1	7.3±0.7	5.3±1.1
28±3.2	29.8±0.9	37.2±3.6	33.82.6	14.5±0.7	12±1.36	11.6±2.9	11±0.8	11.5±2.5	12±1.10	8.8±1.1	10±0.21

MH5		Big toe		2nd toe		Toes345		Hallux angle (°)		Arch index	
LTHFDS	LTHFN	LTHFDS	LTHFN	LTHFDS	LTHFN	LTHFDS	LTHFN	LTHFDS	LTHFN	LTHFDS	LTHFN
5.9±0.6	4.9±0.3	9.25±0.7	9.3±0.4	2.7±1.3	4±0.59	3.1±2.05	7.1±2.2	7.1±5.6	3.9±1.4	0.29±0.03	0.35±0.03
3.7±0.4	5.2±0.2	7.25±1.2	10.4±0.7	3.1±0.6	3.4±0.3	2.8±1.3	5±0.5	9±5.4	4.8±5.5	0.34±0.02	0.23±0.01
4.5±0.9	4.3±0.5	10.5±0.4	7.3±0.14	3.9±0.6	2.2±0.3	5.4±1.3	3.85±1.2	4.5±5.8	2.7±1.9	0.29±0.01	0.26±0.02
3.2±0.6	5.9±0.7	5.7±0.2	6.1±0.8	1.6±0.3	2.7±0.9	3.4±0.4	5.2±1.3	10.6±11.4	10±1.4	0.37±0.02	0.29±0.01
3.5±0.5	4.2±0.4	7.1±1.1	9.2±0.5	3.5±0.5	2.9±0.37	4.7±1.2	5.3±0.6	6.8±5.6	7.8±6.8	0.37±0.02	0.23±0.01
3.7±0.9	5.9±0.6	5.7±4.2	9.2±0.7	3.8±2.3	2.9±0.2	5.8±4.8	3.7±1.5	0	1.6±0.9	0.33±0.01	0.3±0.01
4±0.5	5.7±0.3	7.1±1.5	8.5±1.02	2.9±0.9	2.6±0.4	2.7±2	1.9±1.8	6.5±6	1.7±1.7	0.35±0.01	0.24±0.01
3.7±0.6	5.2±0.4	8.8±0.8	9.3±0.8	2.8±0.4	2.7±0.21	3.2±1.05	5.2±0.6	1.2±1.4	1.9±2.8	0.3±0.01	0.24±0.01
4.6±0.5	3.5±0.5	7.3±1.9	8±0.61	2.6±1.05	2.2±0.3	6.2±0.7	3.3±1.6	10.3±3.2	3.3±1.4	0.36±0.02	0.10±0.05
4.2±0.6	5.6±0.4	4.6±4.1	9±1.19	0.5±1.014	2.5±0.27	0.08±0.14	2.90±0.55	7.3±7.3	4.5±1.5	0.31±0.01	0.31±0.02

MH1: Metatarsal head 1, MH2: Metatarsal head 2, MH3: Metatarsal head 3, MH4: Metatarsal head 4, MH5: Metatarsal head 5, LDS: Left side children with down's syndrome, LN: Left side normal children

Case Report

Incidentally Detected Anomalous Pectoralis Major Muscle During Reconstruction of Oral Cavity Cancer

Abstract

The congenital deficiency of pectoralis major muscle is quite uncommon. Only a few cases are described in the literature that too in cadavers. Recently, we came across a case of deficient pectoralis major while harvesting pectoralis major myocutaneous (PMMC) flap for reconstruction following right composite resection for carcinoma of the right buccal mucosa in a 50-year-old female. The external appearance of the anterior chest wall was normal. During surgery, we found that the clavicular head and sternal portion of the sternocostal head of the right pectoralis major muscle were absent and the costal portion of the sternocostal head was deficient over the medial aspect. A normal pectoralis minor was present. This deficiency may be congenital in nature. We present this case to highlight this uncommon condition, and this may be the only case report till now wherein deficient pectoralis major was used for PMMC flap reconstruction of oral cavity defect.

Keywords: *Deficiency, pectoralis major muscle, pectoralis major myocutaneous flap reconstruction*

Amitabh Jena, Gajjala Sivanath Reddy[1], Rashmi Patnayak[2], Sarla Settipalli[3]

Departments of Surgical Oncology and [2]Pathology, IMS and SUM Hospital, Bhubaneswar, Odisha, Departments of [1]Surgical Oncology and [3]Radiology, Sri Venkateswara Institute of Medical Sciences, Tirupati, Andhra Pradesh, India

Introduction

The pectoralis major is a large thick triangular fan-shaped extrinsic muscle of the anterior thoracic wall. It has clavicular and sternocostal heads. The clavicular head takes origin from the medial third or half of the clavicle. The sternocostal head originates from the sternum, the costal cartilages of the upper six ribs, and the anterior lamina of the rectus sheath. From these two origins, the fibers converge toward their insertion into the lateral lip of the bicipital groove of the humerus[1] [Figure 1a]. The medial pectoral nerve innervates solely the lower pectoralis major segments, and the lateral pectoral nerve is involved in the innervation of the clavicular portion and the upper segments of the sternocostal portion.[2]

There are various anomalies of the pectoralis muscle described in the literature, including few from India.[3,4] However, most of the reported cases were anatomical findings from cadavers.[3]

Anomalies in the pectoralis muscle are more likely to occur in the clavicular portion, being the most proximal and the earliest portion to attach, whereas the sternocostal portion is either reduced or absent.[5]

In our report, we describe a case of deficient pectoralis major muscle in a female patient, incidentally detected while doing reconstruction by pectoralis major myocutaneous (PMMC) flap for carcinoma buccal mucosa. Hereby, we discuss the rarity of the condition and how it affected our surgical management.

Case Report

This is a case of a 50-year-old female diagnosed with carcinoma of the right buccal mucosa. We planned for right composite resection and reconstruction of the defect with PMMC flap. The external appearance of the anterior thoracic wall was apparently normal with well-developed breasts.

While harvesting PMMC flap, we observed that the pectoralis major muscle is only originating from the lateral part of the costal portion of the sternocostal head and was well developed. The clavicular head and the sternal portion of the sternocostal head of the right pectoralis major muscle were completely absent. The medial part of the costal portion of the sternocostal head was also absent. Insertion of the muscle was into the lateral lip of the bicipital groove of the humerus. A normal pectoralis minor was present [Figure 1b]. The vascular supply to

How to cite this article: Jena A, Reddy GS, Patnayak R, Settipalli S. Incidentally detected anomalous pectoralis major muscle during reconstruction of oral cavity cancer. J Anat Soc India 2021;70:XX-XX.

Article Info

Received: 13 December 2019
Accepted: 15 February 2021
Available online: ***

Address for correspondence:
Dr. Rashmi Patnayak, Department of Pathology, IMS and SUM Hospital, Bhubaneswar, Odisha, India. E-mail: rashmipatnayak2002@yahoo.co.in

Access this article online

Website: www.jasi.org.in
DOI: 10.4103/JASI.JASI_239_19
Quick Response Code:

the muscle was found to be intact at its normal anatomical position supplying the pectoralis major by pectoral branch of acromiothoracic vessels [Figure 2]. The deltoid and subclavius muscles were not hypertrophied.

We did not explore the left side, to avoid unnecessary morbidity; also, it was not required for the operative procedure. Hence, the status of the left pectoralis muscles at the time of surgery could not be commented upon. Externally, there was no abnormality noted in the patient's chest wall. As a routine preoperative work-up, chest X-ray was done. Preoperative computed tomography scan or magnetic resonance imaging (MRI) of the chest was not done, as for routine reconstruction with PMMC flap, these investigations were not required.

The skin paddle was marked and was harvested along with the whole muscle. It included the full length of the muscle up to its insertion with intact vascular pedicle [Figure 2]. Then, the flap was used for reconstruction of oral cavity defect.

Postoperative period was uneventful without any complications such as flap necrosis and wound infection. The patient was discharged on the 10th postoperative day with advice to take oral diet.

After a follow-up period of 8 months, we noticed that both the flap donor and reconstructed sites were healthy with acceptable cosmetic result. MRI of the chest showed absent pectoralis major muscle in the right side which was used in toto for reconstruction. Pectoralis minors of both sides and pectoralis major of the left side were intact [Figure 3].

In a previous study, we have reported the outcome of PMMC flap reconstruction in 140 female patients.[6] However, none of those cases showed this type of deficient pectoralis major muscle.

Discussion

In the literature, there are reports of various anomalies of the pectoralis muscle.[1] Even drawings by Leonardo da Vinci in the 16th century demonstrated this type of defect.[1] Poland's syndrome is the most common condition in which pectoral muscle anomalies are noted.[5,7] The combination of a lack of the pectoralis major and/or minor muscles with skeletal, vascular, and surface feature anomalies in the ipsilateral upper limb is referred to as Poland's syndrome.[5] Poland's syndrome is characterized by the absence of the pectoralis major and minor muscles, hypoplasia or complete absence of the breast, costal cartilage and rib defects, and hypoplasia of subcutaneous chest wall tissue.[8] The congenital absence of the pectoralis muscle is usually a common feature of Poland syndrome. Hypoplasia of the sternocostal portion of the pectoralis is the most significant feature. It is most frequently associated with homolateral breast hypoplasia.[8] A nonsyndromic congenital absence of the pectoralis muscle is rare. These types of absences are usually partial and unilateral.[2,9]

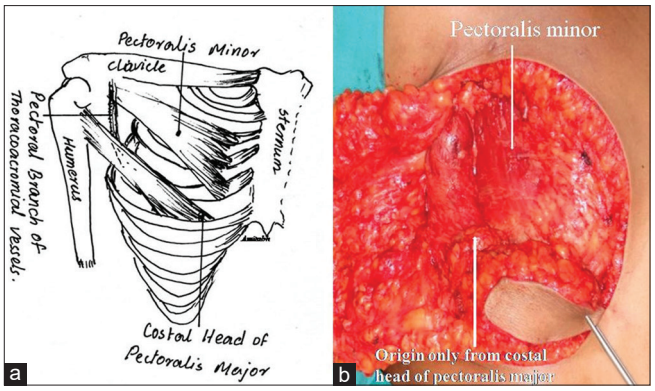

Figure 1: (a) Normal anatomy of pectoralis major. (b) Absence of the clavicular head, sternal and medial part of the costal portion of the sternocostal head of the right pectoralis major muscle, and presence of normal pectoralis minor

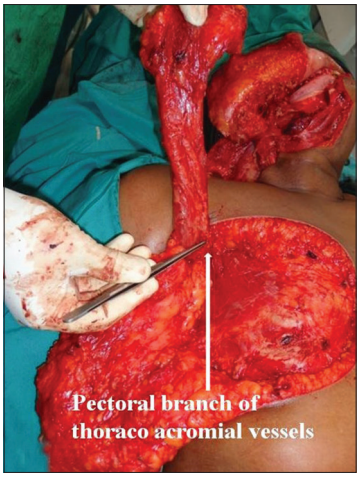

Figure 2: The intact vascular pedicle supplying the pectoralis major

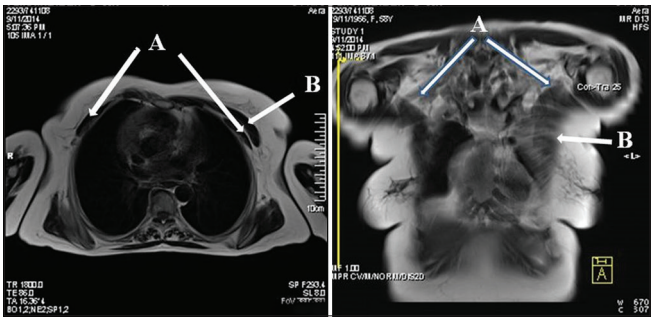

Figure 3: Magnetic resonance imaging (axial and coronal image) of the chest showing absent pectoralis major muscle (A – pectoralis major) in the right side which was used in toto for reconstruction and pectoralis minor (B – pectoralis minor), intact pectoralis major of the left side, and pectoralis minors

The pectoralis major and minor muscles develop from a muscle mass that appears during the 5th month *in utero*.[5,10] The mass of muscle attaches to the clavicle, fans out, and subsequently attaches to the sternum and ribs. Hence, anomalies are more likely in the clavicular portion, whereas the sternocostal portion is either reduced or absent.[5]

The cause of this disease is unknown, most likely the cause being a vascular abnormality that causes failure of development. It is believed that subclavian artery supply disruption sequence may be the underlying cause. It is characterized by an intrauterine damage to the blood supply coming from the subclavian artery.[3] Pectoral muscle anomalies, though not common, were among the most frequently encountered.[5] As far as functional aspect is concerned, several authors agree that the patients with congenital deficits in pectoral muscles have little or no functional deficits in normal daily activities.[5] However, during reconstruction of PMMC flap, an anomalous pectoralis muscle may pose a problem.

In our case, since there was intact vascular supply, this anomalous pectoralis major did not create any problem. The patient is doing well after the reconstruction. In cases where there is a complete absence of pectoralis major muscle option of reconstruction with free flaps should be considered.

We conclude this case of deficient pectoralis muscle incidentally encountered at the time of surgery, by highlighting its relative rarity.

Declaration of patient consent

The authors certify that they have obtained all appropriate patient consent forms. In the form the patient (s) has/have given his/her/their consent for his/her/their images and other clinical information to be reported in the journal. The patients understand that their names and initials will not be published and due efforts will be made to conceal their identity, but anonymity cannot be guaranteed.

Financial support and sponsorship

Nil.

Conflicts of interest

There are no conflicts of interest.

References

1. Standring S, editor. Gray's Anatomy: The Anatomical Basis of Clinical Practice. 40th ed. Edinburgh, Scotland: Churchill Livingstone/Elsevier; 2008.
2. Yuan SM. Non syndromic congenital absence of the pectoralis muscles. J Nippon Med Sch 2018;85:246-9.
3. Garg R, Saheer S, Gupta V, Mehra S. Poland sequence: Series of two cases and brief review of the literature. Ann Thorac Med 2012;7:110-2.
4. Soni S, Rath G, Suri R, Kumar H. Anomalous pectoral musculature. Anat Sci Int 2008;83:310-3.
5. Mosconi T, Kamath S. Bilateral asymmetric deficiency of the pectoralis major muscle. Clin Anat 2003;16:346-9.
6. Jena A, Patnayak R, Sharan R, Reddy SK, Manilal B, Rao LM. Outcomes of pectoralis major myocutaneous flap in female patients for oral cavity defect reconstruction. J Oral Maxillofac Surg 2014;72:222-31.
7. Bannur BM, Mallashetty N, Endigeri P. An accessory muscle of pectoral region: A case report. J Clin Diagn Res 2013;7:1994-5.
8. Huang Y, Pang H, Jin S, Han X, Liu X, Yang L, *et al*. Clinical characteristics of Poland's syndrome associated with breast cancer: Two case reports and a literature review. J Can Res Ther 2018;14:1665-9.
9. Haładaj R, Wysiadecki G, Clarke E, Polguj M, Topol M. Anatomical variations of the pectoralis major muscle: Notes on their impact on pectoral nerve innervation patterns and discussion on their clinical relevance. Biomed Res Int 2019;2019:6212039.
10. Buckwalter VJ, Shah AS. Presentation and treatment of Poland anomaly. Hand (N Y) 2016;11:389-95.

Case Report

An Unusual Variation of Infrahyoid Musculature and Its Clinical Implications

Abstract

Knowledge of the anatomy of musculoskeletal system of the anterior neck region is crucial for the good practice of health personnel. In this area, both muscular and vascular systems are closely related, and the anatomical variations that may occur could alter blood conduction or hinder medical and surgical maneuvers. This study reports a case of unilateral duplicated omohyoid muscle and its merger with an anomalous sternohyoid muscle with an intermediate tendinous formation and discusses its clinical importance. This alteration might have represented a problem at a surgical reconstruction of diverse neck structures, in case of having specified one. Besides, a large-flow collateral vein system has been observed, which could also have played an important role in the consequences of this anatomical muscle variation. Thus, it is considered as of importance to report on the anatomical variations found in human dissections, both for basic science researchers and for professionals dedicated to clinical science.

Keywords: *Anatomical variations, human dissection, infrahyoid musculature, omohyoid, sternohyoid*

Eva María González-Soler, Arantxa Blasco-Serra, Francisco Martínez-Soriano, Alfonso A. Valverde-Navarro

Department of Human Anatomy and Embryology, Faculty of Medicine and Odontology, University of Valencia, Valencia, Spain

Introduction

Over the last decades, interest has grown in the study of anatomical variations of the infrahyoid musculature, given its clinical relevance.[1-3] Infrahyoid musculature is composed of sternothyroid (ST), thyrohyoid (TH), omohyoid (OH), and sternohyoid (SH) muscles.[4] These are embryologically formed from a muscle primordium occurring in the anterior cervical area: ST and TH come from the deep layer of this primordium, and SH and OH come from the superficial layer, specifically from a degeneration of the splenius spread, which is a characteristic of human species.[1,5]

In the case presented in this paper, a unilateral duplicated inferior belly of the OH muscle merging with SH has been found. Besides, a tendinous formation in this SH muscle happened at the same time, and both muscles were found on the right side of the neck. This is a rare case, so it has been considered that it could have significant clinical interest for healthcare professionals.

Case Report

During a regular anatomy dissection of a female cadaver in 2018, a duplicated inferior belly of the OH muscle merged to an anomalous SH muscle with a tendinous formation in its middle (dividing it into two parts) on the right side of the neck was found [Figure 1].

In this case, we found the following duplication variation of the OH muscle: The superior OH muscle showed a typical appearance of the normal superior and inferior bellies with an intermediate tendon in between. The duplicated inferior belly of the OH muscle was similar to the superiorly positioned muscle, without intermediate tendon, and was united with SH muscle at the medial part of the clavicle, next to an intermediate tendon found on SH. The location of the attachment and the innervation for the duplicated inferior belly of the OH muscle were the same as superior OH muscle. This abnormality could belong to two classifications: Type I (double OH) and Type II (as inferior OH merges with SH). Both are innervated by the *ansa cervicalis*. This classification of anatomical OH variations has classical roots and is presented as follows: (1) OH muscle is present and has an intermediate tendon (Type V); (2) attached to the

How to cite this article: González-Soler EM, Blasco-Serra A, Martínez-Soriano F, Valverde-Navarro AA. An Unusual Variation of Infrahyoid Musculature and Its Clinical Implications. J Anat Soc India 2020;69:XX-XX.

Article Info

Received: 08 November 2019
Revised: 30 July 2020
Accepted: 08 August 2020
Available online: ***

Address for correspondence:
Dr. Arantxa Blasco-Serra, Department of Human Anatomy and Embryology, Faculty of Medicine and Odontology, University of Valencia, Avd. Blasco Ibáñez, 1546010 València, Spain.
E-mail: arantxa.blasco@uv.es

Access this article online

Website: www.jasi.org.in
DOI: 10.4103/JASI.JASI_219_19
Quick Response Code:

superior border of the scapula (Type IV); and (3) supplied by the *ansa cervicalis*.[1]

Regarding the anomaly of the SH muscle, an intermediate tendon was found at the level of the medial part of the clavicle and the thyroid gland. It is here that the duplicated inferior belly of the OH muscle appears to be attached [Figure 2]. This merging happens very close to the internal jugular vein (IJV). The intermediate tendon divided SH into a superior and an inferior part.

An anterior jugular vein (AJV) was also found (which was eliminated to continue with the management of dissection), and the anastomosis between AJV and the external jugular vein was through a large-flow communicating vein (LFCV).

Discussion

The clinical relevance of alterations of the anterolateral neck musculature has attracted the attention of many anatomists over recent years, given its surgical importance. Actually, neck surgery is, to this day, one of the basic principles of neck cancer therapy. Therefore, not only surgeons but also all health personnel related to clinical treatment of this region must have an unbeatable

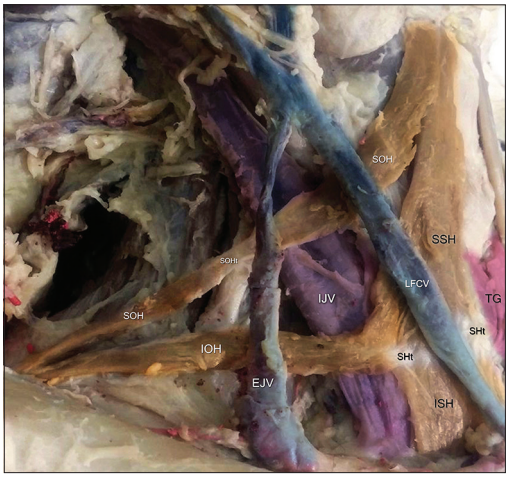

Figure 1: Deep dissection of the right side of the neck of a female cadaver showing the infrahyoid musculature. Note the variations on the omohyoid and sternohyoid muscles. Structures to be valued have been highlighted. SOH: Superior omohyoid muscle, SOHt: tendon of superior omohyoid muscle, IOH: Inferior omohyoid muscle, SSH: Superior sternohyoid muscle, ISH: Inferior sternohyoid muscle, SHt: tendon of sternohyoid muscle, IJV: Internal jugular vein, EJV: External jugular vein, LFCV: Large-flow communicating vein, TG: Thyroid gland

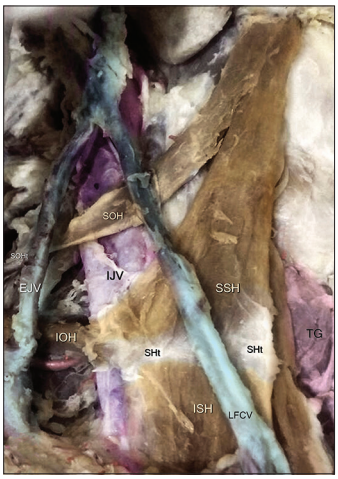

Figure 2: Photograph showing in detail the tendon of superior omohyoid muscle. Structures to be valued have been highlighted. SOH: Superior omohyoid muscle, SOHt: tendon of superior omohyoid muscle, IOH: Inferior omohyoid muscle, SSH: Superior sternohyoid muscle, ISH: Inferior sternohyoid muscle, SHt: tendon of sternohyoid muscle, IJV: Internal jugular vein, EJV: External jugular vein, LFCV: Large-flow communicating vein, TG: Thyroid gland

Figure 3: Photograph of backbone variations. The marked scoliosis has deviated great arteries and venous vessels of the posterior mediastinum, as well as the esophagus; notice how the azygos vein has been completely displaced towards the left. AA: Aorta artery, AV: Azygos vein, VS: Vertebral soma

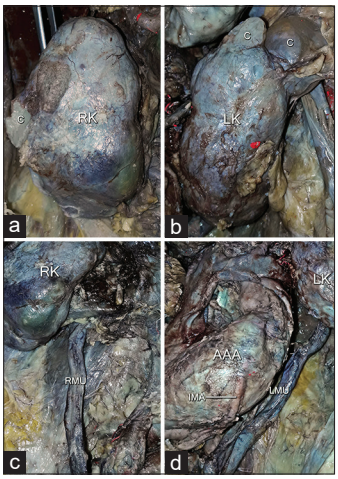

Figure 4: Photograph of urinary system abnormalities. (a and b) Both kidneys can be observed. Notice the cystic formations as well as the remarkable size and morphologic differences. (c and d) The megaureters formation. AAA: Aorta artery aneurism, C: Cyst, IMA: Inferior mesenteric artery, LK: Left kidney, LMU: Left megaureter, RK: Right kidney, RMU: Right megaureter

anatomical base of the anterolateral region of the neck, bearing in mind the possible anatomical variations that could be found, and what complications and risks they could cause.

OH is an anatomical landmark to identify the levels III and IV lymph node metastases of head-and-neck cancers; it has been studied for the treatment of a bowed vocal fold by transpositioning and for the restoration of vocal cord abduction.[6] In the presented case, a duplicated inferior belly of the OH muscle is merged to the abnormal intermediate tendon of the SH muscle. Based on previous studies, it can be hypothesized that this fusion would have confused the level of classification of metastasis and thus alter postoperative therapy and prognosis by altering these anatomical landmarks.[6]

Several authors have theorized a genetic reason of alterations in this musculature: Since *TBX1* gene regulates the myogenic differentiation and cellular fate within the mesoderm, inactivation or deletion of this gene leads to alterations in the morphology of neck muscles.[7] Changes in *TBX1* gene are responsible for many of the features of 22q11.2 deletion syndrome, which has a heterogeneous presentation, including congenital anomalies, such as palatal, gastrointestinal, cardiovascular, and genitourinary abnormalities.[8] In the case presented, both OH and SH muscles presented anatomical variations. These two muscles originate from the superficial layer of the infrahyoid premuscular band, whose development depends on this *TBX1* gene; moreover, a highly marked scoliosis [Figure 3], a discreet micrognathia, and bilateral polycystic kidneys [Figure 4a and b], as well as bilateral dilated megaureters with signs of vesicoureteral reflux [Figure 4c and d] and an abdominal aortic aneurysm [Figure 4d] have also been found.

Intermediate OH tendon is directly adhered to the anterior wall of IJV, connected to it through a thin lamina of the pretracheal layer of the cervical fascia, so the contraction of OH muscle has a direct effect on the lumen of this vessel.[4] The presented case also showed an AJV and an LFCV. The existence of this collateral vein system plays an important role for the insertion of port catheters, pacemaker leads, or other types of central devices, when there is a problem with other accesses considered as more common.[9]

Anomalies on the SH muscle are very uncommon; in fact, the variation of the SH muscle observed in the present case has not been previously reported. Kim *et al*., in 2015, found *in vivo* human cases in which SH muscle arose from the mid-portion of the clavicle and ran toward the hyoid, without fascia and an abnormal muscle color; from a bioscopic perspective, it was presented as a lateral neck mass, and subjects reported symptoms such as mild dysphagia with pain and foreign body sensation in their throat for a long time, with no choking difficulties. These cases were registered under the name of "SH syndrome."[10]

It is important to report these anatomical variations from basic research to clinical fields for the management of diverse interventions, such as neck-and-head surgery. The existence of multidisciplinary clinical-basic work teams is very positive and brings us closer to the understanding of the morphology, physiology, and development of the human body.

Financial support and sponsorship

Nil.

Conflicts of interest

There are no conflicts of interest.

References

1. Rai R, Ranade A, Nayak S, Vadgaonkar R, Mangala P, Krishnamurthy A. A study of anatomical variability of the omohyoid muscle and its clinical relevance. Clinics (Sao Paulo) 2008;63:521-4.
2. Iwanaga J, Tabira Y, Fisahn C, Alonso F, Watanabe K, Kusukawa J, *et al*. Unusual muscle of the anterior neck: Cadaveric findings with surgical applications. Anat Cell Biol 2017;50:239-41.
3. Singh N, Kathole M, Kaur J, Mehta V, Suri RK, Rath G, *et al*. Bilateral clavicular attachment of omohyoid muscle. Morphologie 2018;102:87-90.
4. Moore KL, Dalley AF, Agur AM. Clinically Oriented Anatomy. 8th ed.. Philadelphia: Wolters Kluwer; 2018.
5. Nayak SR, Rai R, Krishnamurthy A, Prabhu LV, Potu BK. An anomalous belly of sternothyroid muscle and its significance. Rom J Morphol Embryol 2009;50:307-8.
6. Kojima H, Hirano S, Shoji K, Omori K, Honjo I. Omohyoid muscle transposition for the treatment of bowed vocal fold. Ann Otol Rhinol Laryngol 1996;105:536-40.
7. Dastjerdi A, Robson L, Walker R, Hadley J, Zhang Z, Rodriguez-Niedenführ M, *et al*. Tb×1 regulation of myogenic differentiation in the limb and cranial mesoderm. Dev Dyn 2007;236:353-63.
8. McDonald-McGinn DM, Sullivan KE, Marino B, Philip N, Swillen A, Vorstman JA, *et al*. 22q11.2 deletion syndrome. Nat Rev Dis Primers 2015;1:15071.
9. Rott G, Boecker F. Port placement via the anterior jugular venous system: Case report, anatomic considerations, and literature review. Case Rep Radiol 2017;2017:2790290.
10. Kim JS, Hong KH, Hong YT, Han BH. Sternohyoid muscle syndrome. Am J Otolaryngol 2015;36:190-4.

Dr. Vishwanath Ramrao Mysorekar (Dec 1931 - Dec 2020)

Anatomy is the base of medical sciences enriched regularly by dedicated contributions from great anatomists worldwide. Among them, one unforgettable personality from India was Dr. V. R. Mysorekar.

Many of his works are cited in Gray's Anatomy (36th, 37th, and 38th Editions) Gardner greys and O' Rahially 4th Edition, Holinshed Vol. 3 (3 Edition) and other books. He was a great teacher known for his excellence in the academics and research. He had at least 56 publications to his credit in both international and national journals.

He was born in December 13, 1931 to Sri Srinivasa rao and Smt. Ramalaxamamma in Mysore. BSC (Hons) – 1949-Pune; MBBS 1954. - B. J. Med College, Pune; MSC (Med. Anatomy) - 1962, - B. J. Med. College, Pune; PhD (Anatomy) - 1972 Pune University. He was also fond of music particularly of Kishorda, which he used to sing often.

He rendered innumerable Guest lectures. He also worked as W.H.O. Fellow at Department of Anatomy, university of New castle-up on Tyne (U.K.) with prof. R. J. Scot Home for a period of 16 months (1967 April–1968 August) and was trained in experimental embryology.

He has been awarded the Chief of Army staff-Commendation Medal and Card on August 15, 1981, for Meritorious and Dedicated Service (sword of honor from AFMC), and his name is inducted into the hall of fame, AFMC, Pune, India.

He was also recipient of prestigious Dr. B.C. Roy National Award for the Category Eminent Medical Teacher - 1983.

Karnataka chapter of Anatomists of Anatomical Society of India conferred him "SUSHRUTA GOLD MEDAL AWARD" - in 2013 - for Excellence in Anatomy.

He has a credit of developing wonderful Anatomy Museums at B.J. Medical College - Pune, Government Medical College – Miraj, AFMC-Pune (Embryology section worth seeing), M.S. Ramaiah Med. College - Bengaluru, SDUMC-Kolar.

His name is listed as a Noteworthy Anatomist, Educator, and Researcher by MARQUIS WHO's WHO.

Dr. Vishwanath Ramrao Mysorekar - Legend in Anatomy (Dec 1931 - Dec 2020)

He is survived by two daughters and a son. On 28-12-2020, I received the sad news of his demise. With Soulful condolences

G. M. Mahesh

Department of Anatomy, BMCH, Chitradurga, Karnataka, India

Address for correspondence: *Dr. G. M. Mahesh, BMCH, Chitradurga, Karnataka, India. E-mail: editorjasi@gmail.com*

Article Info

Received: 02 March 2021
Accepted: 09 March 2021
Available online: ***

Access this article online

Quick Response Code:

Website: www.jasi.org.in

DOI: 10.4103/jasi.jasi_41_21

How to cite this article: Mahesh GM. Dr. Vishwanath Ramrao Mysorekar (Dec 1931 - Dec 2020). J Anat Soc India 2021;XX:XX-XX.

The Editorial Process

A manuscript will be reviewed for possible publication with the understanding that it is being submitted to Journal of the Anatomical Society of India alone at that point in time and has not been published anywhere, simultaneously submitted, or already accepted for publication elsewhere. The journal expects that authors would authorize one of them to correspond with the Journal for all matters related to the manuscript. All manuscripts received are duly acknowledged. On submission, editors review all submitted manuscripts initially for suitability for formal review. Manuscripts with insufficient originality, serious scientific or technical flaws, or lack of a significant message are rejected before proceeding for formal peer-review. Manuscripts that are unlikely to be of interest to the Journal of the Anatomical Society of India readers are also liable to be rejected at this stage itself.

Manuscripts that are found suitable for publication in Journal of the Anatomical Society of India are sent to two or more expert reviewers. During submission, the contributor is requested to provide names of two or three qualified reviewers who have had experience in the subject of the submitted manuscript, but this is not mandatory. The reviewers should not be affiliated with the same institutes as the contributor/s. However, the selection of these reviewers is at the sole discretion of the editor. The journal follows a double-blind review process, wherein the reviewers and authors are unaware of each other's identity. Every manuscript is also assigned to a member of the editorial team, who based on the comments from the reviewers takes a final decision on the manuscript. The comments and suggestions (acceptance/ rejection/ amendments in manuscript) received from reviewers are conveyed to the corresponding author. If required, the author is requested to provide a point by point response to reviewers' comments and submit a revised version of the manuscript. This process is repeated till reviewers and editors are satisfied with the manuscript.

Manuscripts accepted for publication are copy edited for grammar, punctuation, print style, and format. Page proofs are sent to the corresponding author. The corresponding author is expected to return the corrected proofs within three days. It may not be possible to incorporate corrections received after that period. The whole process of submission of the manuscript to final decision and sending and receiving proofs is completed online. To achieve faster and greater dissemination of knowledge and information, the journal publishes articles online as 'Ahead of Print' immediately on acceptance.

Clinical trial registry

Journal of the Anatomical Society of India favors registration of clinical trials and is a signatory to the Statement on publishing clinical trials in Indian biomedical journals. Journal of the Anatomical Society of India would publish clinical trials that have been registered with a clinical trial registry that allows free online access to public. Registration in the following trial registers is acceptable: http://www.ctri.in/; http://www.actr.org.au/; http://www.clinicaltrials.gov/; http://isrctn.org/; http://www.trialregister.nl/trialreg/index.asp; and http://www.umin.ac.jp/ctr. This is applicable to clinical trials that have begun enrollment of subjects in or after June 2008. Clinical trials that have commenced enrollment of subjects prior to June 2008 would be considered for publication in Journal of the Anatomical Society of India only if they have been registered retrospectively with clinical trial registry that allows unhindered online access to public without charging any fees.

Authorship Criteria

Authorship credit should be based only on substantial contributions to each of the three components mentioned below:

1. Concept and design of study or acquisition of data or analysis and interpretation of data;
2. Drafting the article or revising it critically for important intellectual content; and
3. Final approval of the version to be published.

Participation solely in the acquisition of funding or the collection of data does not justify authorship. General supervision of the research group is not sufficient for authorship. Each contributor should have participated sufficiently in the work to take public responsibility for appropriate portions of the content of the manuscript. The order of naming the contributors should be based on the relative contribution of the contributor towards the study and writing the manuscript. Once submitted the order cannot be changed without written consent of all the contributors. The journal prescribes a maximum number of authors for manuscripts depending upon the type of manuscript, its scope and number of institutions involved (vide infra). The authors should provide a justification, if the number of authors exceeds these limits.

Contribution Details

Contributors should provide a description of contributions made by each of them towards the manuscript. Description should be divided in following categories, as applicable: concept, design, definition of intellectual content, literature search, clinical studies, experimental studies, data acquisition, data analysis, statistical analysis, manuscript preparation, manuscript editing and manuscript review. Authors' contributions will be printed along with the article. One or more author should take responsibility for the integrity of the work as a whole from inception to published article and should be designated as 'guarantor'.

Conflicts of Interest/ Competing Interests

All authors of must disclose any and all conflicts of interest they may have with publication of the manuscript or an institution or product that is mentioned in the manuscript and/or is important to the outcome of the study presented. Authors should also disclose conflict of interest with products that compete with those mentioned in their manuscript.

Submission of Manuscripts

All manuscripts must be submitted on-line through the website http://www.journalonweb.com/jasi. First time users will have to register at this site. Registration is free but mandatory. Registered authors can keep track of their articles after logging into the site using their user name and password.

- If you experience any problems, please contact the editorial office by e-mail at editor@jasi.org.in

The submitted manuscripts that are not as per the "Instructions to Authors" would be returned to the authors for technical correction, before they undergo editorial/ peer-review. Generally, the manuscript should be submitted in the form of two separate files:

[1] Title Page/First Page File/covering letter:

This file should provide

1. The type of manuscript (original article, case report, review article, Letter to editor, Images, etc.) title of the manuscript, running title, names of all authors/ contributors (with their highest academic degrees, designation and affiliations) and name(s) of department(s) and/ or institution(s) to which the work should be credited, . All information which can reveal your identity should be here. Use text/rtf/doc files. Do not zip the files.
2. The total number of pages, total number of photographs and word counts separately for abstract and for the text (excluding the references, tables and abstract), word counts for introduction + discussion in case of an original article;
3. Source(s) of support in the form of grants, equipment, drugs, or all of these;
4. Acknowledgement, if any. One or more statements should specify 1) contributions that need acknowledging but do not justify authorship, such as general support by a departmental chair; 2) acknowledgments of technical help; and 3) acknowledgments of financial and material support, which should specify the nature of the support. This should be included in the title page of the manuscript and not in the main article file.
5. If the manuscript was presented as part at a meeting, the organization, place, and exact date on which it was read. A full statement to the editor about all submissions and previous reports that might be regarded as redundant publication of the same or very similar work. Any such work should be referred to specifically, and referenced in the new paper. Copies of such material should be included with the submitted paper, to help the editor decide how to handle the matter.
6. Registration number in case of a clinical trial and where it is registered (name of the registry and its URL)
7. Conflicts of Interest of each author/ contributor. A statement of financial or other relationships that might lead to a conflict of interest, if that information is not included in the manuscript itself or in an authors' form
8. Criteria for inclusion in the authors'/ contributors' list
9. A statement that the manuscript has been read and approved by all the authors, that the requirements for authorship as stated earlier in this document have been met, and that each author believes that the manuscript represents honest work, if that information is not provided in another form (see below); and
10. The name, address, e-mail, and telephone number of the corresponding author, who is responsible for communicating with the other authors about revisions and final approval of the proofs, if that information is not included on the manuscript itself.

[2] Blinded Article file: The main text of the article, beginning from Abstract till References (including tables) should be in this file. The file must not contain any mention of the authors' names or initials or the institution at which the study was done or acknowledgements. Page headers/ running title can include the title but not the authors' names. Manuscripts not in compliance with the Journal's blinding policy will be returned to the corresponding author. Use rtf/doc files. Do not zip the files. **Limit the file size to 1 MB.** Do not incorporate images in the file. If file size is large, graphs can be submitted as images separately without incorporating them in the article file to reduce the size of the file. The pages should be numbered consecutively, beginning with the first page of the blinded article file.

[3] Images: Submit good quality color images. **Each image should be less than 2 MB in size.** Size of the image can be reduced by decreasing the actual height and width of the images (keep up to 1600 x 1200 pixels or 5-6 inches). Images can be submitted as jpeg files. Do not zip the files. Legends for the figures/images should be included at the end of the article file.

[4] The contributors' / copyright transfer form (template provided below) has to be submitted in original with the signatures of all the contributors within two weeks of submission via courier, fax or email as a scanned image. Print ready hard copies of the images (one set) or digital images should be sent to the journal office at the time of submitting revised manuscript. High resolution images (up to 5 MB each) can be sent by email.

Contributors' form / copyright transfer form can be submitted online from the authors' area on http://www.journalonweb.com/jasi.

Preparation of Manuscripts

Manuscripts must be prepared in accordance with "Uniform requirements for Manuscripts submitted to Biomedical Journals" developed by the International Committee of Medical Journal Editors (October 2008). The uniform requirements and specific requirement of Journal of the Anatomical Society of India are summarized below. Before submitting a manuscript, contributors are requested to check for the latest instructions available. Instructions are also available from the website of the journal (www.jasi.org.in) and from the manuscript submission site http://www.journalonweb.com/jasi).

Journal of the Anatomical Society of India accepts manuscripts written in American English.

Copies of any permission(s)

It is the responsibility of authors/ contributors to obtain permissions for reproducing any copyrighted material. A copy of the permission obtained must accompany the manuscript. Copies of any and all published articles or other manuscripts in preparation or submitted elsewhere that are related to the manuscript must also accompany the manuscript.

Types of Manuscripts

Original articles:

These include randomized controlled trials, intervention studies, studies of screening and diagnostic test, outcome studies, cost effectiveness analyses, case-control series, and surveys with high response rate. The text of original articles amounting to up to 3000 words (excluding Abstract, references and Tables) should be divided into sections with the headings Abstract, Key-words, Introduction, Material and Methods, Results, Discussion and Conclusion, References, Tables and Figure legends.

An abstract should be in a structured format under following heads: **Introduction, Material and Methods, Results,** and **Discussion and Conclusion.**

Introduction: State the purpose and summarize the rationale for the study or observation.

Material and Methods: It should include and describe the following aspects:

Ethics: When reporting studies on human beings, indicate whether the procedures followed were in accordance with the ethical standards of the responsible committee on human experimentation (institutional or regional) and with the Helsinki Declaration of 1975, as revised in 2000 (available at http://www.wma.net/e/policy/17-c_e.html). For prospective studies involving human participants, authors are expected to mention about approval of (regional/ national/ institutional or independent Ethics Committee or Review Board, obtaining informed consent from adult research participants and obtaining assent for children aged over 7 years participating in the trial. The age beyond which assent would be required could vary as per regional and/ or national guidelines. Ensure confidentiality of subjects by desisting from mentioning participants' names, initials or hospital numbers, especially in illustrative material. When reporting experiments on animals, indicate whether the institution's or a national research council's guide for, or any national law on the care and use of laboratory animals was followed. Evidence for approval by a local Ethics Committee (for both human as well as animal studies) must be supplied by the authors on demand. Animal experimental procedures should be as humane as possible and the details of anesthetics and analgesics used should be clearly stated. The ethical standards of experiments must be in accordance with the guidelines provided by the CPCSEA and World Medical Association Declaration of Helsinki on Ethical Principles for Medical Research Involving Humans for studies involving experimental animals and human beings, respectively). The journal will not consider any paper which is ethically unacceptable. A statement on ethics committee permission and ethical practices must be included in all research articles under the 'Materials and Methods' section.

Study design:

Selection and Description of Participants: Describe your selection of the observational or experimental participants (patients or laboratory animals, including controls) clearly, including eligibility and exclusion criteria and a description of the source population. *Technical information*: Identify the methods, apparatus (give the manufacturer›s name and address in parentheses), and procedures in sufficient detail to allow other workers to reproduce the results. Give references to established methods, including statistical methods (see below); provide references and brief descriptions for methods that have been published but are not well known; describe new or substantially modified methods, give reasons for using them, and evaluate their limitations. Identify precisely all drugs and chemicals used, including generic name(s), dose(s), and route(s) of administration.

Reports of randomized clinical trials should present information on all major study elements, including the protocol, assignment of interventions (methods of randomization, concealment of allocation to treatment groups), and the method of masking (blinding), based on the CONSORT Statement (http://www.consort-statement.org).

Reporting Guidelines for Specific Study Designs

Initiative	Type of Study	Source
CONSORT	Randomized controlled trials	http://www.consort-statement.org
STARD	Studies of diagnostic accuracy	http://www.consort-statement.org/stardstatement.htm
QUOROM	Systematic reviews and meta-analyses	http://www.consort- statement.org/Initiatives/MOOSE/moose.pdf statement.org/Initiatives/MOOSE/moose.pdf
STROBE	Observational studies in epidemiology	http://www.strobe-statement.org
MOOSE	Meta-analyses of observational studies in epidemiology	http://www.consort- statement.org/Initiatives/MOOSE/moose.pdf

Statistics: Whenever possible quantify findings and present them with appropriate indicators of measurement error or uncertainty (such as confidence intervals). Authors should report losses to observation (such as, dropouts from a clinical trial). When data are summarized in the Results section, specify the statistical methods used to analyze them. Avoid non-technical uses of technical terms in statistics, such as 'random' (which implies a randomizing device), 'normal', 'significant', 'correlations', and 'sample'. Define statistical terms, abbreviations, and most symbols. Specify the computer software used. Use upper italics (*P* 0.048). For all *P* values include the exact value and not less than 0.05 or 0.001. Mean differences in continuous variables, proportions in categorical variables and relative risks including odds ratios and hazard ratios should be accompanied by their confidence intervals.

Results: Present your results in a logical sequence in the text, tables, and illustrations, giving the main or most important findings first. Do not repeat in the text all the data in the tables or illustrations; emphasize or summarize only important observations. Extra- or supplementary materials and technical detail can be placed in an appendix where it will be accessible but will not interrupt the flow of the text; alternatively, it can be published only in the electronic version of the journal.

When data are summarized in the Results section, give numeric results not only as derivatives (for example, percentages) but also as the absolute numbers from which the derivatives were calculated, and specify the statistical methods used to analyze them. Restrict tables and figures to those needed to explain the argument of the paper and to assess its support. Use graphs as an alternative to tables with many entries; do not duplicate data in graphs and tables. Where scientifically appropriate, analyses of the data by variables such as age and sex should be included.

Discussion: Include summary of *key findings* (primary outcome measures, secondary outcome measures, results as they relate to a prior hypothesis); *Strengths and limitations* of the study (study question, study design, data collection, analysis and interpretation); *Interpretation and implications* in the context of the totality of evidence (is there a systematic review to refer to, if not, could one be reasonably done here and now?, what this study adds to the available evidence, effects on patient care and health policy, possible mechanisms); *Controversies* raised by this study; and *Future research directions* (for this particular research collaboration, underlying mechanisms, clinical research).

Do not repeat in detail data or other material given in the Introduction or the Results section. In particular, contributors should avoid making statements on economic benefits and costs unless their manuscript includes economic data and analyses. Avoid claiming priority and alluding to work that has not been completed. New hypotheses may be stated if needed, however they should be clearly labeled as such. About 30 references can be included. These articles generally should not have more than six authors.

Review Articles:

These are comprehensive review articles on topics related to various fields of Anatomy. The entire manuscript should not exceed 7000 words with no more than 50 references and two authors. Following types of articles can be submitted under this category:

- Newer techniques of dissection and histology
- New methodology in Medical Education
- Review of a current concept

Please note that generally review articles are by invitation only. But unsolicited review articles will be considered for publication on merit basis.

Case reports:

New, interesting and rare cases can be reported. They should be unique, describing a great diagnostic or therapeutic challenge and providing a learning point for the readers. Cases with clinical significance or implications will be given priority. These communications could be of up to 1000 words (excluding Abstract and references) and should have the following headings: Abstract (unstructured), Key-words, Introduction, Case report, Discussion and Conclusion, Reference, Tables and Legends in that order.

The manuscript could be of up to 1000 words (excluding references and abstract) and could be supported with up to 10 references. Case Reports could be authored by up to four authors.

Letter to the Editor:

These should be short and decisive observations. They should preferably be related to articles previously published in the Journal or views expressed in the journal. They

should not be preliminary observations that need a later paper for validation. The letter could have up to 500 words and 5 references. It could be generally authored by not more than four authors.

Book Review: This consists of a critical appraisal of selected books on Anatomy. Potential authors or publishers may submit books, as well as a list of suggested reviewers, to the editorial office. The author/publisher has to pay INR 10,000 per book review.

Other:

Editorial, Guest Editorial, Commentary and Opinion are solicited by the editorial board.

References

References should be *numbered* consecutively in the order in which they are first mentioned in the text (not in alphabetic order). Identify references *in text*, tables, and legends by Arabic numerals in superscript with square bracket after the punctuation *marks. References cited only* in tables or figure legends should be numbered in accordance with the sequence established by the first identification in the text of the particular table or figure. Use the style of the examples below, which are based on the formats used by the NLM *in Index Medicus*. The titles of journals *should be abbreviated* according to the style used in Index Medicus. Use complete name of the journal for non-indexed journals. Avoid using abstracts as references. Information from manuscripts submitted but not accepted should be cited in the text as "unpublished observations" with written permission from the source. Avoid citing a "personal communication" unless it provides essential information not available from a public source, in which case the name of the person and date of communication should be cited in parentheses in the text. The commonly cited types of references are shown here, for other types of references such as newspaper items please refer to ICMJE Guidelines (http://www.icmje.org or http://www.nlm.nih.gov/bsd/uniform_requirements.html).

Articles in Journals

1. Standard journal article (for up to six authors): Parija S C, Ravinder PT, Shariff M. Detection of hydatid antigen in the fluid samples from hydatid cysts by co-agglutination. Trans. R.Soc. Trop. Med. Hyg.1996; 90:255–256.
2. Standard journal article (for more than six authors): List the first six contributors followed by *et al*.

Roddy P, Goiri J, Flevaud L, Palma PP, Morote S, Lima N. *et al*., Field Evaluation of a Rapid Immunochromatographic Assay for Detection of Trypanosoma cruzi Infection by Use of Whole Blood. J. Clin. Microbiol. 2008; 46: 2022-2027.

3. Volume with supplement: Otranto D, Capelli G, Genchi C: Changing distribution patterns of canine vector borne diseases in Italy: leishmaniosis vs. dirofilariosis. Parasites & Vectors 2009; Suppl 1:S2.

Books and Other Monographs

1. Personal author(s): Parija SC. Textbook of Medical Parasitology. 3rd ed. All India Publishers and Distributors. 2008.
2. Editor(s), compiler(s) as author: Garcia LS, Filarial Nematodes In: Garcia LS (editor) Diagnostic Medical Parasitology ASM press Washington DC 2007: pp 319-356.
3. Chapter in a book: Nesheim M C. Ascariasis and human nutrition. In Ascariasis and its prevention and control, D. W. T. Crompton, M. C. Nesbemi, and Z. S. Pawlowski (eds.). Taylor and Francis,London, U.K.1989, pp. 87–100.

Electronic Sources as reference

Journal article on the Internet: Parija SC, Khairnar K. Detection of excretory *Entamoeba histolytica* DNA in the urine, and detection of *E. histolytica* DNA and lectin antigen in the liver abscess pus for the diagnosis of amoebic liver abscess. *BMC Microbiology* 2007, **7**:41. doi:10.1186/1471-2180-7-41. http://www.biomedcentral.com/1471-2180/7/41

Tables

- Tables should be self-explanatory and should not duplicate textual material.
- Tables with more than 10 columns and 25 rows are not acceptable.
- Number tables, in Arabic numerals, consecutively in the order of their first citation in the text and supply a brief title for each.
- Place explanatory matter in footnotes, not in the heading.
- Explain in footnotes all non-standard abbreviations that are used in each table.
- Obtain permission for all fully borrowed, adapted, and modified tables and provide a credit line in the footnote.
- For footnotes use the following symbols, in this sequence: *, †, ‡, §, ||,¶ , **, ††, ‡‡
- Tables with their legends should be provided at the end of the text after the references. The tables along with their number should be cited at the relevant place in the text

Illustrations (Figures)

- Upload the images in JPEG format. The file size should be within 1024 kb in size while uploading.
- Figures should be numbered consecutively according to the order in which they have been first cited in the text.
- Labels, numbers, and symbols should be clear and of uniform size. The lettering for figures should be large enough to be legible after reduction to fit the width of a printed column.

- Symbols, arrows, or letters used in photomicrographs should contrast with the background and should be marked neatly with transfer type or by tissue overlay and not by pen.
- Titles and detailed explanations belong in the legends for illustrations not on the illustrations themselves.
- When graphs, scatter-grams or histograms are submitted the numerical data on which they are based should also be supplied.
- The photographs and figures should be trimmed to remove all the unwanted areas.
- If photographs of individuals are used, their pictures must be accompanied by written permission to use the photograph.
- If a figure has been published elsewhere, acknowledge the original source and submit written permission from the copyright holder to reproduce the material. A credit line should appear in the legend for such figures.
- Legends for illustrations: Type or print out legends (maximum 40 words, excluding the credit line) for illustrations using double spacing, with Arabic numerals corresponding to the illustrations. When symbols, arrows, numbers, or letters are used to identify parts of the illustrations, identify and explain each one in the legend. Explain the internal scale (magnification) and identify the method of staining in photomicrographs.
- Final figures for print production: Send sharp, glossy, un-mounted, color photographic prints, with height of 4 inches and width of 6 inches at the time of submitting the revised manuscript. Print outs of digital photographs are not acceptable. If digital images are the only source of images, ensure that the image has minimum resolution of 300 dpi or 1800 x 1600 pixels in TIFF format. Send the images on a CD. Each figure should have a label pasted (avoid use of liquid gum for pasting) on its back indicating the number of the figure, the running title, top of the figure and the legends of the figure. Do not write the contributor/s' name/s. Do not write on the back of figures, scratch, or mark them by using paper clips.
- The Journal reserves the right to crop, rotate, reduce, or enlarge the photographs to an acceptable size.

Protection of Patients' Rights to Privacy

Identifying information should not be published in written descriptions, photographs, sonograms, CT scans, etc., and pedigrees unless the information is essential for scientific purposes and the patient (or parent or guardian, wherever applicable) gives informed consent for publication. Authors should remove patients' names from figures unless they have obtained informed consent from the patients. The journal abides by ICMJE guidelines:

1. Authors, not the journals nor the publisher, need to obtain the patient consent form before the publication and have the form properly archived. The consent forms are not to be uploaded with the cover letter or sent through email to editorial or publisher offices.
2. If the manuscript contains patient images that preclude anonymity, or a description that has obvious indication to the identity of the patient, a statement about obtaining informed patient consent should be indicated in the manuscript.

Sending a revised manuscript

The revised version of the manuscript should be submitted online in a manner similar to that used for submission of the manuscript for the first time. However, there is no need to submit the "First Page" or "Covering Letter" file while submitting a revised version. When submitting a revised manuscript, contributors are requested to include, the 'referees' remarks along with point to point clarification at the beginning in the revised file itself. In addition, they are expected to mark the changes as underlined or colored text in the article.

Reprints and proofs

Journal provides no free printed reprints. Authors can purchase reprints, payment for which should be done at the time of submitting the proofs.

Publication schedule

The journal publishes articles on its website immediately on acceptance and follows a 'continuous publication' schedule. Articles are compiled in issues for 'print on demand' quarterly.

Copyrights

Checklist

Covering letter

- Signed by all contributors
- Previous publication / presentations mentioned
- Source of funding mentioned
- Conflicts of interest disclosed

Authors

- Last name and given name provided along with Middle name initials (where applicable)
- Author for correspondence, with e-mail address provided
- Number of contributors restricted as per the instructions
- Identity not revealed in paper except title page (e.g. name of the institute in Methods, citing previous study as 'our study', names on figure labels, name of institute in photographs, etc.)

Presentation and format

- Double spacing
- Margins 2.5 cm from all four sides
- Page numbers included at bottom
- Title page contains all the desired information
- Running title provided (not more than 50 characters)
- Abstract page contains the full title of the manuscript
- Abstract provided (structured abstract of 250 words for original articles, unstructured abstracts of about 150 words for all other manuscripts excluding letters to the Editor)
- Key words provided (three or more)
- Introduction of 75-100 words
- Headings in title case (not ALL CAPITALS)
- The references cited in the text should be after punctuation marks, in superscript with square bracket.
- References according to the journal's instructions, punctuation marks checked
- Send the article file without 'Track Changes'

Language and grammar

- Uniformly American English
- Write the full term for each abbreviation at its first use in the title, abstract, keywords and text separately unless it is a standard unit of measure. Numerals from 1 to 10 spelt out
- Numerals at the beginning of the sentence spelt out
- Check the manuscript for spelling, grammar and punctuation errors
- If a brand name is cited, supply the manufacturer's name and address (city and state/country).
- Species names should be in italics

Tables and figures

- No repetition of data in tables and graphs and in text
- Actual numbers from which graphs drawn, provided
- Figures necessary and of good quality (colour)
- Table and figure numbers in Arabic letters (not Roman)
- Labels pasted on back of the photographs (no names written)
- Figure legends provided (not more than 40 words)
- Patients' privacy maintained (if not permission taken)
- Credit note for borrowed figures/tables provided
- Write the full term for each abbreviation used in the table as a footnote

Journal of
The Anatomical Society of India

Salient Features:

- Publishes research articles related to all aspects of Anatomy and Allied medical/surgical sciences.
- Pre-Publication Peer Review and Post-Publication Peer Review
- Online Manuscript Submission System
- Selection of articles on the basis of MRS system
- Eminent academicians across the globe as the Editorial board members
- Electronic Table of Contents alerts
- Available in both online and print form.

The journal is registered with the following abstracting partners:
Baidu Scholar, CNKI (China National Knowledge Infrastructure), EBSCO Publishing's Electronic Databases, Ex Libris – Primo Central, Google Scholar, Hinari, Infotrieve, Netherlands ISSN center, ProQuest, TdNet, Wanfang Data

The journal is indexed with, or included in, the following:
SCOPUS, Science Citation Index Expanded, IndMed, MedInd, Scimago Journal Ranking, Emerging Sources Citation Index.

Impact Factor® as reported in the 2018 Journal Citation Reports® (Clarivate Analytics, 2019): 0.168

Editorial Office:
Dr. Vishram Singh, Editor-in-Chief, JASI
OC-5/103, 1st floor, Orange County Society,
Ahinsa Khand-I, Indirapuram, Ghaziabad,
Delhi, NCR- 201014.
Email: editorjasi@gmail.com
(O) | Website: www.asiindia.in

The journal is owned and run by The Anatomical Society of India